SCALE AND ORGANISMAL FORM: AN ECOLOGICAL GENETIC PERSPECTIVE

by

JAMES MICHAEL NOVAK

(Under the Direction of I.Lehr Brisbin, Jr.)

ABSTRACT

Spatial variation in skull form was analyzed for white-tailed deer (*Odocoileus virginianus*) from eight sites within three physiographic regions [upper (UCP) and lower coastal plain (LCP) and barrier islands (BI)] of the Southeast. Components of skull form vary among the physiographic regions. Deer from BI were smaller than mainland deer, and together with LCP deer, exhibited increased fluctuating asymmetry (FA) compared to UCP deer. LCP deer exhibited decreased shape variation compared to animals from either the UCP or BI. Form components for sites within regions appeared to be influenced more by recent processes such as hunting regime, restocking effort and habitat change. Evidence for maintaining the subspecific status of *O. v. hiltonensis* appeared weak.

Fluctuating asymmetry occurs on a smaller scale than the original character and measurement error represents a significant proportion of FA. Mixed-model ANOVA allows group-level FA to be corrected for measurement. Currently, individual-level FA estimates include measurement error. Best linear unbiased predictors (BLUP) can provide error-corrected estimates of individual FA. A simulated data set showed BLUP estimates were more efficient than arithmetic means at error reduction. An analysis of a *Gambusia* hybridization study showed the usefulness of individual-level FA analysis.

Form is a composite character and cannot be measured. Path analysis was utilized to develop individual-level models of skull form evolution for the hispid cotton rat (*Sigmodon hispidus*). Path coefficients are essentially selection coefficients and translate into relative time scales. Structural size operated over the shortest time scale in six models and an intermediate scale in two models. Mass operated over the shortest time scale in four models and an intermediate scale in four models. Age operated over the shortest time scale in four models but sex operated over the shortest time scale in one model and an intermediate scale in the remaining three. Density class operated on an intermediate time scale in all models. Heterozygosity class acted over intermediate (2 models) or long (6 models) time scales. Path models allowed the identification of covariates when utilizing form as a biomarker. Structural size, mass and age together accounted for 89.8% to 95.7% of explained variation.

INDEX WORDS: Form, Fluctuating Asymmetry, Size, Shape, Geometric Morphometrics, Landmarks, Mixed-Model ANOVA, Best Linear

Unbiased Predictor, Path Analysis, Measurement Error, Simulation, *Gambusia affinis*, *Gambusia heterochir*, *Odocoileus virginianus*, *Sigmodon hispidus*

SCALE AND ORGANISMAL FORM: AN ECOLOGICAL GENETIC PERSPECTIVE

by

JAMES MICHAEL NOVAK

B.S., University of Illinois, 1978

M.S., University of Illinois, 1981

A Dissertation Submitted to the Graduate Faculty of The University of Georgia in Partial Fulfillment of the Requirements for the Degree

DOCTOR OF PHILOSOPHY

ATHENS, GEORGIA

2003

SCALE AND ORGANISMAL FORM: AN ECOLOGICAL GENETIC PERSPECTIVE

by

JAMES MICHAEL NOVAK

Major Professor: I.Lehr Brisbin, Jr.

Committee: Wyatt W. Anderson
Justin D. Congdon
J Vaun McArthur
Michael H. Smith

Electronic Version Approved:

Maureen Grasso
Dean of the Graduate School
The University of Georgia
August 2003

DEDICATION

I dedicate this dissertation to my parents, Dolores and Michael, who always encouraged me to follow my heart and my mind, to all my mentors in my educational odyssey and most of all to my wife, Karen, without whose support and inspiration I would not be as happy with my life and career.

ACKNOWLEDGEMENTS

I would like to thank Hayward Simmons who allowed access to Cedar Knoll plantation for the collection of white-tailed deer skulls and was extremely helpful in securing the hunters cooperation. The deer skulls from Hilton Head Island were collected by Bob Warren and his students and graciously donated for use in this research. I would also like to thank Rick Purdue for demonstrating the correct methodology for collecting skulls from a gut pile and Paul Johns for help in collection, sharing information about deer biology and providing invaluable help and friendship. The staff of both the south Carolina and Georgia departments of natural resources helped to facilitate our white-tailed deer collections. Without their help the collection process would have been much more laborious.

I would like to thank Phil Dixon for initial discussions about the usefulness of BLUP for estimating FA values and help in some of the more obscure aspects of the SAS MIXED procedure. Craig Stockwell and Elizabeth Gatlin kindly allowed the use of the *Gambusia* hybrid data.

I would like to thank my committee members Wyatt W. Anderson, Justin D. Congdon, and, J Vaun McArthur for their support and guidance. I would also like to particularly thank my two major professors Michael H. Smith and I.Lehr Brisbin, Jr.. Mike was instrumental in the completion of this dissertation through his support and friendship during my long and somewhat tortuous tenure as a Ph.D. student. Bris made

the process easier to complete by stepping up in the twelfth-hour and through his genuine interest in the topics of this dissertation.

Constructive comments on all chapters were provided by Wyatt W. Anderson, I.Lehr Brisbin, Jr., Justin D. Congdon, Karen F. Gaines, J Vaun McArthur and Michael H. Smith but all errors of omission or commission are strictly mine. This research was partially supported by the Environmental Remediation Sciences Division of the Office of Biological and Environmental Research, U.S. Department of Energy through the Financial Assistance Award no. DE-FC09-96SR18546 to the University of Georgia Research Foundation and the Savannah River Ecology Laboratory.

TABLE OF CONTENTS

CHAPTER 1

INTRODUCTION AND OVERVIEW

WHENCE FORM

Webster's dictionary defines form as: "Form – 1. The shape or outline of anything; figure; structure, excluding color, texture, and density." (McKechnie, 1978) and thus for an organism, form can be defined as the outward physical appearance of an individual excluding color, texture and density. Traditionally form has been defined as being composed of size and shape (Dryden and Mardia, 1998), which are components of form defined by their invariance to changes in location (translation), changes in position (rotation) or changes in size (scaling) (Slice *et al.*, 1996; Figure 1). Symmetry has not traditionally been included as a component of form, which makes the definition of form incomplete for several reasons. First, the components of form are defined by differences in their invariance to transformations. Size is defined as those aspects of form that are invariant to translation and rotation but not scale whereas shape is invariant to changes brought about by translation, rotation and scale (Slice *et al.*, 1996). Similarly, symmetry is that aspect of form that is invariant to changes brought about through translation and scale, but not rotation. Second, it is well known in geometric morphometrics that traditional landmark-based analyses do not work well on a configuration of landmarks that is symmetrical (Bookstein, 1996), however, this is only because the symmetry is not addressed in the analysis (Klingenberg *et al.*, 2002) since it is not included in the definition of form components. Lastly, there has been a long debate between users of

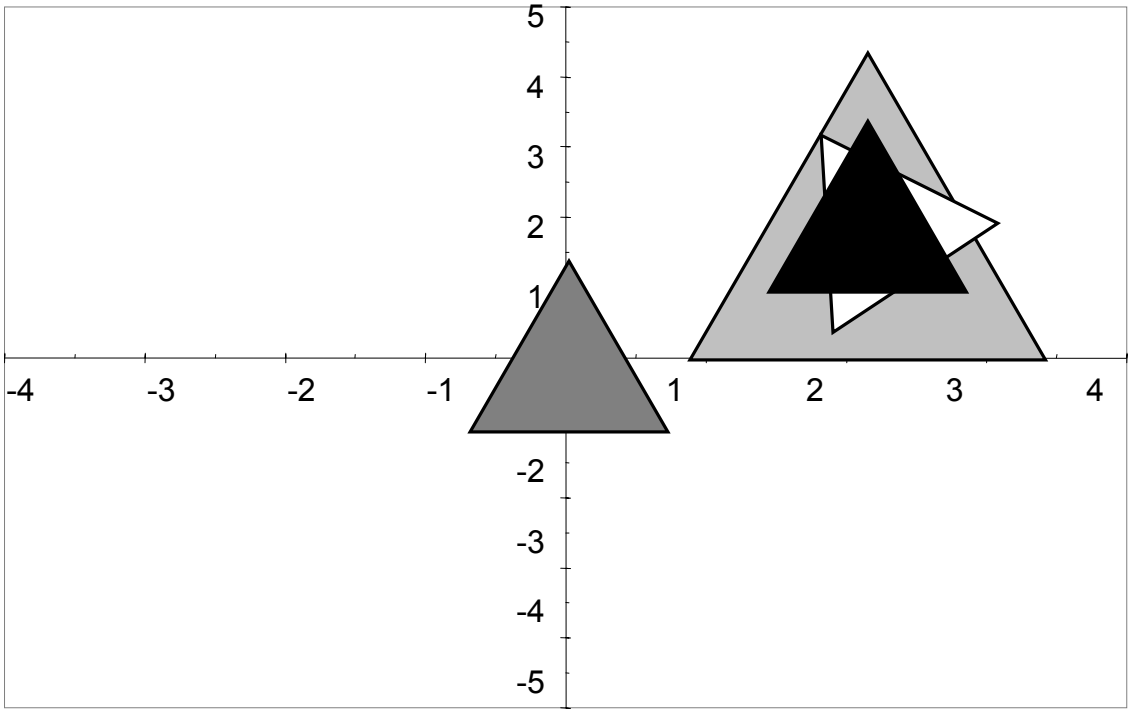

Figure 1. Diagrammatic representation of the geometric processes of translation, rotation and scaling. Starting with the black triangle we can translate it to the dark gray triangle, rotate it to the white triangle or scale it (larger) to the light gray triangle.

Euclidean distance matrix analysis-based techniques (EDMA) and those utilizing landmark-based approaches based upon Procrustes superimposition techniques (Rohlf, 2000a; Rohlf, 2000b; Richtsmeier *et al.*, 2002). A large portion of the discrepancy between the two techniques results from the fact that EDMA techniques analyze the whole form, not even addressing what components are included within form, whereas Procrustes methods analyze components of form. If symmetry is a large component of the form the expectation is that the results of EDMA and Procrustes analysis will differ since traditional Procrustes methods do not include symmetry as a component in the form analysis.

Form is therefore composed of size, shape and symmetry as well as all the covariances among these three components of form (Figure 2). This makes form a composite character; in the same sense as, fitness is a composite character composed of reproductive and survival components (Stearns, 1992). Composite characters are defined and estimated through their components and not directly (Roff, 1992). Components of form can be summarized for groups of individuals, but form itself is a property of an individual, thus, we can only analyze form using individual-based models and analyses (DeAngelis and Rose, 1992; Judson, 1994).

COMPONENTS OF FORM AND THEIR ANALYSIS

Each component of form is both a morphological and life-history trait and has a quantitative genetic basis (Klingenberg, 2001b; Klingenberg, 2001a). While size has a long history as an important life history trait, shape and symmetry have not been considered in the life-history literature to any great extent (Roff, 1992; Stearns, 1992). The shift from components of form being viewed as morphological versus life-history

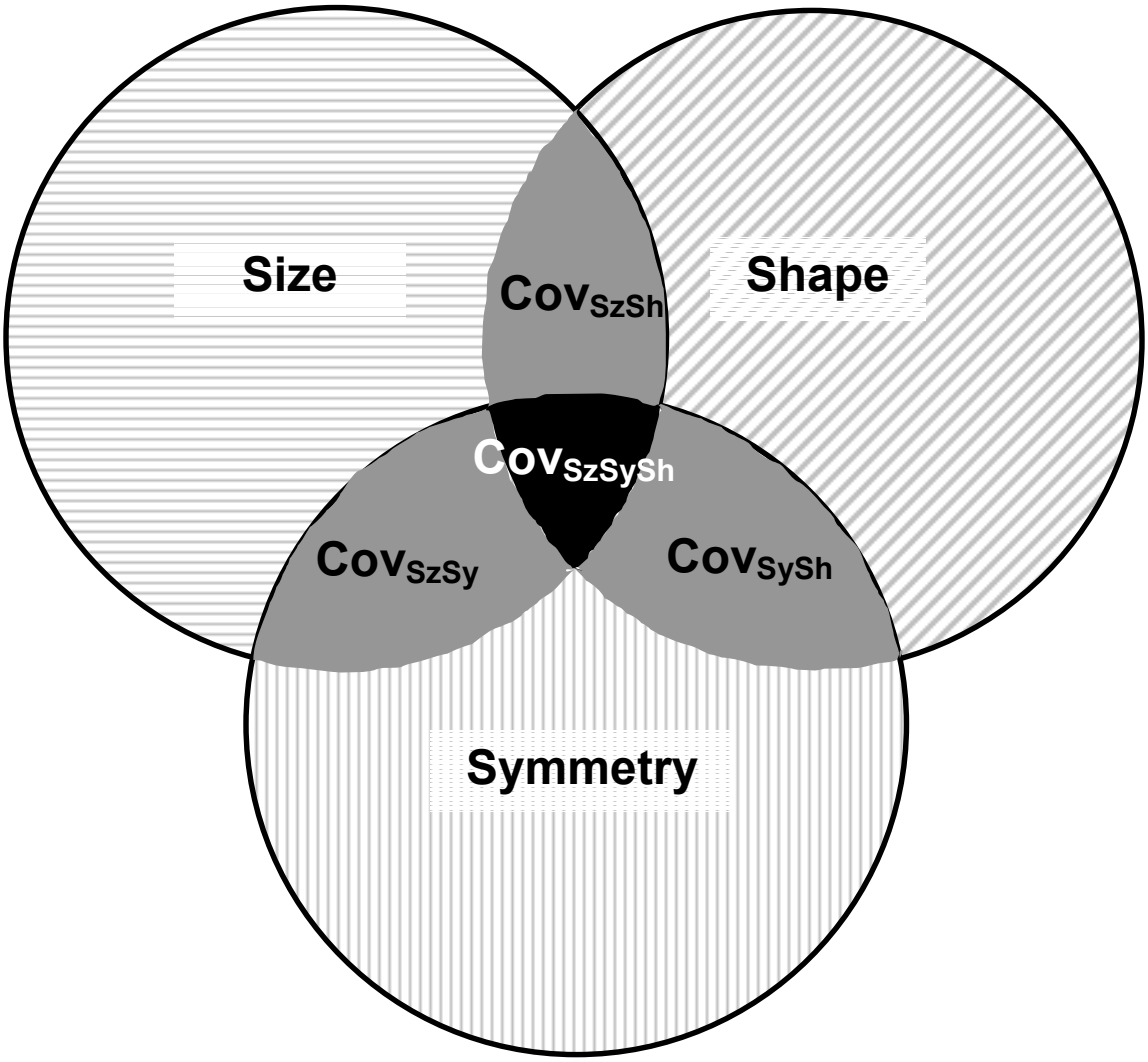

Figure 2. Heuristic representation of form and the components of form. The solid light gray areas represent the covariances of pairs of form components while the black area represents the covariance of all three components. The actual areas of each component as well as the relative areas of the covariances may vary in size and need not be equal in magnitude as depicted here. All three components and the covariances among them together define form.

traits comes when we place a temporal or developmental constraint upon the component. Thus, size is a morphological trait but size-at-maturity is a life-history trait. Since size is but one component of form, placing a constraint defining a temporal point in an organisms life history, allows the use of any component of form to be analyzed as a life-history trait. In addition, components of form can be considered primary or fundamental life-history traits since they define life history traits such as of size (or shape or symmetry) specific reproductive rates and mortality schedules (Stearns, 1992).

From a statistical viewpoint, estimation of form is primarily a problem in the estimation and combination of its component parts (size, shape and symmetry). Geometric morphometrics provides a statistically accurate and biologically meaningful metric for both size (centroid size) and shape (Procrustes distance and partial/relative warps) based upon the statistical analysis of a relatively small subset of discrete landmarks that capture the essential form of the object under study. Excellent recent reviews of geometric morphometric concepts can be found in the volume by Small (1996) for theoretical underpinnings and those of Marcus *et al.* (1996) and Dryden and Mardia (1998) for statistical analysis and excellent examples of how shape can be estimated from relatively few landmarks. The history of geometric morphometrics is well illustrated in the reviews of Bookstein (1989), Rohlf and Marcus (1993), Monteiro *et al.* (2000) and Adams *et al.* (2003) all of which provide more in depth descriptions of the logic behind geometric morphometrics.

Geometric morphometrics is based upon the Euclidean approximation of a space tangential to Kendall's shape space, which allows us to use standard univariate and multivariate techniques in the analysis (Small, 1996; Dryden and Mardia, 1998). The

form of the character or organism is summarized using a series of landmarks digitized from or onto an image of the object or organism. A landmark is defined as a specific point located on an object according to a specific rule (Slice *et al.*, 1996). The key point is that the rule allows us to define the landmarks as homologues between individuals. If the landmarks can be defined as homologous based upon strong histological evidence, such as a suture point or foramina they are type I landmarks (Slice *et al.*, 1996). Type II landmarks are defined purely by geometry (e.g. a point of greatest curvature) and type III landmarks have at least one deficient coordinate (e.g. either end of a longest diameter) (Slice *et al.*, 1996) and grade into semi-landmarks (landmarks based upon the position of one or more other landmarks) for estimating the form of curved surfaces (Bookstein, 1997).

Once we have a set of landmarks we can proceed to a Procrustes superimposition. The first step involves translating each set of landmarks to a common point, rotating each landmark configuration to a common baseline, and scaling each configuration to a predefined size. Most commonly, each individual landmark configuration is scaled to a centroid size of 1, which is the convention followed for all analyses. The scaling also defines our relevant size variable as centroid size since it will be uncorrelated with shape except for any real covariance between the parameters due to allometry (Bookstein, 1997). Centroid size is defined as the square root of the sum-of-squared distances of a set of landmarks from their centroid (Slice *et al.*, 1996; Figure 3). The centroid, which is the center of density of the landmark configuration, is calculated simply as the mean of the x and the mean of the y coordinates of all landmarks. After all individual landmark configurations have been translated, rotated and scaled, the consensus landmark

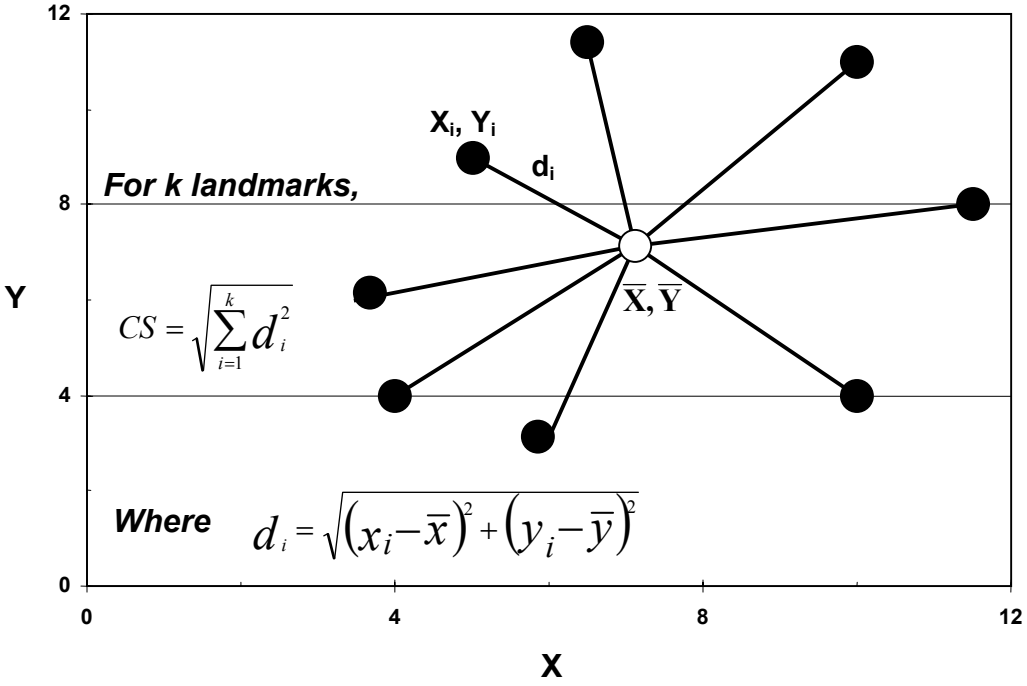

Figure 3. Diagrammatic representation of the calculation of centroid size for a configuration of eight landmarks (solid circles). The centroid, $\overline{X}, \overline{Y}$ is represented by an open circle and CS is centroid size.

configuration is calculated as the Procrustes mean of all configurations. Each individual is "fit" to the consensus form by aligning the centroid of the two forms followed by a series of orthogonal transformations using a least-squares minimization criterion to obtain the closest fit of the individual to the consensus. The resultant set of x and y coordinates for each individual is the set of Procrustes residuals. Procrustes residuals are simply the deviance of a landmark for an individual from the consensus coordinates of that landmark. Procrustes residuals can be used to extract size-free shape and symmetry components.

As stated earlier, symmetry has not been included in the geometric morphometrics definition of form. In fact the definition of symmetry and its analysis has proceeded along an independent pathway as a surrogate for developmental stability. Excellent reviews of the history of, and analytical techniques for, both fluctuating asymmetry and developmental stability can be found in the volumes by Markow (1994), Møller and Swaddle (1997), and Polak (2003). Symmetry itself is a composite character and may contain antisymmetry, directional asymmetry, or fluctuating asymmetry (Van Valen, 1962; Figure 4). Directional asymmetry (DA) obtains when one side of a bilateral character differs and the difference is always in the same direction. Statistically, DA will move the mean of the distribution of left/right differences left (right-biased DA) or right (left-biased DA) from zero (Figure 4). Antisymmetry (AS) occurs when one side of a bilateral character always differs but the direction of the difference is random across individuals. Statistically, AS will cause the distribution of left/right differences to deviate from normality, usually by causing platykurtosis or bimodality in the distribution (Figure 4). Fluctuating asymmetry (FA) results differences between the sides of a bilateral

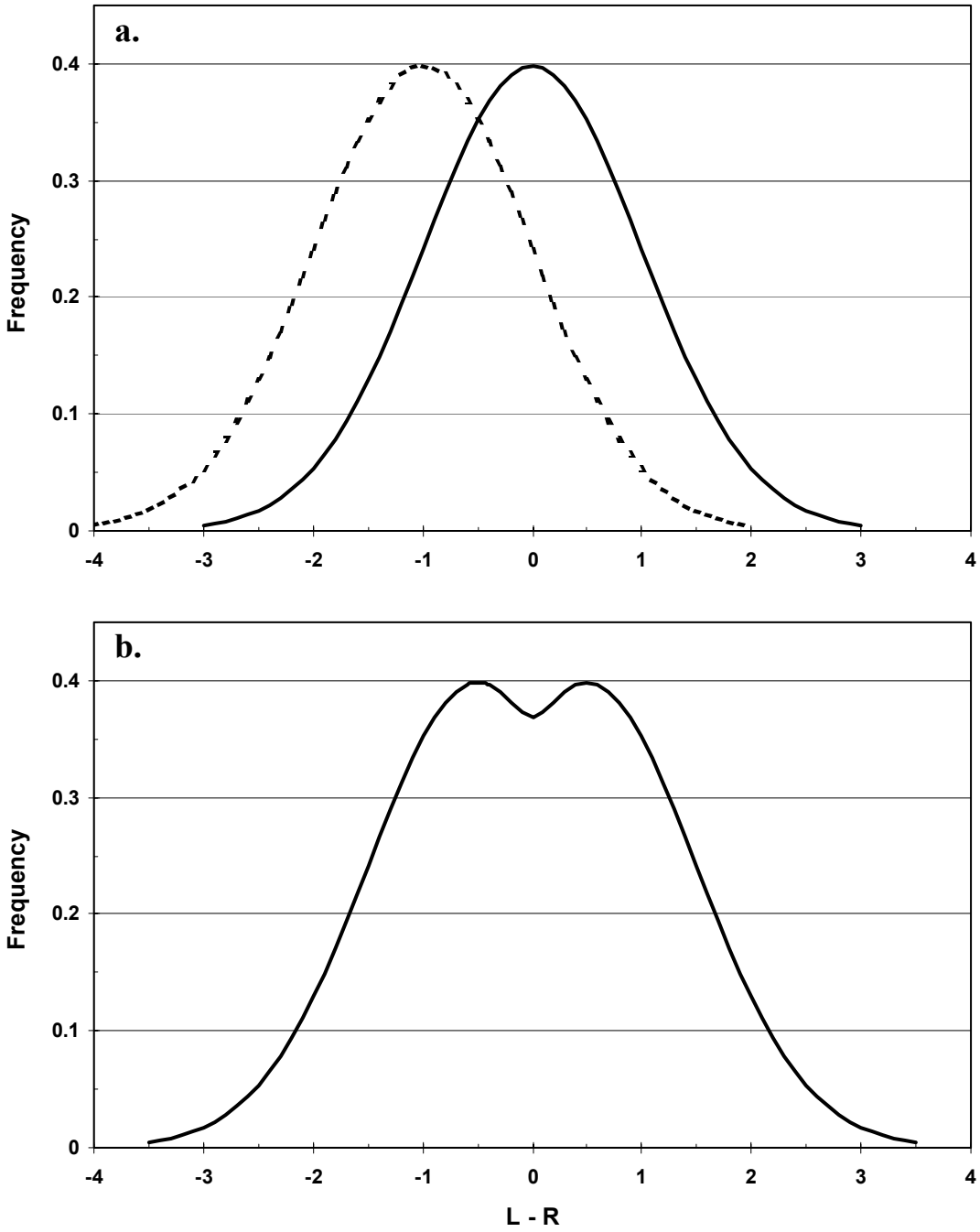

Figure 4a.) The solid line is the distribution of left minus right differences for a trait exhibiting fluctuating asymmetry (FA) with mean equal to zero and variance equal to FA. The dashed line is the distribution for a trait exhibiting right biased directional

asymmetry (DA) with mean equal to –1 and variance equal to FA + σ^2_{DA}, that is, the variance of the distribution contains components due to fluctuating asymmetry and also a component of unknown magnitude due to variation in directional asymmetry. 4b.) The distribution of left minus right differences for a trait exhibiting an extreme form of antisymmetry (AS) resulting from a mixture of two normal distributions with mean=0 and modes at –0.5 and 0.5 and variance equal to $FA_1 + FA_2$. A trait exhibiting a less extreme form of antisymmetry would exhibit platykurtosis rather than bimodality.

character that are random in both direction and magnitude across individuals such that the mean difference between sides is zero and FA is the variance of that distribution (Van Valen, 1962). Most researchers agree that only FA is a legitimate surrogate for developmental stability since its phenotypic basis is largely due to environmental variance rather than genetic variance (Palmer and Strobeck, 1986; Møller and Swaddle, 1997). However, a few studies have implied that directional asymmetry, antisymmetry or both, may also be used as surrogate measures for developmental stability (McKenzie and Clarke, 1988; Graham *et al.*, 1993; Møller, 1994). As a component of form only FA is likely to be a universal feature of all characters. FA should occur in any trait that is not totally canalized in its development whereas AS and DA will be trait dependent since they are generally functional and have a significant, but largely unknown, genetic basis (Palmer and Strobeck, 1992). Therefore, only fluctuating asymmetry will be analyzed in any detail in the following chapters. Directional asymmetry and antisymmetry will only be analyzed in so far as to insure they are not confounding the analysis of FA.

Since FA represents the variance of a distribution, a reasonable method is to estimate it as a variance component. The variance component for FA is obtained from a mixed-model analysis of variance (ANOVA) with replicate measurements on all individuals (Palmer and Strobeck, 1986; Table 1). In the mixed-model analysis, side (left or right) is a fixed effect that estimates the magnitude of directional asymmetry, individual is a random effect that estimates size or shape variation (in this case, we have removed size by standardizing to unit centroid size so that only symmetric shape variation is estimated), the residual error term represents measurement error, and the interaction of side and individual is a random effect and its variance component is our measurement

Table 1. Mixed-model ANOVA for the estimation of group-level FA.

Effect	Expected Mean Square	Estimated Component
Sides (S)	$\sigma_m^2 + M\left\{\sigma_i^2 + [J/(S-1)]\sum a^2\right\}$	Directional asymmetry
Individuals (J)	$\sigma_m^2 + M\left(\sigma_i^2 + S\,\sigma_j^2\right)$	Size/Shape variation[1]
Interaction(I) (SxJ)	$\sigma_m^2 + M\,\sigma_i^2$	Antisymmetry, FA / # reps, Measurement error
Measurements (M)	σ_m^2	Measurement error

[1] In a Procrustes-based analysis this component represents shape variation and allometric variation (Size x Shape Interaction) since all individuals are scaled to unit centroid size prior to superimpositioning. In addition, for studies performing a Procrustes analysis on a structure with object symmetry, any size asymmetry will be included in this component.

error-corrected estimate of FA. Performing this analysis in a geometric morphometrics framework requires a slight modification of the mixed-model ANOVA (Klingenberg and McIntyre, 1998). A separate ANOVA is performed for each of the x and y coordinates for every landmark; thus for 12 landmarks, 24 ANOVA's are calculated. The sums-of-squares for all model effects (side, individual, side*individual and error) are summed and divided by the degrees-of-freedom to obtain an overall mean square for each effect. The degrees-of-freedom for each effect is calculated as the degrees of freedom from the univariate analysis multiplied by 2 times the number of landmarks minus 4, for traits exhibiting matching symmetry or, 2 times the number of paired landmarks plus the number of midline landmarks minus 2, for traits exhibiting object symmetry (see below). For our example of twelve landmarks the degrees-of –freedom for each effect would be multiplied by 20, for matching symmetry or by 22 for object symmetry (11 landmark pairs and two midline landmarks). The resultant values are the Procrustes mean squares. The methodology of Klingenberg and McIntyre (1998) is based upon the work of Goodall (1991), which assumes that variation among landmarks is equal, isotropic (non-directional) and independent. Thus, we must check the degree to which these assumptions are violated or perform a fully multivariate analysis, which has its own set of assumptions and a much more stringent sample size requirement. Variation of points around the landmark can be estimated as the sum-of-squared distances of the points from the centroid. We can test for homogeneity of variance among the landmarks with a Levene's test on the distance values (Palmer and Strobeck, 2003), for isotropy with a Rayleigh test of uniformity (Mardia and Jupp, 2000), and for independence among the landmarks with a semivariogram based upon a spherical model (Piegorsch and Bailer, 1997).

When analyzing a structure such as the vertebrate skull that exhibits object symmetry (i.e. the plane of symmetry is part of the structure) one often has both paired and unpaired (midline) landmarks. For traits exhibiting object symmetry, the midline points contain useful information and throwing them out and analyzing only the paired points as a right and left half-configuration is not the best methodology. Instead the analysis can proceed using the full configuration of landmarks as one side and a reflected set of landmarks as the other side (Klingenberg *et al.*, 2002) prior to the Procrustes superimposition. This allows the simultaneous estimation of both symmetric shape (individual main effect) and fluctuating asymmetry (side*individual interaction) from the mixed model ANOVA since the mean of a landmark configuration and its reflection is absolutely symmetric.

WHENCE SCALE

The usual context in which scale is discussed is in terms of spatial or temporal scale. In the context of this dissertation scale will also refer to the scale of analysis as either individual-level or group (of individuals) level. The scale of the analysis imposes a spatio-temporal scale for the processes structuring the measured variables (Pascual and Levin, 1999). It is well known in both ecology (Begon *et al.*, 1998) and evolutionary biology (Futyma, 1998), that not only may the magnitude of the underlying process change non-linearly from the individual to the group level, but the process itself may not transcend scales. Thus the choice of analysis scale is a function of both the hypothesis being tested as well as the underlying ecological and evolutionary processes that are part of that hypothesis.

For the components of form, size and shape, analyses either at the individual level or at some higher level of aggregated individuals, is performed identically. However, fluctuating asymmetry presents some problems at the individual level. First, the definition of fluctuating asymmetry makes it clear that FA is a variance and an individual does not have a variance. However, an individual does have two sides so we can estimate its FA as the difference or deviance between the sides (Møller and Swaddle, 1997). The problem with using either the signed or unsigned difference as an individual-level estimator of FA is that the estimate also includes measurement error. For a group-level mixed model ANOVA with replicate measurements, the variance component of the interaction term provides a measurement-error corrected estimate of FA (Palmer and Strobeck, 1986; Table 1). The reason measurement error is a bigger problem for estimates of FA compared to estimates of size or shape also has to do with scale. Since FA values are a difference between sides actual values of FA are usually 2 or 3 orders of magnitude smaller than the character itself (Møller and Swaddle, 1997). For example, if we measure the left and right trait of our organism as 35.60mm and 35.65mm with a measurement error 0.05mm our percentage error relative to character size is 0.14% however our percentage error relative to the difference between the sides is 100%. The usual method to address a measurement error problem is to calculate a mean over several replicates. Means are inefficient at removing error and are technically not appropriate when dealing with a random effect (Verbeke and Molenberghs, 1997). Since we are estimating group-level fluctuating asymmetry with a mixed-model ANOVA we can utilize the technique of best linear unbiased predictors (BLUP) to estimate an error corrected estimate of FA for an individual (Robinson, 1991). For our purposes we can

think of the BLUP as a random effects analog to a fixed effects arithmetic mean. The BLUP differs from an arithmetic mean in that it is a regression of the individual value towards the overall group mean based upon the variance components of the relevant model effects (Littell *et al.*, 1996). Thus it is a shrinkage estimator, which shrinks individual values toward the overall mean consistent with the ratio of the relevant variance components. Attenuation of the shrinkage of extreme means by the prior knowledge of the underlying variability is an inherently Bayesian approach which has the effect of reducing data misinterpretation for random effects. The use of BLUP for the estimation of individual-level FA allows the use of individual-level methods in cases where the amount of measurement error may have previously necessitated the use of a group-level analysis.

The scale of analysis (individual or group) should be decided based upon the level at which the underlying structuring processes are acting. As stated previously, form is a composite trait and is the property of an individual. Since, we can only measure the components of form, and not form itself, we can only estimate form by reconstructing it from its individual components. The reconstruction of form from its measured components can be most easily performed at the level of the individual not groups. At any level above the individual any reconstruction of form is limited by sample size (the number of groups) and by our inability to know if the underlying processes are the same in magnitude and kind at both the individual and group level. Thus our goal is to reconstruct an unmeasured trait, form, from its measured components, size, shape and symmetry. One way to do this is to use the analytical framework of path analysis to estimate mechanistic effects on form similar to its use for the estimation of selection

(Kingsolver and Schemske, 1991) and fitness (Svensson *et al.*, 2002). Path analysis was first utilized by Sewell Wright for incorporating genetic relatedness into between-generation analyses of quantitative genetic variation (Wright, 1921). However, it is actually part of a larger statistical framework called structural equation or causal modeling that also includes such techniques as principal components analysis and factor analysis (Hatcher, 1994). The usefulness of path models comes from the fact that path coefficients are simply partial regression coefficients on standardized variables (Li, 1975), they can be converted to coefficients of determination (Li, 1975) and path models can contain both manifest (measured) and latent (unmeasured) variables (Hatcher, 1994). In addition, path models are a representation of a hypothesis for causal links among the variables in the models so they are perfectly suited for developing mechanistic models. Separate mixed-model ANOVA's are utilized to generate BLUP estimates of the x and y coordinates of all landmarks and these BLUP estimates are analyzed via separate path analyses for each x and y coordinate. The sum-of-squares summation technique of Klingenberg and McIntyre (1998) is utilized to generate Procrustes mean squares which in turn are used to calculate composite path coefficients for symmetric shape (mean of the original value and its reflection) and fluctuating asymmetry (difference between the original value and its refection). Only a single path analysis is necessary for centroid size since it is a univariate measure.

OVERVIEW AND SUMMARY

This dissertation is an exposition of the analysis of form from an ecological genetic perspective. I define ecological genetics broadly to encompass aspects of both evolutionary ecology and evolutionary ecotoxicology. It starts with a group-level

analysis, develops a new methodology for estimating a measurement error-corrected value of fluctuating asymmetry, and ends with an individual-based form analysis that integrates size shape and symmetry into an overall estimate of form.

In chapter two we will perform a group-level analysis of white-tailed deer (*Odocoileus virginianus*) along a transect following the Savannah River and along the coast and barrier islands of South Carolina and Georgia. White-tailed deer were chosen as subjects for this analysis as 1.) they are the single most important game species in the United States; 2.) within the area of South Carolina and Georgia, there are five named subspecies; one mainland form and four barrier island forms; and 3.) previous work with both allozyme and mtDNA has shown that deer in this part of the Southeast exhibit relatively strong female philopatry, which results in spatial genetic structure patterned at a relatively small scale for an organism of its size and vagility. Analysis of spatial variation in the components of form (size, shape and symmetry) will proceed utilizing deer skulls collected from eight sites within three physiographic regions (upper/middle coastal plain, lower coastal plain and barrier islands).

The components of skull form varied for white-tailed deer inhabiting different physiographic areas of South Carolina and Georgia. Size and fluctuating asymmetry covaried spatially to a degree. However, symmetric shape appears relatively spatially independent relative to size and fluctuating asymmetry. Deer collected from barrier islands were smaller than mainland deer and together with lower coastal plain deer exhibited increased fluctuating asymmetry compared to deer collected from the upper/middle coastal plain. Deer collected from the lower coastal plain exhibited decreased symmetric shape variation compared to animals from either the upper/middle

coastal plain or barrier islands. Components of form for sites within areas varied on a smaller spatio-temporal scale and appeared to be influenced more by relatively recent processes such as hunting regimes, restocking efforts and habitat changes associated with anthropogenic development. There was only weak evidence for the subspecific designation, *O. v. hiltonensis*, for deer inhabiting Hilton Head Island, SC. Form analysis provided useful information for evolutionary, ecological and management inferences concerning white-tailed deer using a group-level analysis. However, only weak inferences for form and the covariation of form components could be drawn at the group-level due to statistical and theoretical considerations.

Chapter three will provide a new methodology for the estimation of a measurement error-corrected estimate of individual-level fluctuating asymmetry (FA). Fluctuating asymmetry has become a favorite estimator of developmental stability but there are some important statistical considerations when estimating FA. Estimates of FA are usually at a reduced scale compared to the original character, thus measurement error can represent a significant proportion of the total estimate. Estimates of FA for a group can be corrected for measurement error using replicated measurements within a mixed-model ANOVA framework. However, group-level analysis is not appropriate for all questions and these individual-level estimates, usually raw signed or unsigned differences, remain uncorrected for measurement error. The technique of best linear unbiased predictors (BLUP) will be utilized in a novel manner to provide estimates of individual-level FA corrected for measurement error as part of the original analysis. A simulated data set will be used to illustrate that BLUP estimates are much more efficient than simple means at removing measurement error. Finally, an analysis of data from a study of hybridization

between western mosquitofish (*Gambusia affinis*) and the endangered Clear Creek *Gambusia* (*Gambusia heterochir*) will show the usefulness of this technique when the analysis can be done at the individual rather than the group-level. The measurement error-corrected individual-level FA estimates allow more latitude in determining the scale of analysis for asymmetry research and provide estimates suitable for integrating into an estimate of form, which must be done at the scale of the individual not an aggregation of individuals.

Chapter four will illustrate an individual-based analysis of form for a meta-population of hispid cotton rats (*Sigmodon hispidus*). Form is a composite character composed of size, shape, symmetry and their covariances and is a property of individuals. Thus, form itself cannot be easily measured directly, but only through its components. Path analysis provides the analytical framework to develop mechanistic models for the evolution of unmeasured (latent) variables such as form. The path coefficients can be interpreted as selection coefficients. Thus, for evolutionary models path coefficients translate into rates of evolution and thus indicate the relative time scales for effects of exogenous and mediator variables. A total of eight models will be analyzed utilizing four endogenous variables (centroid size, symmetric shape, fluctuating asymmetry, and form), two mediator variables (mass and structural size) and (grid density class, heterozygosity class, and age class or sex). Separate models will be analyzed for sex and age class because of sampling considerations. We will also utilize the path models to identify covariates for utilizing form and form components as effects biomarkers in ecotoxicological research.

In all but two models, the effects of structural size operated over the shortest time scale and acted over an intermediate time scale in those two. The effects of mass operated over the shortest time scale in four models and over an intermediate time scale in the remaining four. Effects of age operated over the shortest time scale in the four models in which it was included but the effects of sex operated over the shortest time scale in only one of the four models it was included in and over an intermediate time scale in the remaining three. The effects of density class operated on an intermediate time scale in all eight models. The effects of heterozygosity class acted over intermediate (2 models), long (4 models) or very long (2 models) time scales. We captured 89.8% to 95.7% of the variation utilizing only structural size, mass, and age as model components compared to full models that included the more laborious and costly variables, density class and heterozygosity. Thus individual-based models allowed us to analyze the components of form more efficiently, estimate the composite trait, form and allowed the identification of necessary covariates when using form and its components as effects biomarkers for the individual-level based comparisons among impacted and reference sites in ecotoxicological research.

CHAPTER 2

EVOLUTIONARY DYNAMICS OF SKULL FORM AMONG POPULATIONS OF WHITE-TAILED DEER

INTRODUCTION

White-tailed deer (*Odocoileus virginianus*) are arguably the most important game animal in North America. They are most certainly the most important game animal in South Carolina in terms of biomass harvested, effort and dollars spent (Ruth, 2003). This has led to a large amount of research on white-tailed deer in the United States. This is unusual only in the fact that a large proportion of this research was actually more basic than applied and in subject areas that are atypical for the research performed on most wildlife species. For example, white-tailed deer were one of the first wildlife species to have extensive research done on their genetic structure (Smith *et al.*, 1984) especially in the Southeast (Ellsworth *et al.*, 1994a; Ellsworth *et al.*, 1994b). One important result of this genetic research, from an ecological point of view, was the confirmation of the relatively strong philopatry of white-tailed deer, especially females (Smith, 1991) through its resultant effect upon spatial genetic heterogeneity (Purdue *et al.*, 2000).

Purdue *et al.* (2000) examined a series of 6 populations that formed a transect down the Savannah River from the United States Department of Energy's Savannah River Site (N 33° 14' W 81° 31'), just below the fall line, to the coast and southward along the coast into Georgia. Using data from both Allozyme and mitochondrial DNA markers, Purdue *et al.* (2000) confirmed that females disperse less than males, estimated that females

account for only 13% of the gene flow exhibited among these populations, and had a functional migration distance of < 50km. They also concluded that the magnitude of the genetic differences among populations were relatively large for this relatively small spatial scale given a white-tailed deer's potential vagility (Mech and Korb, 1978) and both the magnitude (Novak *et al.*, 1991) and type (Scribner *et al.*, 1985) of hunting involved. In addition, demographic characteristics also differ within a small area (803 km^2) for white-tailed deer in South Carolina (Dapson *et al.*, 1979).

The major subspecies within the area surveyed by Purdue *et al.* (2000) is *O. v. virginianus* which occurs on the mainland of South Carolina and in most, except for the extreme southern portions, of Georgia where *O. v. seminolus* occurs. In addition, there are four recognized subspecies that occur on barrier islands (*O. v. taurinsulae*, Bull's Island, SC; *O. v. venatorius*, Hunting Island, SC; *O. v. hiltonensis*, Hilton Head Island, SC and *O. v. nigribarbis*, Blackbeard Island, GA) off the coast of South Carolina and Georgia (Goldman and Kellogg, 1940). The subspecific designations were applied to these populations primarily because of smaller structural size, smaller mass and coat color differences of individuals compared to the mainland form as well as some skull shape differences, especially in the rostral and braincase areas. Purdue *et al.* (2000) did not include any deer from these or other barrier islands in their analysis and so did not address the genetic validity of these subspecific designations.

Since, the barrier island subspecies of deer were defined in terms of size and skull shape characteristics, skull form metrics may be a better way to evaluate these taxonomic designations as opposed to mtDNA or allozyme markers (Hillis and Wiens, 2000). Form is traditionally defined as being composed of size and shape (Dryden and Mardia, 1998).

Symmetry is not included and makes the definition incomplete for several reasons. First, the components of form are defined by differences in their invariance to transformations. Size is defined as those aspects of form that are invariant to translation and rotation but not scale while shape is invariant to changes brought about by translation, rotation and scale (Slice *et al.*, 1996). Similarly, symmetry is that aspect of form that is invariant to changes brought about through translation and scale, but not rotation. Second, it is well known in geometric morphometrics that traditional landmark-based analyses do not work well on a configuration of landmarks that is symmetrical (Bookstein, 1996). The reason symmetry is a problem in a standard geometric morphometrics analysis is because the symmetry is not directly included in the analysis (Klingenberg *et al.*, 2002). Lastly, there has been a rather long debate between users of Euclidean distance matrix analysis (EDMA)-based techniques and those utilizing landmark-based approaches utilizing Procrustes superimposition techniques (Rohlf, 2000a; Rohlf, 2000b; Richtsmeier *et al.*, 2002). A large portion of the discrepancy between these techniques results from the fact that EDMA analyzes the whole form whereas Procrustes methods only analyze two components of form, size and shape. Thus, if symmetry is a large component of the form, traditional Procrustes methods will differ from EDMA-based estimates since symmetry is not included as a component in the form analysis.

Our general objective is to extend the analysis of Purdue *et al.* (2000) utilizing a similar sampling scheme for selecting populations but using a character, organismal form, that has a quantitative genetic basis. Specifically we will estimate the components of form (size, shape and symmetry) and determine their pattern of spatial variation among selected populations of white-tailed deer from the upper/middle coastal plain, from the

lower coastal plain and from barrier islands of South Carolina and Georgia. In addition, the pattern of spatial covariation among the components of form will be examined. Lastly, the subspecific designation of *O. v. hiltonensis* will be evaluated in light of the data we have gathered.

MATERIALS AND METHODS

SAMPLING LOCALITIES AND SPECIMENS

White-tailed deer skulls were obtained from hunters at the following 8 sampling locations (sites) located in Georgia and South Carolina (Figure 5). Savannah River Site, SC (SRS; N 33° 14' W 81° 31'; n=14), Cedar Knoll Hunt Club, SC (N 32° 52' W 81° 27'; n=11), Laurel Hill Hunt Club, GA (N 31° 46' W 81° 17'; n=11), Glynn Co., GA (N 31° 14' W 81° 25'; n=2), McIntosh Co., GA (N 31° 16' W 81° 34'; n=1), Sapelo Island, GA (N 31° 29' W 81° 15'; n=12), St. Catherine's Island, GA (N 31° 38' W 81° 9'; n=2), and Hilton Head Island, SC (N 32° 12' W 80° 44'; n=8). All collected deer were sexed and aged (Severinghaus, 1949) prior to collecting of skulls. Only skulls of female deer aged 2.5 years or older were collected. Skulls were cleaned and prepared at The Illinois State Museum using standard techniques (Martin *et al.*, 2000). Only a single deer was collected from McIntosh Co., which did not differ significantly in form from the two deer collected from Glynn Co. Therefore, it was merged with the two deer from Glynn Co. into a single sample (labeled Other in figures) for all analyses.

MEASUREMENTS AND ANALYSIS

Individual skulls were placed on a ball of modeling clay and leveled using a bubble-level with one edge aligned to the distal end of the incisive foramina (Figure 6). A photograph was taken of the ventral surface of the skull using a Nikon n90s camera with

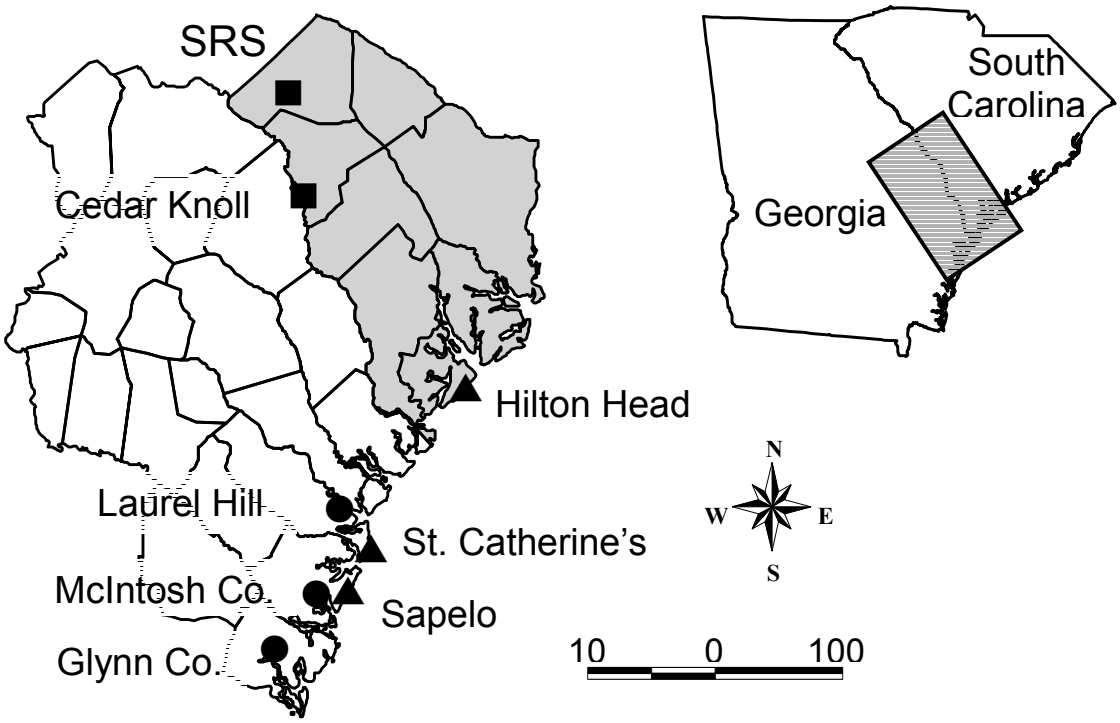

Figure 5. White-tailed deer sampling localities in Georgia (unshaded) and South Carolina (shaded). Squares are upper/middle coastal plain populations, circles are lower coastal plain populations and triangles are barrier island populations. The scale bar is referenced to the map containing the sampling locations.

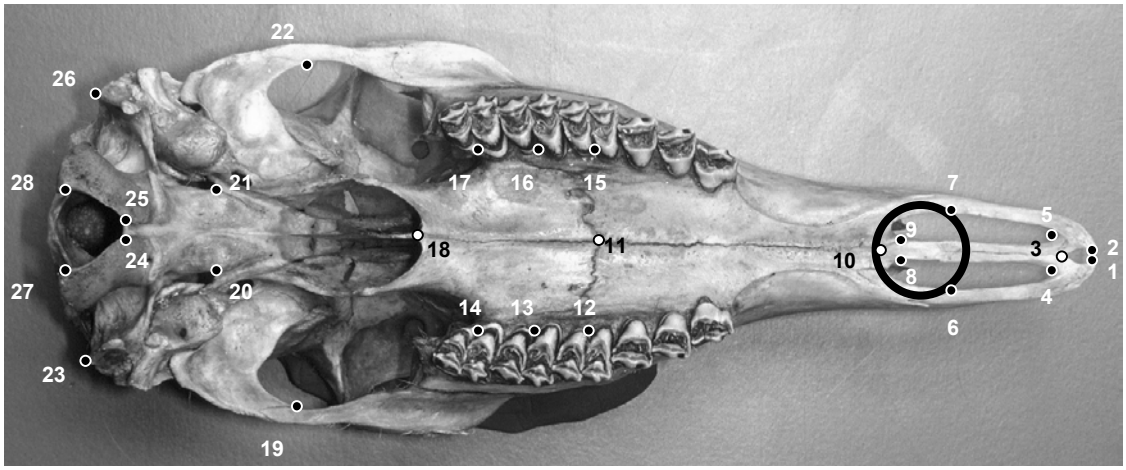

Figure 6. Locations on the ventral skull surface of the 28 landmark points utilized in the current study. Midline points are white with a black border and black numbers (4 landmarks) and paired points are black with a white border and white numbers (12 pairs of landmarks). The large open circle represents the position of the bubble-level prior to image acquisition. Landmark points are described in Appendix A.

a flat-field 60mm macro lens (ASA 100; f = 16). We chose the ventral surface of the skull as it presented a relatively flat surface compared to the dorsal and lateral surfaces and thus distortion from the creation of a 2-dimensional image from a 3-dimensional object would be relatively less in this plane. The camera was attached to a copy stand at a height that allowed the skull to fill most of the image frame. The camera was also leveled using a bubble-level centered upon the back plane of the camera. Photographic slides were taken for a series of skulls; the skulls were then repositioned and leveled and a replicate slide was taken for each skull in the series. Thus each individual was photographed twice with individuals randomized between replicates. Each slide was then scanned to a 7Mb 24bit color bitmap image using a Nikon LS-2000 slide scanner. Each bitmap was used to digitize a series of 28 landmarks (4 midline and 12 pairs; Figure 6; Appendix A) twice. Again, individuals were randomized prior to digitization of landmarks and between replicates. The final result was each individual having two images, each with two sets of digitized landmarks providing four sets of replicate landmarks per individual.

The basic analysis followed a geometric morphometrics protocol (Adams *et al.*, 2003) and is based upon the x and y coordinates of each landmark point and not upon distances derived from those points. Size was estimated as the centroid size of the landmark configuration, which is simply the square root of the sum of the squared distance between each landmark and the centroid of the configuration (Bookstein, 1991). Centroid size was utilized because it is independent of the shape estimate except for the contribution of allometry (the interaction of size and shape). Antisymmetry was assessed utilizing the test for normality in PROC UNIVARIATE (SAS, 1999) as well as a test of Kurtosis (Zar, 1999). Fluctuating asymmetry (FA) was estimated using a mixed model analysis of

Table 2. Mixed-model ANOVA for the estimation of group-level FA

Effect	Expected Mean Square	Estimated Component
Sides (S)	$\sigma_m^2 + M\left\{\sigma_i^2 + [J/(S-1)]\sum a^2\right\}$	Directional asymmetry
Individuals (J)	$\sigma_m^2 + M\left(\sigma_i^2 + S\,\sigma_j^2\right)$	Size/Shape variation[1]
Interaction(I) (SxJ)	$\sigma_m^2 + M\,\sigma_i^2$	Antisymmetry, FA / # reps, Measurement error
Measurements (M)	σ_m^2	Measurement error

[1] In a Procrustes-based analysis this component represents shape variation and allometric variation (Size x Shape Interaction) since all individuals are scaled to unit centroid size prior to superimpositioning. In addition, for studies performing a Procrustes analysis on a structure with object symmetry, any size asymmetry will be included in this component.

variance (ANOVA) with side (left or right) as a fixed effect, individual as a random effect and the variance component of the interaction of side and individuals providing the measurement error-corrected group estimate of FA (Palmer and Strobeck, 1986; Table 2). Directional asymmetry was estimated to determine if differences in the magnitude of directional asymmetry among sites or areas confounded our fluctuating asymmetry estimate (Lamb *et al.*, 1990). Since we utilized a landmark-based approach, the ANOVA was modified for the requirements of geometric morphometrics and Procrustes methods (Klingenberg and McIntyre, 1998). The mammalian skull exhibits object symmetry (i.e. the plane of symmetry is contained within the object) and our landmark configuration included twelve sets of paired landmarks. To overcome the problems inherent in estimating shape with symmetric landmark configurations, the method of Klingenberg *et al.* (2002) was utilized to separate the symmetric shape estimate from the FA estimate. Both of the methods by Klingenberg and colleagues are extensions of the work of Goodall (1991), which assumes that variation among landmarks is equal, isotropic (i.e. non-directional) and independent. To assess homogeneity of variance we calculated the centroid of each landmark based upon the digitized points, calculated the squared distance of each point from the centroid, and summed those distances over all individuals. The result of the summing was four estimated variances around each landmark, one for each replicate. We then performed an ANOVA on the absolute value of each squared distance value from the mean value of all squared distances, which is analogous to a Levene's test of homogeneity of variances (Palmer and Strobeck, 2003). For visualization of the relative variances around each landmark we used a bubble plot. Since we were interested in visualizing the variance between individuals, and not

digitization error, we first calculated the best linear unbiased prediction (BLUP) (Robinson, 1991) of the x and y coordinate for each landmark and individual. The model for BLUP estimation utilized individual nested within site as a random effect. Independence of landmarks was assessed using a semivariogram based upon a spherical model with a spherical model of covariation (Piegorsch and Bailer, 1997). The isotropy of the digitized points around their centroid was assessed using a Rayleigh test for uniformity, with isotropy as the null hypothesis (Mardia and Jupp, 2000).

ANOVA calculations to estimate symmetry and BLUP were performed using the SAS® procedure MIXED with REML estimation, the semivariogram was calculated using the SAS® procedures VARIOGRAM and NLIN, and the among site and among area ANOVA's for centroid size and the Levene's test were performed using the SAS® procedure GLM (SAS, 1999). Procrustes superimposition was carried out using the tpsRelw, v. 1.31, program (Rohlf, 2003).

RESULTS

CENTROID SIZE

We first analyzed differences in the centroid size of skulls among sites within physiographic areas (Figure 7) utilizing mixed-model ANOVA with sites as a fixed effect and individuals nested within site as a random effect. Differences among sites were tested using the nested effect as the error term. Within the upper/middle coastal plain, deer from the SRS had significantly larger skulls compared to deer from Cedar Knoll ($F_{1,23} = 7.23$, $P = 0.013$). Within the lower coastal plain, there were no significant difference between the skull size of deer from Laurel Hill compared to the deer from Glynn and McIntosh Counties (Other) ($F_{1,12} = 3.72$, $P = 0.078$). Within the barrier island area, there was a

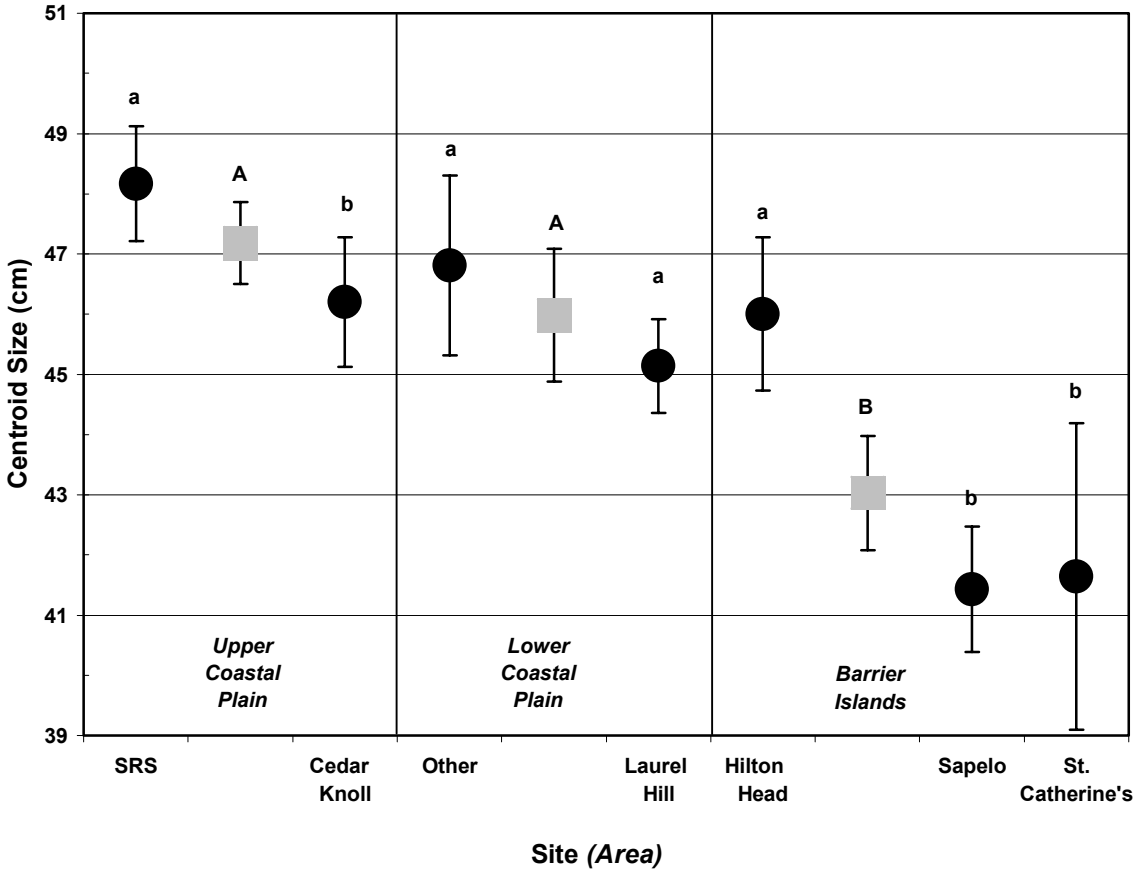

Figure 7. Least squared means and 95% confidence intervals of skull centroid size from white-tailed deer collected from the eight sampling sites (black circles) and the three physiographic regions (gray squares). Only seven sampling sites are represented since the site labeled Other represents the combination of the two individuals from Glynn Co., GA and the one individual from McIntosh Co., GA. Different letters represent significant differences between least squared means. Lowercase letters are for tests between or among sites within areas and uppercase letters are for tests among areas. A Bonferroni correction was applied to tests with more than two groups.

significant difference in skull size among the sites ($F_{2,19} = 15.52$, $P = 0.0001$) with deer collected from Hilton Head being significantly larger ($|t_{18}| = 5.44$, $P < 0.0001$ and $|t_8| = 3.00$, $P = 0.022$, respectively) compared to deer collected from Sapelo and St. Catherine's islands, which did not differ significantly in size ($|t_{12}| = 0.15$, $P = 1.000$).

Differences among physiographic areas (Figure 7) were tested utilizing two different mixed-model ANOVA. The first model set area as a fixed effect, sites nested within area as a fixed effect and individuals nested within site within area as a random effect. The second model differed in modeling sites nested within area as a random effect. Centroid size differed significantly among areas in the first model ($F_{2,54} = 26.57$, $P < 0.0001$) but did not differ in the second model ($F_{2,4.022} = 2.41$, $P = 0.205$). Centroid size also differed significantly as a function of sites nested within area ($F_{4,54} = 11.33$, $P < 0.0001$) and the same result obtained with either model.

VARIATION OF LANDMARKS

There was no evidence of heterogeneity of variance among landmarks ($F_{27,84} = 0.92$, $P = 0.590$; Figure 8). The midline points and the rostral points appeared to exhibit anisotropy (Figure 9) but the descriptive statistics and a Rayleigh test for circular uniformity showed no deviation from isotropy (Table 3). The variance around landmarks exhibited significant positive spatial autocorrelation for points less than 0.2 units apart (Figure 10).

SHAPE

Variation in shape among sites is illustrated in figure 11. Within the upper/middle coastal plain area white-tailed deer skulls sampled from Cedar Knoll exhibited significantly greater symmetric shape variation compared to deer skulls from SRS

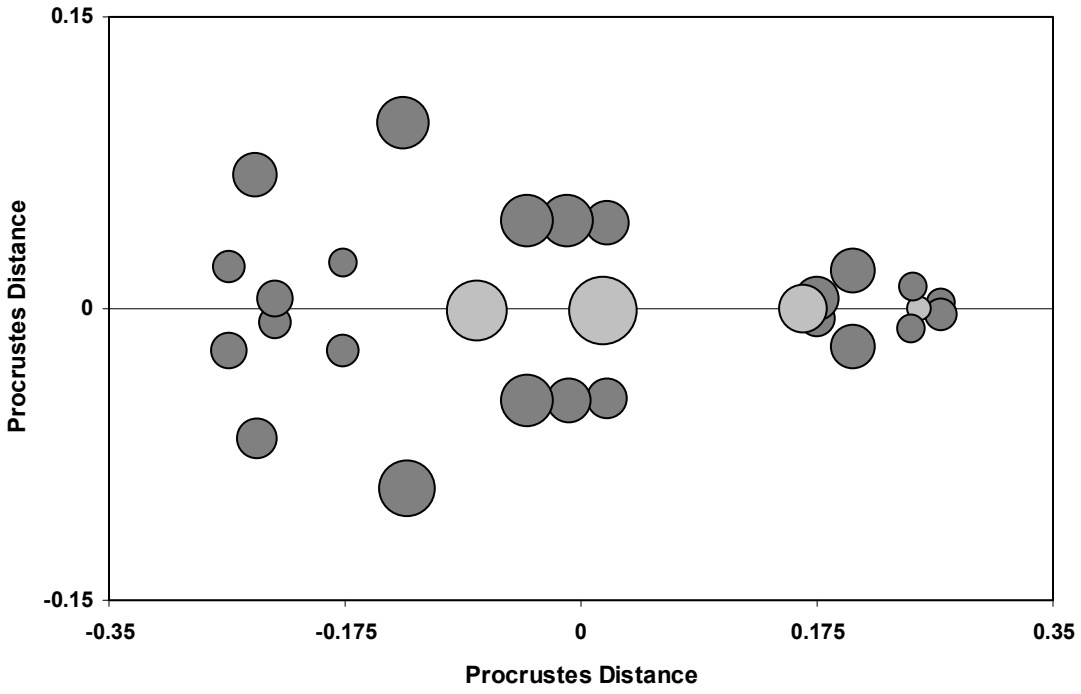

Figure 8. Bubble plot of sum-of-squared distances after Procrustes superimposition for the best linear unbiased prediction estimate for all individuals. The sum of the squared distances was calculated as the sum of the squared distance between each estimated point and the centroid of all estimated points for a landmark. Light gray bubbles represent the midline landmarks and the dark gray bubbles represent the paired landmarks. The area of the bubble represents the variation around a landmark relative to all other landmarks. Landmarks are as depicted in Figure 6. Procrustes distance is unitless.

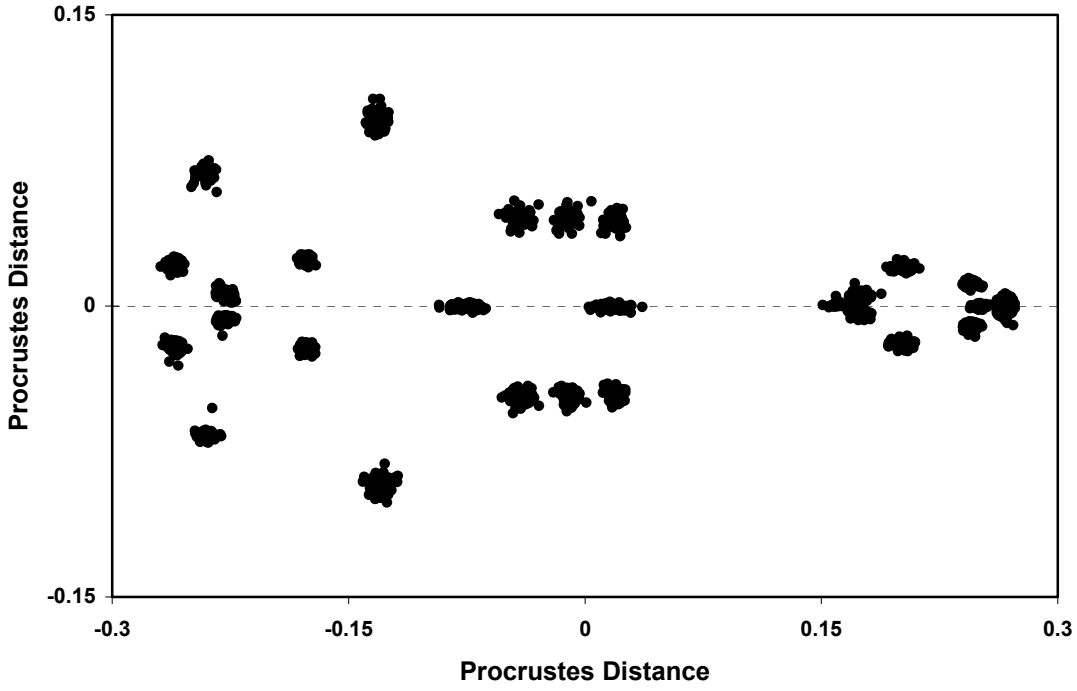

Figure 9. Scatter plot of the best linear unbiased prediction estimate for each of the 28 landmarks after Procrustes superimposition for all individuals. Each cloud consists of 61 points. Landmarks are as depicted in Figure 6 and their position would be at the centroid of each of the 28 clouds of points. Procrustes distance is unitless.

Table 3. The mean and median angle, mean length, angular deviation and results of a Rayleigh test for uniformity of best linear unbiased predictions for each of the 28 landmarks. Landmark numbers are as designated in Figure 6. The sample size for each landmark is 61.

Landmark	Mean Angle	Median Angle	Mean Length	Angular Deviation	Rayleigh Statistic	P
1	26.46	181.93	0.023	80.084	0.0107	0.9947
2	85.92	166.37	0.037	79.523	0.0269	0.9866
3	88.71	169.39	0.080	77.725	0.1278	0.9381
4	92.68	159.22	0.084	77.542	0.1422	0.9314
5	316.68	175.32	0.018	80.291	0.0065	0.9968
6	58.57	179.40	0.056	78.747	0.0615	0.9697
7	278.05	177.66	0.015	80.428	0.0043	0.9978
8	256.67	182.65	0.073	77.995	0.1080	0.9474
9	235.24	183.97	0.061	78.530	0.0735	0.9639
10	177.51	180.01	0.004	80.855	0.0004	0.9998
11	211.77	178.96	0.071	78.112	0.0999	0.9513
12	226.14	166.00	0.021	80.192	0.0084	0.9958
13	26.45	156.84	0.078	77.803	0.1219	0.9409
14	17.64	178.52	0.028	79.887	0.0156	0.9923
15	105.19	177.25	0.064	78.395	0.0816	0.9600
16	85.99	172.90	0.048	79.068	0.0455	0.9775
17	3.84	167.30	0.070	78.146	0.0976	0.9524
18	328.61	178.07	0.027	79.947	0.0140	0.9930
19	200.25	172.67	0.039	79.419	0.0308	0.9847
20	162.49	162.51	0.045	79.203	0.0395	0.9804
21	154.93	175.54	0.004	80.872	0.0003	0.9999
22	335.81	187.34	0.068	78.214	0.0931	0.9545
23	303.74	186.24	0.087	77.439	0.1506	0.9275
24	34.90	157.28	0.140	75.145	0.4002	0.8187
25	333.29	169.25	0.117	76.162	0.2749	0.8716
26	87.43	161.65	0.101	76.829	0.2054	0.9024
27	173.67	185.26	0.045	79.166	0.0411	0.9797
28	186.27	186.90	0.052	78.888	0.0541	0.9733

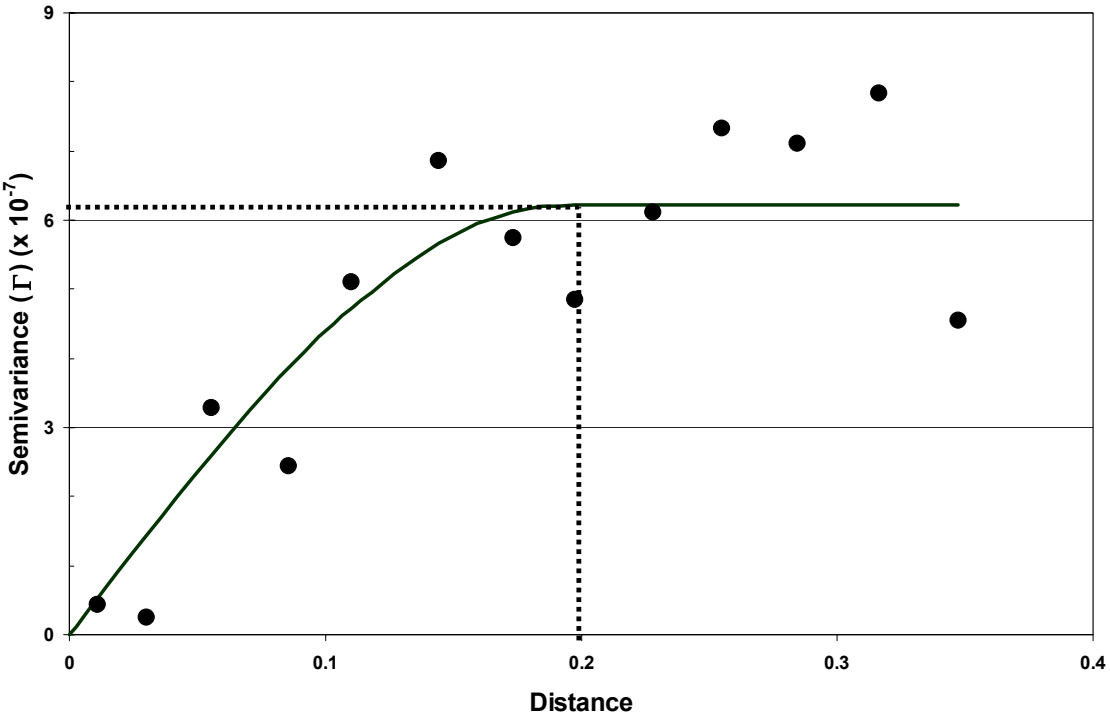

Figure 10. Semivariogram of sum-of-squared distances after Procrustes superimposition for the best linear unbiased prediction estimate for all individuals. The sum of the squared distances was calculated as described in figure 4. The horizontal dotted line represents the sill and the vertical dotted line the scale or range of the data. The nugget is zero.

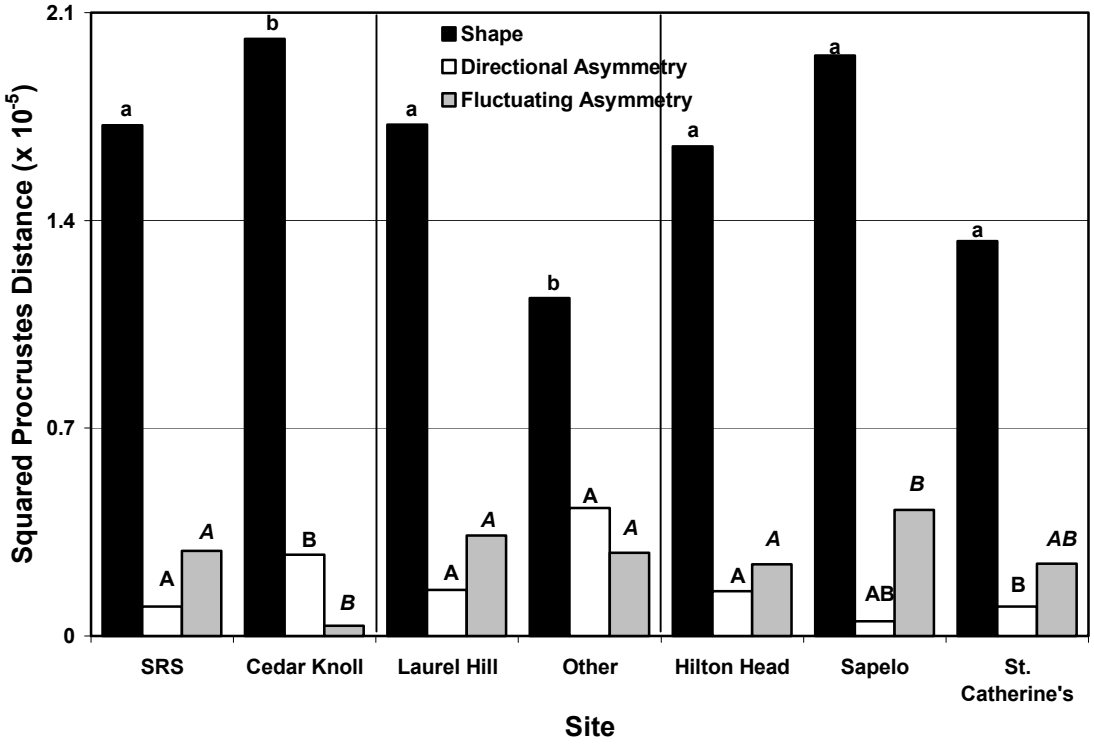

Figure 11. Variance components of Procrustes mean squares of symmetric skull shape, fluctuating asymmetry and directional asymmetry from white-tailed deer collected from the eight sampling sites. Only seven sampling sites are represented since the site labeled Other represents the combination of the two individuals from Glynn Co., GA and the one individual from McIntosh Co., GA. Different letters represent significant differences between variance components from an F-test (2 groups) or series of F-tests (3 groups). A Bonferroni correction was applied to the probability values of the associated F-tests for > 2 groups. Lowercase letters are for tests between or among sites for shape, uppercase black letters are for tests between or among sites for directional asymmetry and uppercase gray italic letters are for tests between or among sites for fluctuating asymmetry.

($F_{260,338}$ = 1.23, P = 0.036). Within the lower coastal plain area white-tailed deer skulls sampled from Laurel Hill exhibited significantly greater symmetric shape variation compared to skulls from Glynn and McIntosh Co. (Other) ($F_{260,52}$ = 1.48, P = 0.044). None of the barrier island samples of deer skulls differed in symmetric shape variation from each other (HH/SAP; $F_{286,182}$ = 1.22, P = 0.071: HH/STC; $F_{186,26}$ = 1.22, P = 0.278: SAP/STC; $F_{286,26}$ = 1.50, P = 0.109).

Variation in shape among physiographic areas is illustrated in figure 12. White-tailed deer sampled from the lower coastal plain exhibited significantly lower symmetric shape variation compared to deer sampled from either the upper/middle coastal plain ($F_{624,338}$ = 1.24, P = 0.014) or barrier islands ($F_{546,338}$ = 1.28, P = 0.007). White-tailed deer sampled from the upper/middle coastal plain did not differ in symmetric shape variation compared to deer sampled from barrier islands ($F_{546,624}$ = 1.03, P = 0.345).

SYMMETRY

There was no deviation from normality nor was there a deviation from the normal expectation for kurtosis for the distribution of left-minus-right differences.

Directional Asymmetry

Variation in directional asymmetry among sites is illustrated in figure 11. Within the upper/middle coastal plain area white-tailed deer skulls sampled from Cedar Knoll exhibited significantly greater directional asymmetry compared to deer skulls from SRS ($F_{26,26}$ = 2.12, P = 0.030). Within the lower coastal plain area white-tailed deer skulls sampled from Laurel Hill and deer skulls from Glynn and McIntosh Co. (Other) did not differ in directional asymmetry ($F_{26,26}$ = 1.30, P = 0.252). Deer collected from Hilton Head exhibited significantly greater directional asymmetry compared to those collected

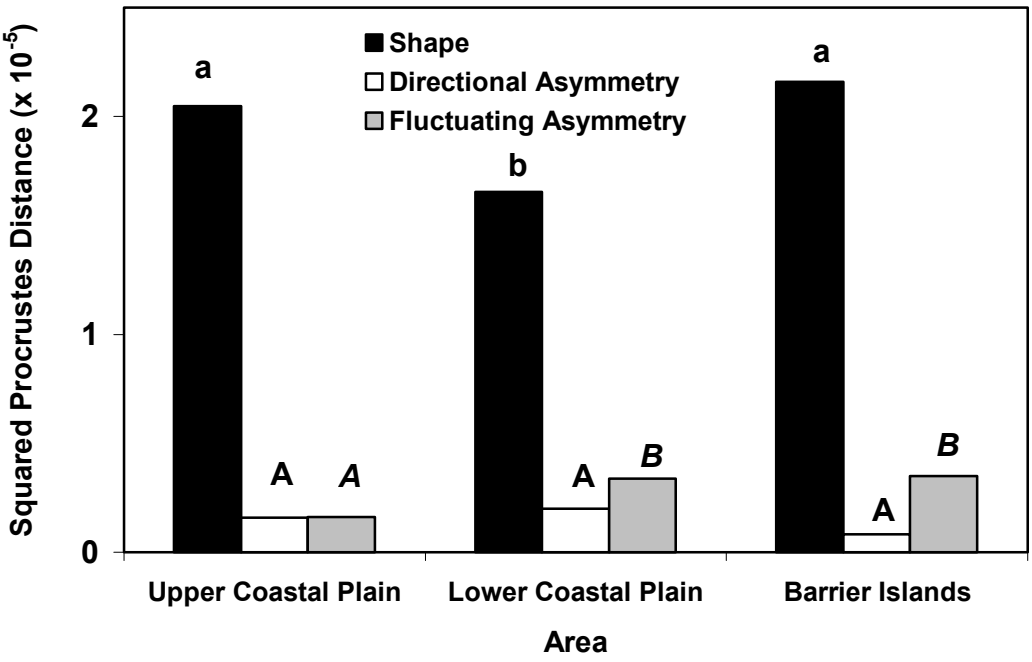

Figure 12. Variance components of Procrustes mean squares of symmetric skull shape, fluctuating asymmetry and directional asymmetry from white-tailed deer collected from the three physiographic areas. Different letters represent significant differences between variance components from a series of F-tests (3). A Bonferroni correction was applied to the probability values of the associated F-tests. Lowercase letters are for tests among areas for shape, uppercase black letters are for tests among areas for directional asymmetry and uppercase gray italic letters are for tests among areas for fluctuating asymmetry.

from St. Catherine's Island ($F_{26,26} = 3.29$, P = 0.002). Deer samples from Hilton Head did not differ from those collected from Sapelo in directional asymmetry ($F_{26,26} = 1.43$, P = 0.184) nor did deer collected from Sapelo differ from those collected from St. Catherine's ($F_{26,26} = 2.30$, P = 0.019).

Variation in directional asymmetry among physiographic areas is illustrated in figure 12. None of the physiographic areas differed significantly from any other in the amount of directional asymmetry measured in sampled deer (UCP/LCP; $F_{26,26} = 1.40$, P = 0.198: UCP/ISL; $F_{26,26} = 2.05$, P = 0.036: LCP/ISL; $F_{26,26} = 1.47$, P = 0.168).

Fluctuating Asymmetry

Variation in fluctuating asymmetry among sites is illustrated in figure 11. Within the upper/middle coastal plain area white-tailed deer sampled from Cedar Knoll exhibited significantly less fluctuating asymmetry compared to those from SRS ($F_{260,338} = 1.96$, P < 0.0001). Within the lower coastal plain area white-tailed deer sampled from Laurel Hill did not differ in fluctuating asymmetry compared to those sampled from Glynn and McIntosh Co. (Other) ($F_{260,52} = 1.26$, P = 0.171). Deer collected from Hilton Head exhibited significantly less fluctuating asymmetry compared to those collected from Sapelo ($F_{286,182} = 1.65$, P = 0.0001). Deer samples from Hilton Head did not differ from those collected from St. Catherine's island in fluctuating asymmetry ($F_{182,26} = 1.08$, P = 0.432) nor did deer collected from Sapelo differ from those collected from St. Catherine's ($F_{286,26} = 1.78$, P = 0.040).

Variation in fluctuating asymmetry among physiographic areas is illustrated in figure 12. White-tailed deer sampled from the upper/middle coastal plain exhibited significantly lower fluctuating asymmetry compared to deer sampled from either the lower coastal

plain ($F_{624,338} = 1.24$, P = 0.012) or barrier islands ($F_{546,624} = 1.20$, P = 0.013). White-tailed deer sampled from the lower coastal plain did not differ in fluctuating asymmetry compared to deer sampled from barrier islands ($F_{546,338} = 1.03$, P = 0.371).

ODOCOILEUS VIRGINIANUS HILTONENSIS

The centroid size of white-tailed deer skulls from Hilton Head were not significantly smaller than white tailed deer skulls from either the SRS ($|t_{20}| = 2.82$, P = 0.140), Cedar Knoll ($|t_{17}| = 0.24$, P = 1.000), Laurel Hill ($|t_{17}| = 1.07$, P = 1.000), or Glynn and McIntosh Counties (Other) ($|t_{9}| = 0.69$, P = 1.000) (Figure 7). To compare the skull shape between the two subspecies we can compare the consensus configurations of *O. v. virginianus* and *O. v. hiltonensis*. Figure 13 illustrates the consensus configuration after Procrustes superimposition for *O. v. hiltonensis* and mainland (upper and lower coastal plain) *O. v. virginianus*. Deer from Hilton Head tend to be broader compared to mainland deer. This is most evident at the maxilla/premaxilla suture (points 6 and 7), the squamosal/jugal suture (points 19 and 22), the paraoccipital process (points 23 and 26) and at the intersection of the occipital with the anterior margin of the foramen magnum (points 24 and 25).This can also be seen to a lesser degree in several other paired landmark points. In addition the palatine extends further posteriorly in the mainland *O. v. virginianus* subspecies (point 18).

DISCUSSION

White-tailed deer collected from barrier islands exhibited a significantly smaller skull size compared to deer from either the lower coastal plain or the upper/middle coastal plain. The model with sites nested within area as a fixed effect is highly significant whereas the random effects model is not. The true model is more likely to be closer to the

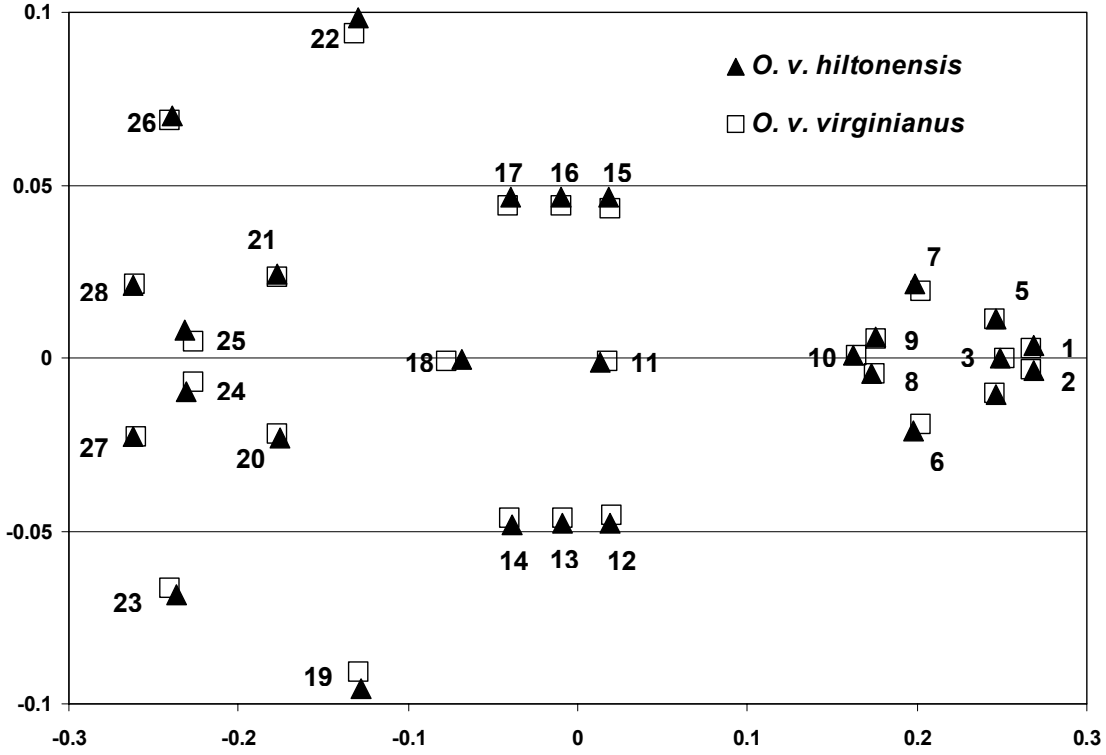

Figure 13. Consensus configuration after Procrustes superimposition for white-tailed deer collected from Hilton Head Island (n=8) and mainland deer from the upper and lower coastal plain (n=39)

fixed effects model for the following reasons. First, the random effects model uses a very conservative denominator degrees-of-freedom for the F-test. Thus the low sample size populations (Other and St. Catherine's) cause an extreme reduction in the Sattherthwaite approximated degrees-of-freedom. We are currently gathering more data from these populations to assess this effect. Second, in the random effects model, we are comparing the size variation between areas to that within areas. Although, this sounds correct at first (and is statistically) the spatial scale within areas and between is not comparable. The more serious problem is that spatial and temporal scales are not independent. Thus, the comparison involves skull variation generated by underlying processes acting across different spatio-temporal scales. The between area size difference may represent a longer time-scale effect compared to differences among sites within areas although this may not be the case for barrier islands.

Even though our primary interest is in form differences among deer from the three physiographic areas, the variation in form between sampling sites within areas is also of interest. There is significant between site heterogeneity in skull size within both the upper/middle coastal plain area and the barrier islands. These differences likely result from two causes. First, the underlying ecological and evolutionary processes structuring the variation between sites act over relatively shorter time scales compared to the processes structuring the variation among physiographic areas. Anthropogenically influenced processes such as deer management strategies and recent ecological habitat changes are likely candidates and described below. Second, comparisons among sites have lower sample sizes and thus we expect variation to be increased compared to among

area comparisons. We are currently increasing our sample sizes to address the influence small sample sizes are having on between site variability.

Within the upper/middle coastal plain, SRS deer exhibit a significantly larger skull size compared to those from Cedar Knoll hunt club. This is most likely a function of the differing hunting rules between the two sites. The goal of deer management on the SRS is to keep the herd size small to minimize deer-car accidents (Novak *et al.*, 1991), whereas the deer herd on Cedar Knoll (and Laurel Hill) is managed to optimize trophy quality (P. Johns, personal communication). There is no special doe permitting on the SRS and hunters are instructed to kill any deer or hog that is driven past their stand. Trophy deer management focuses the largest hunting pressure on mature bucks and limits the take on does and yearling bucks. Thus, herds managed for trophy deer tend to exhibit a higher density and a different sex-age structure compared to those that are not (McCullough, 1984). Although, population size estimates for the SRS are available (Novak *et al.*, 1991), estimates for Cedar Knoll are not. Therefore, at this time the reasons for the skull size differences between SRS and Cedar Knoll remain as hypotheses.

Within the barrier island area, deer collected from Hilton Head Island exhibited a significantly larger skull size compared to deer collected from Sapelo and St. Catherine's Islands. The interior of St. Catherine's Island is closed to the public, with only the beach areas having general access. Sapelo Island is reachable only by ferry and is a national estuarine reserve. Both St. Catherine's and Sapelo Islands are largely undeveloped for residential use. Hilton Head Island, on the other hand, is a highly developed resort community. The increased residential horticultural plantings, irrigation, and fertilization by residents has vastly improved the forage quality on Hilton Head Island compared to

less developed barrier islands (Caudell and Warren, 1997). Since barrier islands are not completely isolated from the mainland like oceanic islands, the presumed cause of the smaller mass and structural size of barrier island deer has been poorer forage quality compared to mainland areas (Tall Timbers Research Inc., 1992). We are currently increasing our sample of recent animals from Hilton Head Island and examining museum specimens to investigate any recent changes in skull size of deer from the island coincident with the forage quality changes.

Goldman and Kellogg (1940) described the skull characteristics of *Odocoileus virginianus hiltonensis* as follows: "Skull.—Similar in general to that of *Odocoileus virginianus virginianus* but smaller; vault of brain case more highly arched; frontal profile more convex; suproccipital region narrower, tending to project farther posteriorly on the median line over foramen magnum; nasals less depressed anteriorly, narrower posteriorly, and more encroached upon by lachrymal vacuities; dentition relatively about as in *virginianus*". In our data set the skull size of female deer from Hilton Head Island were not significantly smaller than those collected from any of the other mainland sites. In addition, the skulls of female deer from Hilton Head were wider compared to the skulls of mainland deer. At this point we are reticent to conclude that deer inhabiting Hilton Head Island are not a unique subspecies for several reasons. First, we did not examine most of the skull characteristics that Goldman and Kellogg (1940) examined, the type specimen is a male specimen, and the final determination should be done in a focused study using several different genetic and morphological markers. Nevertheless, we conclude that at this point the evidence for subspecific status for *O. v. hiltonensis* is weak.

The largest component of shape variation was the symmetric component, which was significantly greater than directional asymmetry or fluctuating asymmetry in all areas. White-tailed deer collected from the lower coastal plain area exhibited significantly lower symmetric shape variation compared to deer collected from the upper/middle coastal plain and barrier islands. Thus deer within the lower coastal plain were more similar to each other in symmetric shape compared to deer from either the upper/middle coastal plain or barrier islands.

Compared to the lower coastal plain, barrier islands represent smaller, more fragmented and slightly more isolated habitats (Tall Timbers Research Inc., 1992). Thus barrier islands may support smaller, more rapidly evolving populations that are influenced to a larger extent by the dynamics of colonization and extinction processes. If this is the case then the barrier island deer may represent a more heterogeneous population compared to the mainland herds. Unlike size, symmetric shape variation did not differ among the three barrier island deer samples. Thus, whatever the underlying cause of the greater skull size of Hilton Head Island deer compared to those from Sapelo and St. Catherine's Islands, it did not affect shape, or affected it to a lesser degree so that larger sample sizes or longer time periods would be needed for differences to become manifest.

Fragmentation is not a viable explanation for the shape difference between lower coastal plain compared to upper/middle coastal plain deer. Populations in the upper/middle coastal plain region of the southeast underwent large population depressions and extirpations during the late 19th and early 20th centuries, followed by either restocking efforts or rapid population increases, whereas those in the lower coastal

plain were less impacted (Blackard, 1971; Hillestad, 1984). In fact, the major source of reintroduced deer in the upper/middle coastal plain and piedmont of South Carolina was the Francis Marion forest in the lower coastal plain (Hillestad, 1984). The history of the deer herd on the SRS is well known and exhibits a typical pattern for a protected population. Prior to the formation of the SRS in 1951, white-tailed deer were uncommon on the agricultural lands of the area (Jenkins and Provost, 1964). Once the site was closed to the public and the lands reverted to either old-field or planted pine, the deer herd expanded in size and range from the swamp herds until a site-wide hunt was deemed necessary in 1965 (Urbston, 1967). Such spatio-temporal variation may have acted to increase variation of quantitative genetic traits such as symmetric shape, which are likely to have significant variance components due to environment and gene-by-environment interactions (Roff, 1997). The history of the white-tailed deer herd on Cedar Knoll is not as well known. Since it is relatively close to the SRS, the expansion of the SRS herd likely also impacted the deer herd at this location. In addition, since Cedar Knoll is a private hunt club, restocking efforts may have occurred in an attempt to increase the body mass of individuals (P. Johns, personal communication). Restocking efforts should increase the genetic variance component of the total phenotypic variance for a quantitative trait. In fact, within the upper and lower coastal plain areas, Cedar Knoll and Laurel Hill, respectively exhibited a larger amount of symmetric shape variation compared to deer collected from either the SRS (upper/middle coastal plain) or Glynn and McIntosh Co. (lower coastal plain). Whether, this is due to restocking efforts by the hunt clubs is not known at this time, but it remains an intriguing possibility.

Directional asymmetry did not differ among areas and thus was unlikely to confound our estimates of fluctuating asymmetry. Fluctuating asymmetry was significantly lower in deer collected from the upper/middle coastal plain area compared to those collected from either the lower coastal plain or the barrier islands. If we assume that fluctuating asymmetry is reflecting the underlying stability of the developmental process (Møller and Swaddle, 1997; Polak, 2003) then deer from the upper/middle coastal plain exhibit significantly greater developmental stability compared to those from either the lower coastal plain or barrier islands. There are numerous potential causes of increased developmental instability (Møller and Swaddle, 1997), but all can be classified as either increases of environmentally induced-stress or decreases in the buffering ability of the developmental process resist the effects of environmental stress. The lower value of fluctuating asymmetry within the upper/middle coastal plain area is driven primarily by the very low value for deer collected from Cedar Knoll. One potential causative agent may be related to increased genetic variability due to restocking at the hunt club. Purdue *et al.* (2000) found that deer from Cedar Knoll hunt club exhibited a much higher mtDNA haplotype diversity ($h = 0.67$) compared to deer collected from the SRS ($h = 0.27$) but the sites did not differ significantly in direct count heterozygosity for allozyme loci ($H = 0.24$ and $H = 0.23$). This is the expected pattern for populations which have experienced a relatively recent restocking, given the faster evolutionary dynamics of mtDNA (Chesser and Baker, 1996), the greater philopatry of female white-tailed deer (Nelson and Mech, 1987; Nixon *et al.*, 1991), and the sex and age structure of harvest from a herd managed for trophy quality (Deyoung, 1990; Jenks *et al.*, 2002). The increased symmetric shape variation of deer skulls collected from Cedar Knoll compared to white-tailed deer skulls

collected from the SRS is also consistent with the restocking hypothesis. Nevertheless, at this time there is no direct record of restocking at Cedar Knoll hunt club, and thus restocking at Cedar Knoll remains a hypothesis.

Fluctuating asymmetry did not differ between sites within the lower coastal plain but did differ among barrier island sites. Deer collected from Hilton Head Island had significantly lower fluctuating asymmetry compared to those from Sapelo but not from deer collected from St. Catherine's Island. This difference is consistent with the better foraging habitat on Hilton Head discussed previously in discussing the relatively larger skull size of Hilton Head deer compared to those from Sapelo and St. Catherine's Islands. Because of the higher quality forage on Hilton Head, the deer herd living there should experience much less nutritional stress compared to deer living on relatively undeveloped barrier islands such as Sapelo and St. Catherine's. The lack of a difference in fluctuating asymmetry for deer skulls from Hilton Head Island compared to those from St. Catherine's Island is most likely a function of the low sample size from St. Catherine's Island.

The covariation of form components among the three physiographic areas is an interesting question as it can provide insight into the evolutionary processes structuring form variation. Size and fluctuating asymmetry do appear to show a degree of negative covariation. That is structurally larger animals exhibit reduced fluctuating asymmetry. However, the observed covariation was not very strong in this study. Whereas mainland deer (both upper and lower coastal plain) were larger than barrier island deer, deer from the upper/middle coastal plain exhibited lower levels of fluctuating asymmetry compared to both lower coastal plain and barrier island deer. Symmetric shape variation exhibited a

third pattern with deer collected from the lower coastal plain exhibiting reduced variation compared to deer from both the upper/middle coastal plain and barrier islands. In addition, we have no *a priori* expectation of the direction of covariation between symmetric shape variation and either size or fluctuating asymmetry. Although we could have utilized a Mantel test (Mantel, 1967) to compare the covariance matrices of the form components, this would have been an extremely weak test and only served to provide the impression of more precision without providing further quantitative information. The scale of our question was at the level of physiographic areas and a Mantel test using 3 x 3 matrices would have had little chance of showing significant correlations due to the small size of the matrices. Utilizing matrices with all seven sites begins to approach the minimal necessary size but, as discussed earlier, sites represented a different spatio-temporal scale compared to physiographic areas. Thus processes acting to structure variation between sites were likely to differ in both kind and magnitude from those acting at the scale of physiographic area. The potential differences in processes among scales could have been partially addressed by modifying the permutations to keep sites within areas together, however we would then be back to performing permutations on a roughly 3 x 3 matrix.

Form is expressed at the scale of an object or individual (Slice *et al.*, 1996) but its components can be summarized at any larger scale consisting of groups of objects or individuals. Thus, an individual-based model should provide a more appropriate framework for analyzing covariation among form components in more detail and should circumvent "sample size" problems encountered when performing a group-level analysis. Such models can use more powerful statistical techniques such as path analysis to derive

both predictive and inferential models (Kingsolver and Schemske, 1991; Scheiner *et al.*, 2000). The appropriate scale for analysis is a function of the exact hypothesis to be tested as well as the scale imposed limitations on the raw data. In the present analysis our primary spatio-temporal scale was at the level of physiographic areas. The data itself was limited in spatial extent to the groups of individuals at sites. Limitations in our knowledge of exact collection locations of individuals for all sites except the SRS and the known vagility of white-tailed deer limited our ability to perform an individual-based analysis for analyzing the covariation of form components. At the spatial scale of sites and areas utilized in this study, female deer are fairly philopatric. However, analysis at scales smaller than the sites defined here are compromised by no small-scale spatial information from hunters. Thus given the size of female home ranges in the south (63 ± 17 ha; Ivey and Causey, 1981), the use of dogs to drive deer in many areas (Scribner *et al.*, 1985), and the potential for even females to move several kilometers even without pressure from hunting (Kammermeyer and Marchinton, 1976), an individual-based model was deemed inappropriate for this data set.

The components of skull form do vary for white-tailed inhabiting different physiographic areas of South Carolina and Georgia. Size and fluctuating asymmetry do spatially covary to a degree but symmetric shape appears relatively spatially independent relative to size and fluctuating asymmetry. Deer collected from barrier islands are smaller than mainland deer and together with coastal plain deer exhibit increased fluctuating asymmetry compared to deer collected from the upper/middle coastal plain. Deer collected from the lower coastal plain exhibit decreased symmetric shape variation compared to animals from either the upper/middle coastal plain or barrier islands.

Components of form for sites within areas varied on a smaller spatio-temporal scale and appear to be influenced more by relatively recent processes such as hunting regimes, restocking efforts and habitat changes associated with anthropogenic development. Thus, form analysis provides useful information for evolutionary (phenotypic variance and rates of evolution), ecological (individual and population growth) and management (hunting regimes and restocking efforts) inferences concerning white-tailed deer. However, the information at the group level is limited. Since form is the property of an individual, it is at that level where the components of form can be analyzed to provide an estimate of the composite trait, form.

CHAPTER 3

THE USE OF BEST LINEAR UNBIASED PREDICTION (BLUP) FOR ESTIMATING INDIVIDUAL FLUCTUATING ASYMMETRY: FORM AND FUNCTION MEETS STATISTICS

INTRODUCTION

Fluctuating asymmetry has become a popular surrogate measure for estimating developmental stability, mostly because of the apparent ease of estimation (Markow, 1994; Møller and Swaddle, 1997; Polak, 2003). As such, FA has been used as an indicator of developmental effects of genetic and/or environmental stress, an effects biomarker of performance, a signal for sexual selection and a fitness correlate (Møller and Swaddle, 1997). However, heterogeneity in results among studies (Leung and Forbes, 1997; Møller, 1997; Møller and Thornhill, 1997) has called into question the utility of using FA as a biomarker of stress (Hoffmann and Woods, 2003; Leung *et al.*, 2003). Theoretical models of the relationship between FA and developmental stability also come to different conclusions regarding the utility of FA as a surrogate measure of developmental stability (Gangestad and Thornhill, 1999; Klingenberg and Nijhout, 1999; Houle, 2000) suggesting additional empirical studies may be necessary before the relationship between FA and developmental stability. Unfortunately, fluctuating asymmetry is not as easily estimated as the earliest practitioners thought and much of the variation in outcomes of studies utilizing FA may be due to differences in the magnitude

of error associated with the FA estimates (Palmer and Strobeck, 1986; Palmer and Strobeck, 1992; Møller and Swaddle, 1997; Palmer and Strobeck, 2003; Van Dongen e*t al*., 2003)

Analyses of FA have a long history going back to Ludwig (1932) and Mather (1953) with a formal description by Van Valen (1962) that defined FA as a population characteristic and formally defined directional asymmetry (DA) and antisymmetry (AS). If only FA is present, a distribution of left minus right differences should be normally distributed with mean zero and a variance equal to the magnitude of FA (Palmer and Strobeck, 1986). Directional asymmetry will cause the mean to be displaced to the right or left of zero while antisymmetry will cause the distribution to deviate from normality usually by causing the distribution to be platykurtic (Palmer and Strobeck, 1986). Unfortunately, many early studies on FA failed to account for either the confounding effects of other forms of asymmetry or measurement error (ME) on estimated FA. Palmer and Strobeck (1986) made clear both the magnitude of the measurement error problem as well as a solution for group-level FA estimates. Briefly, since FA is a difference between sides it is usually 1 or 2 orders of magnitude smaller than the character itself. Thus a measurement error that is 1% of the original character may be of the same magnitude as FA and represent ME of almost 100% relative to FA. Levels of ME of this magnitude are not unreasonable as they have been reported in the literature (Greene, 1984; Palmer, 1996). Palmer and Strobeck (1986) suggested the use of a mixed-model analysis of variance (ANOVA) with repeated measurements on individuals with side as a fixed effect, individuals as a random effect and the variance component for the interaction of

side and individual providing a group-level estimate of FA corrected for ME (Table 4). Part of the heterogeneity among group-level FA analyses undoubtedly results from differential success in removing ME from estimates of FA among studies.

More recently, the interest has shifted from group-level FA to individual-level FA, or more appropriately, individual left/right differences (Van Dongen *et al.*, 2003). At first, this may seem like a paradox, since FA has previously been defined as the variance of left/right differences for a group of individuals. Møller and Swaddle (1997) provide a nice explanation of asymmetry as a population statistic and an individual property, as well as some examples where individual-level analyses are more appropriate than group-level analyses. The argument is similar to that of fitness, fitness itself is a property of individuals as replicators of genes but is relative to, and can be estimated at the level of, a group or population (Futyma, 1998). The usual way individual-level FA values are estimated is as either signed (Palmer and Strobeck, 2003) or unsigned (Swaddle *et al.*, 1994) left/right differences. If repeated measures are taken, arithmetic means of the replicates are utilized as the best estimate of FA. However, even with repeated measures, these differences are inflated by measurement error, and thus are biased estimates of FA (Palmer and Strobeck, 2003). In addition, individual left/right differences when interpreted as individual FA estimates become random effects whereas simple arithmetic means are only appropriate for fixed effects (Robinson, 1991).

Recently Van Dongen and colleagues (Van Dongen *et al.*, 1999; 2003) have developed an unbiased estimate of individual-level FA using a multi-trait mixed model regression with restricted maximum-likelihood (REML) estimation. The multi-trait mixed model differs from the mixed model ANOVA described above by parameterizing

Table 4. Mixed-model ANOVA for the estimation of group-level FA

Effect	Expected Mean Square	Estimated Component
Sides (S)	$\sigma_m^2 + M\left\{\sigma_i^2 + [J/(S-1)]\sum a^2\right\}$	Directional asymmetry
Individuals (J)	$\sigma_m^2 + M\left(\sigma_i^2 + S\,\sigma_j^2\right)$	Size/Shape variation
Interaction(I) (SxJ)	$\sigma_m^2 + M\,\sigma_i^2$	Antisymmetry, FA / # reps, Measurement error
Measurements (M)	σ_m^2	Measurement error

side as a continuous random covariate rather than as a fixed effect with two values (left and right). Parameterizing side as a continuous covariate, the intercept side estimates the amount of directional asymmetry and the slope provides an unbiased estimate of FA for an individual. Although, the model is appropriate from a statistical viewpoint, treating side as a continuous covariate is not realistic biologically. It places the variation, which is biologically among individuals, among traits within an individual. If a single trait analysis is performed the among individual variation is moved into the between side component within individuals. In addition, the multi-trait mixed model forces one to run separate models for group-level and individual-level FA, which is unnecessary.

Because of the relationship between individual- and group-level variance components, the problem of estimating FA for an individual bears a striking resemblance to the estimation of breeding value in quantitative genetics (Lynch and Walsh, 1998). An individual's breeding value is the sum of the additive effects of its genes. In practice, it only exists in relation to a group as it is calculated by mating the individual to many randomly chosen individuals and subtracting the offspring mean from the group mean and multiplying by two. Individual-level FA, and its relationship to ME, is similar since ME occurs at the individual-level but can only be removed at that level in reference to the group-level ME and FA. The currently favored methodology for estimating breeding value is through the use of best linear unbiased predictors (BLUP) (Robinson, 1991; Lynch and Walsh, 1998). Best linear unbiased predictor methodology should allow the estimation of individual-level FA that is unbiased and corrected for ME. In addition

BLUP methodology exists within in a well-established statistical framework and does not require additional models or parametric assumptions to be made over and above the standard mixed model ANOVA assumptions.

The objective of this paper is to provide a method of estimating individual-level FA values that is unbiased and not inflated by ME through the use of BLUP in a mixed-model analysis with REML estimation. In this way, the choice of analysis level (group or individual) can be based upon the level that is appropriate for the question and not upon the magnitude of ME present in the data. The efficacy of BLUP estimates of individual FA is evaluated using two data sets. A simulated data set is utilized to assess the accuracy and the efficiency of BLUP estimates compared to simple arithmetic means averaged over replicate measurements. An unpublished data set for hybridization in *Gambusia* is used to compare individual analysis using simple arithmetic means to BLUP FA values.

MATERIALS AND METHODS

BEST LINEAR UNBIASED PREDICTION

Robinson (1991) provides a very thorough derivation of BLUP estimates from frequentist and Bayesian perspectives as well as providing example applications of BLUP. Simply put, a BLUP is a random effects analog to a fixed effects arithmetic mean. The BLUP differs in that it is a regression of the individual value towards the group mean based upon the variance components of the relevant model effects (Littell *et al.*, 1996). Thus a BLUP is a shrinkage estimator, which shrinks individual values toward the overall mean consistent with the ratio of the relevant variance components. The attenuation of the shrinkage of extreme means by the prior knowledge of the underlying variability is an inherently Bayesian approach which has the effect of reducing data misinterpretation.

For the mixed model ANOVA of FA illustrated in Table 4, the shrinkage estimator (Mood, 1950; Littell *et al.*, 1996) is:

(1) $$\hat{\mu}_i^S = \hat{\mu} + \frac{\hat{\mu}_i + \hat{\mu}}{\hat{\sigma}_I^2 / \left[\left(\hat{\sigma}_I^2 + \hat{\sigma}_W^2\right) / N\right]}$$

Where,

$\hat{\mu}_i^S =$ The shrinkage estimator for the ith individuals left/right difference
$\hat{\mu} =$ The overall left/right difference
$\hat{\mu}_i =$ The ith individuals left/right difference
$\hat{\sigma}_I^2 =$ The variance component for left/right differences between individuals
$\hat{\sigma}_W^2 =$ The variance component for left/right differences within individuals
$N =$ The number of observations per individual

The BLUP estimates for individual left/right differences are actually shrunk too much, since the model shrinks the estimates for each side independently, and need to be corrected as:

(2) $$\hat{\mu}_i^C = \hat{\mu}_i^S x \sqrt{\frac{|\hat{\mu}_i|}{|\hat{\mu}_i^S|}}$$

where,

$\hat{\mu}_i^C =$ The corrected shrinkage estimator for the ith individuals left/right difference

Formula 2 preserves the sign of the original estimator and should be utilized unsimplified for signed differences but can be simplified if unsigned differences are required. Utilizing formula 2 also allows a single analysis for both group and individual measurement corrected FA estimates.

SIMULATION DATA

A simulated data set was generated utilizing a modification of the additive model proposed by Palmer and Strobeck (1992). The Palmer and Strobeck model included terms for mean character size, character size variation, directional asymmetry, antisymmetry, variation in DA (sDA) and developmental noise of the right and left side. An additional term for ME was added to the model utilized in this analysis. Character size variation was modeled using a uniform distribution (IMSL routine DRNUN) while all other variance terms were modeled as normal variates (IMSL routine DRNNOR) and scaled appropriately to the required magnitude (Microsoft, 1995). Developmental noise (FA) was added independently to each side among individuals while ME was added independently to each side among replicates within individuals. Thus, true FA only varied among individuals whereas ME varied among replicates and individuals. The model parameters and realized values are listed in Table 5. Although 10,000 individuals were generated, BLUP's were generated on 100 sets of 100 individuals for computational reasons as well as to allow more reasonable standard deviation estimates. It is unlikely that many FA studies would have a sample size of 10,000. In essence the data are analyzed as 100 sampling events of 100 individuals from a population of 10,000. All data were generated using FORTRAN 90 and BLUP's were estimated using the SAS® procedure MIXED with REML estimation (SAS Institute Inc., 1999).

GAMBUSIA HYBRIDIZATION DATA

Hybridization in endangered species is an important conservation issue, and is the source of both political and scientific controversy (O'Brien *et al.*, 1990; Lehman *et al.*, 1991; Bullini, 1994). Anthropogenically induced hybridization between endangered

Table 5. Model parameters and realized values for simulated data using the modified additive model of Palmer and Strobeck (1992).

Parameter	Expectation	Realized Value
Number of Individuals	10000	10000
Number of Replicates	10	10
Mean Trait Size	12.50	12.497
Trait Size Variation	3.00	2.980
Antisymmetry (AS)	0.00	0.000
Directional Asymmetry (DA)	0.00	0.000
Variation in DA (sDA)	0.00	0.000
Fluctuating Asymmetry	0.25	0.256
Measurement Error	0.25	0.253

species and closely related congeners has become a serious problem in the conservation of biodiversity. Data for a relatively recent hybrid zone between the endangered Clear Creek Gambusia (*Gambusia heterochir*) and the more common western mosquitofish (*G. affinis*) are analyzed. The Clear Creek Gambusia is endemic to the headwaters of Clear Creek in central Texas (Hubbs, 1957; Hubbs, 1959; Hubbs, 1971; Edwards and Hubbs, 1985). Individual *Gambusia affinis*, *G. heterochir* and their hybrids were collected between 26 August 1983 and 21 February 1987 in 5 sites above and 2 sites below a farm pond dam on Clear Creek, Menard County, Texas (30º 55' N, 100º 57' 30" W); (Edwards and Hubbs, 1985). The collections have been maintained at the Texas Memorial Museum at the University of Texas at Austin. Individuals were stored unsorted and uncatalogued with regard to sex and hybrid status.

Individuals were sorted according to sex and age and given a unique identification code. Each adult individual was then scored for a series of phenotypic traits described by Hubbs (1959). The hybrid index scores were totaled and the distributions analyzed to determine the range of values indicative of the different hybrid classes. The empirically derived ranges resulted in 34 individuals identified as *G. affinis*, 61 individuals identified as *G. heterochir*, and 77 individuals identified as hybrids (Table 6). Since hybridization scores for males and females are based on different characters, the scores were standardized to prevent sexual differences in the magnitude of the scores from confounding the results.

Measurements of FA were performed using the MorphoSys digital imaging system (Meacham and Duncan, 1990). Each frame was labeled with the individual's identification code and side of fish being measured. First, a body contour was digitized

Table 6 Hybrid category, sex and sample sizes for the *Gambusia* analysis

Sex	Hybrid Class		
	Gambusia affinis	*Gambusia heterochir*	Hybrids
Female	18	20	40
Male	16	41	37

and then predetermined landmark points were digitized on both the left and right sides of each individual (Figure 14). After all individuals were measured, a replicate set of contours and points was obtained. All individuals were measured by a single investigator in random order for each replicate and blind with regard to species designation. Four traits were analyzed: snout to ventral insertion of operculum (SVO), operculum length (OPL), dorsal pectoral fin length (DPFL), and ventral pectoral fin length (VPFL): (Figure 14). Individual FA values were generated as simple arithmetic means over replicates and as BLUP's using the SAS® procedure MIXED with REML estimation (SAS Institute Inc., 1999). The individual FA values were analyzed as signed differences in an ANCOVA with hybrid designation, sex and site (above or below dam) as class variables and hybrid score as a continuous covariate. The use of individual hybrid scores allowed the quantification of the influence of hybrid score variation within hybrid classes on FA variation. A separate model was fit for each character by first fitting a full model, removing the most complex or least significant effect, refitting the model and comparing the corrected Akaike Information Criterion (AICc) for the two models (Akaike, 1974). The model-fitting procedure was terminated when AICc failed to become smaller for the simpler model. In addition, all effects contained in significant interaction terms were kept in the model as main effects. The ANCOVA was performed using the SAS® procedure GLM (SAS Institute Inc., 1999).

The results presented here should be considered preliminary and are utilized solely for the elucidation of BLUP on a field sampled data set. The complete analysis will use a landmark-based approach rather than a character-based approach. Therefore, no inferences should be drawn from this analysis beyond the effect of BLUP estimates.

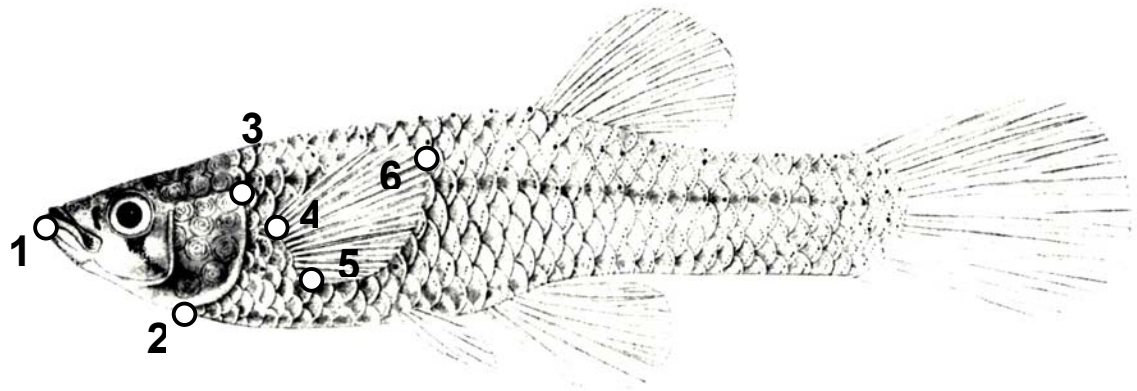

Figure 14. Measurements used for the analysis of FA in *Gambusia* hybrids. Snout to ventral insertion of operculum (SVO) (1 to 2), operculum length (OPL) (2 to 3), dorsal pectoral fin length (DPFL) (4 to 6), and ventral pectoral fin length (VPFL) (5 to 6). All measurements are straight-line distances between points.

RESULTS

SIMULATION DATA

Simple arithmetic means will always overestimate the true FA when ME is present as illustrated in Figure 15. Even with 10 replicate measures per individual, the FA estimate is inflated by 10.51%, whereas the BLUP using two replicate measures per individual only overestimates FA by 0.95%. Since a sample size of 10,000 is unrealistic for most FA studies, Table 7 presents summary statistics for the deviance of arithmetic averages and BLUP from the parametric expectation of each of the 100 samples of 100 individuals. The arithmetic mean is always inflated and averages over 50% inflation. The BLUP estimate is unbiased and averages less than 1% inflation. The absolute value of the deviance of the BLUP estimate varies from the true value of FA by slightly more than 12%. The standard deviation of the BLUP FA values is less than the parametric FA value and decreases with increasing numbers of replicates while the standard deviation of the arithmetic mean FA values is greater than the parametric FA value and increases with increasing numbers of replicates (Figure 16).

GAMBUSIA HYBRIDIZATION DATA

Results for all the final models are presented in Tables 8 a and b. The model for SVO showed general congruence using both arithmetic and BLUP FA values. The terms for hybrid score and the interaction of hybrid category, sex and hybrid score showed a slight difference being non-significant for the raw values ($F_{1,160}$=3.88, P=0.051 and $F_{3,160}$=2.55, P=0.058 respectively), but significant for the BLUP values ($F_{1,160}$=5.19, P=0.024 and $F_{3,160}$=2.68, P=0.049 respectively). The models for OPL were virtually indistinguishable between the raw and BLUP FA values for all model effects except the interaction term

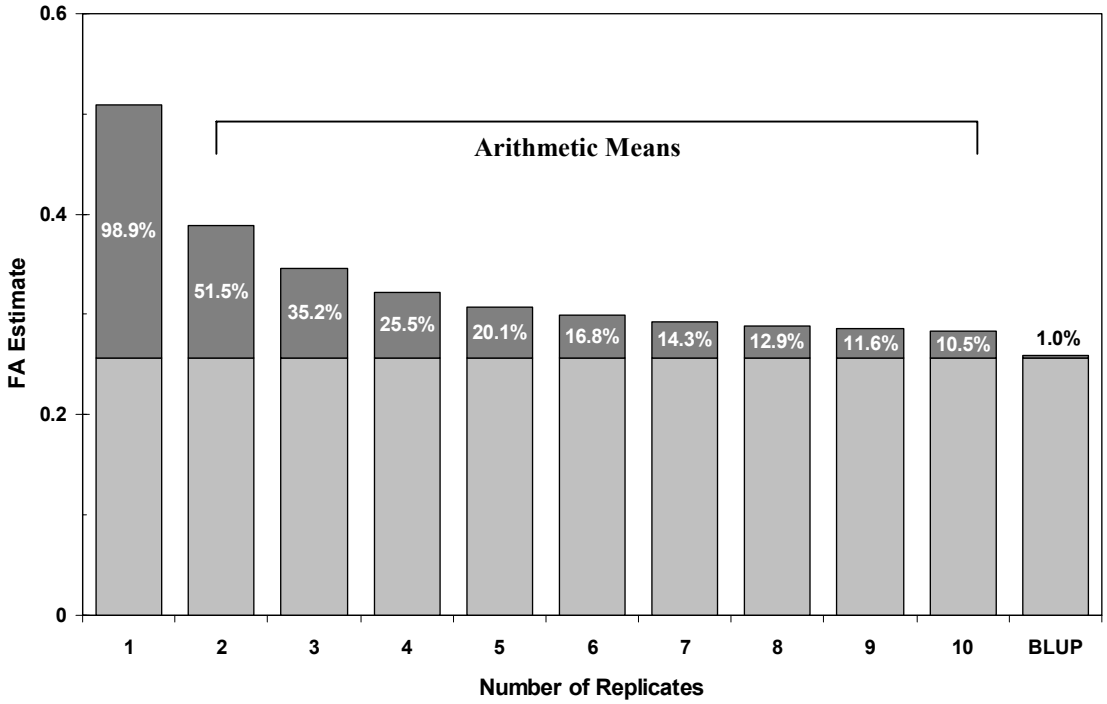

Figure 15. Percentage overestimation of the true FA in a simulated data set for a single replicate, simple arithmetic means using 2 to 10 replicate measurements per individual and a best linear unbiased predictor (BLUP) using 2 replicates. The light gray shading indicates the true FA value and the dark shading the overestimate.

Table 7. Parametric values for 100 samples of 100 simulated data points and percentage deviance of the FA estimates from the true value of FA using arithmetic means and BLUP. Both estimates are based upon two replicate measurements per individual.

Statistic	Parametric FA	Arithmetic Mean Deviance	BLUP Signed Deviance	BLUP Unsigned Deviance
Mean	0.2563	52.46%	0.84%	12.17%
Maximum	0.3599	97.79%	46.77%	46.77%
Minimum	0.1575	16.36%	-29.29%	0.18%

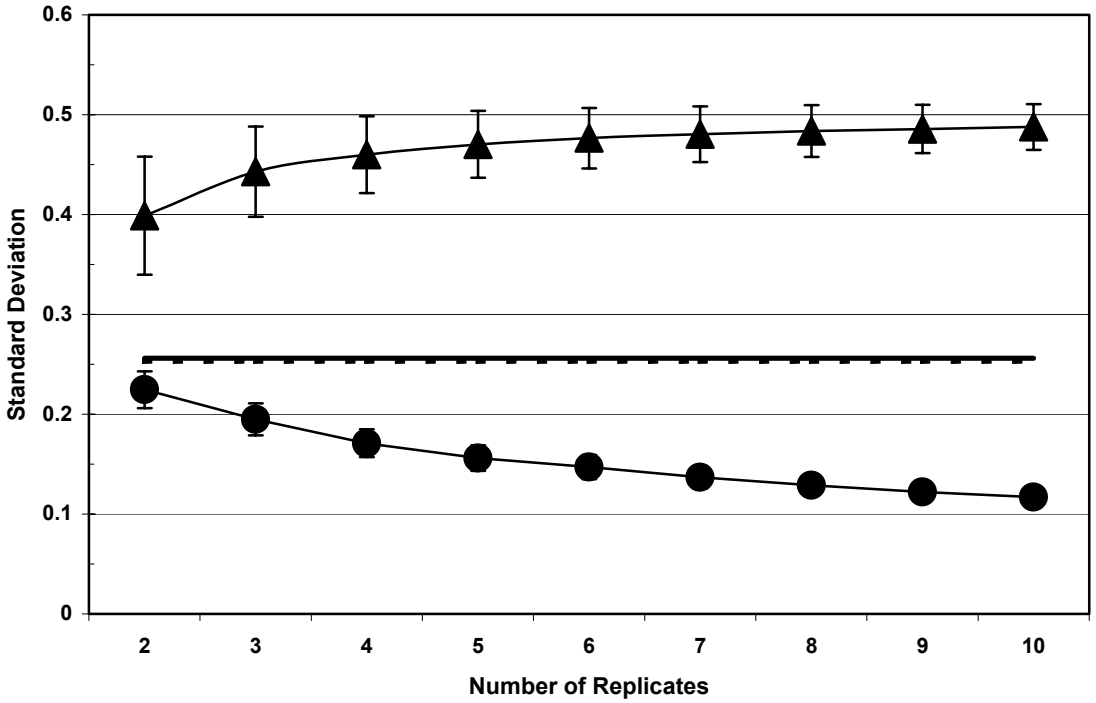

Figure 16. Standard deviations (circles and triangles) and 95% confidence intervals (vertical bars) for BLUP FA values (circles) and arithmetic mean FA values (triangles) using from 2 to 10 replicate measurements. The solid horizontal line is the true parametric value of FA in the simulated data set (0.256) and the dashed horizontal line is the true parametric value of ME in the simulated data (0.253).

Table 8. Results of the ANCOVA for the *Gambusia* hybridization study a.) for snout to ventral operculum (SVO) and operculum length (OPL) and b.) for dorsal pectoral fin length (DPFL) and ventral pectoral fin length (VPFL). A value of *na* indicates that the given effect was not a component of the final model for that trait.

a.

Effect	df	SVO			SVO BLUP			OPL			OPL BLUP		
		MS	F	P	MS	F	P	MS	F	P	MS	F	P
Hybrid Category (HC)	2	0.57	4.83	0.009	0.19	5.51	0.005	*na*	*na*	*na*	*na*	*na*	*na*
Sex	1	0.02	0.15	0.697	0.01	0.39	0.531	5.70	29.05	0.0001	3.34	27.57	0.0001
HC x Sex	2	0.36	3.08	0.049	0.11	3.33	0.038	*na*	*na*	*na*	*na*	*na*	*na*
Hybrid Score (HS)	1	0.46	3.88	0.051	0.18	5.19	0.024	1.01	5.14	0.025	0.50	4.09	0.045
HC x HS	2	0.84	7.13	0.001	0.24	7.03	0.001	*na*	*na*	*na*	*na*	*na*	*na*
Sex x HS	2	*na*	*na*	*na*	*na*	*na*	*na*	0.58	2.96	0.087	0.48	3.97	0.048
HC x Sex x HS	3	0.30	2.55	0.058	0.09	2.68	0.049	*na*	*na*	*na*	*na*	*na*	*na*

b.

Effect	Df	DPFL			DPFL BLUP			VPFL			VPFL BLUP		
		MS	F	P	MS	F	P	MS	F	P	MS	F	P
Sex	1	1.89	7.16	0.008	0.28	3.19	0.076	2.24	5.61	0.019	0.64	3.76	0.054

for sex and hybrid score which was non-significant for the raw values ($F_{1,160}$=2.96, P=0.087) but significant for the BLUP values ($F_{1,160}$=3.97, P=0.048). The final models for both DPFL and VPFL contained only sex as a significant term in the models. However, in both cases, while the raw values indicated a significant difference in FA due to sex ($F_{1,160}$=7.16, P=0.008 for DPFL and $F_{1,160}$=5.61, P=0.019 for VPFL), the BLUP FA values did not indicate any sexual differences in FA ($F_{1,160}$=3.19, P=0.076 for DPFL and $F_{1,160}$=3.76, P=0.054 for VPFL).

DISCUSSION

The simulation results reveal that BLUP values for individual FA are a more efficient estimator compared to arithmetic means. In this case, the BLUP estimate with 2 replicates produced an overestimate which had a magnitude of less than 10% of the overestimate produced using an arithmetic mean from 10 replicates. Reasonable sample sizes of 100 individuals produced reasonable (relative to the parametric amount of ME) standard deviations of the BLUP values with only four replicate measurements per individual (For 100 samples; Mean = 0.171, Minimum = 0.155, Maximum = 0.188). The mean standard deviation for a BLUP FA value using 4 replicates was 37.2% of the arithmetic mean FA estimate using the same number of replicates. As expected, the BLUP standard deviation decreased with both an increase in the number of individuals and with the number of replicates. Increasing the number of replicates above 2 resulted in a greater decrease in the standard deviation when corrected for effort compared to increasing the number of individuals. For example, 100 individuals with 4 replicate measurements each, had a comparable standard deviation for the BLUP FA values to that for 200 individuals with 2 replicate measurements. In both cases, 400 measurements per

character were required but the effort required to procure an additional 100 individuals is not necessary for the first case. The example assumes that the magnitude of FA differences among individuals and ME among replicate measurements is approximately equal, as in the simulation study. In situations using data from sampled populations, the magnitude of both FA and ME can be estimated (Palmer and Strobeck, 1986) from either previous data or a pilot study to determine the best compromise between the number of individuals and the number of replicate measurements per individual.

The significance of using BLUP FA values compared to arithmetic means varied among characters for the *Gambusia* study. This implies that either FA varied among traits, ME varied among traits, or that both measures varied. Table 9 b. lists the average standardized values (standardized to the total sums-of-squares) of FA, ME and the ratio of ME to FA, for each of the measured characters. Since the data is utilized here solely for a comparison of arithmetic mean and BLUP FA values, and no other conclusions should be drawn from the data, the actual group-level FA and ME are less relevant than standardized values presented as percentages for comparing among traits. All three variables vary significantly among traits with VPFL having the maximal value for both FA and ME but with DPFL exhibiting the maximal value of the ratio of ME to FA. In this case the use of BLUP FA values had the greatest influence using DPFL as the focal character and the least influence when using OPL as a character, reinforcing the results of the comparison of F values from the ANCOVA models.

In data sets from field-sampled populations, both FA and ME may vary among groups. Averaging over all characters, ME varied much less among hybrid classes (Table 9a) and between sexes (Table 9c) than does FA, indicating less group influence on ME

Table 9. Averaged scaled values of FA, ME and the ratio of ME to FA for a.) hybrid classes, b.) characters, and c.) sex. The mean squares for FA and ME were scaled to the total sums-of-squares for each model to facilitate comparisons among grouping variables.

a.

Class	FA	ME	Ratio
hybrid	100.00%	129.48%	344.33%
G. affinis	187.43%	112.18%	206.69%
G. heterochir	212.41%	100.00%	100.00%

b.

Character	FA	ME	Ratio
SVO	100.00%	120.85%	203.19%
DPFL	204.52%	212.17%	249.24%
OPL	262.28%	100.00%	100.00%
VPFL	351.33%	301.13%	147.41%

c.

Sex	FA	ME	Ratio
M	100.00%	100.00%	131.29%
F	440.46%	119.92%	100.00%

than FA. The ratio of ME to FA varies less between sexes (Table 9c) but more among hybrid classes (Table 9a) compared to between character variation (Table 9b). Variation among the classes of grouping variables such as sex or hybrid class in the relative amounts of FA and ME can confound biological inferences from FA analyses. If sample sizes are adequate, the best solution to eliminating the confounding effect would be to model separate ME values for each group (i.e. each sex or hybrid class) using the repeated statement in PROC MIXED as suggested by Van Dongen *et al.* (1999). For the *Gambusia* hybridization data this would involve 12 (4 traits, 3 hybrid classes) or 24 (4 traits, 3 hybrid classes, 2 sexes) ME estimates. The best model or models should be generated using an information theoretic approach in a multi-model inference structure as proposed by Burnham and Anderson (2002). We will utilize a landmark-based analysis of the *Gambusia* hybridization data with separate modeled ME estimates for each group in an upcoming paper and the complete methodology will be fully elaborated in that paper.

The necessity for individual-level FA estimates is readily seen in the recent literature. The last three chapters of the book by Møller and Swaddle (1997) all deal with FA as a surrogate of developmental stability and individual-level phenomena (performance, signaling and fitness) and comprise roughly 33% of the book. Perhaps the greatest area of interest recently has been the use of FA as a surrogate for developmental stability in studies of sexual selection (Møller and Pomiankowski, 1993; Palmer, 1999; Thornhill *et al.*, 1999; Møller and Cuervo, 2003; Tomkins and Simmons, 2003). Since sexual selection is an individual-level phenomenon, studies of sexual selection should be analyzed at the level of individuals. Unfortunately, the lack of a useful methodology to remove ME from individual-level FA estimates has forced many studies to be performed

at a group-level. A recent meta-analysis reveals that of 132 studies with an explicit indication of the scale of the analysis, 58 (44%) were conducted at the group-level (Tomkins and Simmons, 2003). Although some investigators chose to analyze the problem at the group level, the lack of an unbiased individual-level FA value was explicitly pointed out as a fundamental problem in many of these studies (Tomkins and Simmons, 2003). The use of FA in studies of sexual selection has been rather contentious and has led to heated debate on both methodological concerns about FA as well as the overall usefulness of FA as a descriptor of developmental stability. Two recent reviews and meta-analyses illustrate the salient points of the debate and the import of measurement error assessment.

Tomkins and Simmons (2003) present a meta-analysis of studies analyzing FA and sexual selection conducted between 1990 and 2000. One of the conclusions of their meta-analysis is that replicate measures are necessary to assess repeatability. They also state that if repeatability is high ($r \geq 0.9$) then replicate measures on all individuals may not be necessary. This can lead to unreliable within group FA estimates and incorrect probability values for FA comparisons among groups when dealing with more than a single group. The fact that repeatability is high within several groups of interest is only relevant if in addition there is a significant correlation of the repeatabilities among groups. For an individual-level analysis, this implies a significant correlation of repeatabilities among individuals. If repeatabilities are low to moderate, Tomkins and Simmons (2003) suggest that arithmetic averages of two replicate measures should be utilized. For reasons previously stated in this paper, BLUP FA values are superior to simple means and the same problems with multiple groups and the correlation of

repeatability among groups applies here. However, Tomkins and Simmons (2003) go on to state that more robust FA estimates will be realized if replicates are taken on all individuals and if more than two replicates are taken. The results of the comparison of BLUP and arithmetic mean estimates of FA fully support the last two conclusions of Tomkins and Simmons.

Møller and Cuervo (2003) also provide a meta-analysis of studies analyzing FA and sexual selection. Of relevance to the question of measurement error and FA is their comparison of unadjusted FA values to values adjusted using the mixed-regression technique (Van Dongen *et al.*, 1999). The analysis by Møller and Cuervo correlated the adjusted values for several organisms utilizing ungrouped samples as well as samples grouped by sex and age using Pearson product-moment correlations. The average correlation coefficient was 0.94 and thus they concluded that measurement error would not likely bias the results of these studies. Unfortunately, their analysis does not address the effect of ME on FA. A simple example will illustrate the fallacy in their analysis. Create two groups of five individuals with the following character measurements: (Group1: 1, 2, 3, 4, 5 and Group 2: 3, 6, 9, 12, 15). A simple ANOVA reveals a significant difference between groups ($F_{1,8} = 7.2$, $P = 0.028$). Adding a fixed ME of 5 to each group 1 member and 3 to each group 2 member results in the following values (Group1: 6, 7, 8, 9, 10 and Group 2: 6, 9, 12, 15,18). The difference between groups is no longer significant ($F_{1,8} = 3.2$, $P = 0.111$) even though there is a Pearson's correlation of 0.98 over all 10 individuals or a Pearson's r of 1 within each group. The use of Pearson's r as an assay tool in this case assumed that ME is constant or nearly so between or among groups or individuals. Although the example is contrived, ME is different among groups

in the *Gambusia* hybridization study presented earlier and is known to vary among groups in other studies (Van Dongen *et al.*, 2003). Therefore, the analysis of Møller and Cuervo (2003) with regard to the lack of importance of ME in studies of sexual selection is wholly unconvincing and repeated measurements and appropriate statistical analyses should become de rigour for sexual selection studies at both the group and individual-level.

Recently, a series of papers have proposed the use of a mixed regression analysis for the estimation of unbiased individual FA values (Van Dongen *et al.*, 1999; Van Dongen, 2000; Van Dongen *et al.*, 2003). The methodology of Van Dongen and colleagues is similar to that proposed here in that both utilize a mixed-model procedure and REML estimation of parameters. In the BLUP methodology the standard ANOVA model of Palmer and Strobeck (1986) is utilized with side being a fixed effect classification variable. In the mixed-regression approach, side is utilized as both a fixed and random continuous covariate to avoid overparameterization. Such overparameterization in a mixed-model ANOVA only occurs when side is treated as a random effect. The problem with treating a truly fixed effect as random is that the model results become dependent on how the effect is coded. Coding side as –1 and +1 will not obtain the same results as coding side 0.1 and –0.1 or any other set of values. For example, Van Dongen *et al.* (2003) gives a worked example using three individuals with side coded as 0.5 and –0.5 which results in calculated vales of 0.727, 1.074 and –1.801 for the three individuals. Using the same data, but with side coded as 1 and –1 as previously suggested (Van Dongen *et al.*, 1999), values of 0.3635, 0.537 and –0.9005 are obtained for the three individuals. The values using the 1/-1 coding are exactly half the values using the 0.5/-0.5

coding, as expected, but the absolute magnitude of the values are totally dependent on the coding scheme. Therefore, by not utilizing the variable in its native state a subjective bias can be introduced into our model. Such recoding is not necessary since the BLUP estimates are consistent, unbiased, and require no subjectivity in recoding. Lastly, by treating side as a continuous covariate, part of the variance among individuals is partitioned into the side covariate. Depending on how the data is scaled prior to analysis, this amounts to confounding the FA within individuals with size or shape variation between individuals. Whether or not this has a significant effect will be dependent upon the relative magnitude of the variation in FA compared to the variation in size and/or shape. In most data sets the results of both methods, with proper recoding, will be similar so the choice may not be significant for the overall result. However, the use of BLUP FA values and a mixed-model ANOVA does not require a change in either model or interpretation, is supported by a large body of literature on BLUP procedures, and does not require any subjective recoding of parameters.

The choice of the level of analysis (group or individual), should be based upon the level at which the underlying process of interest is acting. For FA values, this choice no longer requires a decision on how important ME is to the results. Measurement error can be assessed and removed at both the group and individual-level through the utilization of replicated measurements, mixed-model analysis and for individual-level FA, best linear unbiased prediction. The use of the MIXED procedure in SAS with either maximum likelihood or restricted maximum likelihood estimation also frees the analysis of some of the constraints imposed by least-squares analysis. This can result in more realistic and accurate modeling of FA in at least two ways. First, a single ME value does not have to

be assumed for all groups or individuals (Van Dongen *et al.*, 2003) and one can model as many separate error estimates as the sample size allows. Second, grouping variables such as sex, age, sample areas, etc. do not have to be assumed independent as non-zero covariance terms can also be modeled with or without spatial and/or temporal structure (Littell *et al.*, 1996). The use of individual ME corrected FA values also allows one to use other statistical tools such as path (Li, 1975) and causal (Hatcher, 1994) analysis to explore and model the link between FA (the measured variable) and developmental stability (the unmeasured, latent variable).

CHAPTER 4

PATH ANALYSIS OF SKULL FORM WITHIN A METAPOPULATION OF HISPID COTTON RATS (*SIGMODON HISPIDUS*)

INTRODUCTION

Form was defined in the previous chapters as a character consisting of three components, size, shape and symmetry, as well as all the covariances among them. From an evolutionary perspective, form is thus a composite character and its phenotypic variance is an amalgam of the phenotypic variances and covariances of all of the constituent components. The components of form have a genetic basis, but the proportion of the total phenotypic variance due to genetic variance is likely to vary among the components as will the environmental variances and the gene-by-environment interaction. Both quantitative genetic analysis (Klingenberg, 2001b) and QTL analysis (Klingenberg, 2001a) of geometric morphometric estimates of size, shape and symmetry have indicated that the components of form for the mouse mandible have different underlying genetic bases that may include significant covariances among the components of form. Thus, form, like fitness, cannot be measured directly, but only indirectly through simultaneous analysis of its components or by surrogate overall measures (Roff, 1992).

In addition, like fitness, form is a characteristic of the individual but the components of both form and fitness can be summarized for groups of individuals (Stearns, 1992). However, any such aggregation imposes a spatial and temporal scale, which defines, and limits, the ecological and evolutionary processes that influence the aggregation (Pascual

and Levin, 1999). Furthermore, ecological and evolutionary processes do not necessarily transcend scales linearly, if at all (Pascual and Levin, 1999), and thus we study micro- and macroevolutionary processes separately (Futyma, 1998) and study population and community ecology as separate subdisciplines (Begon *et al.*, 1998). Since the underlying ecological and evolutionary processes structuring form occur at the level of the individual, a process-based mechanistic model is only possible at the individual-level and becomes phenomenological (i.e we can only interpret the outcome, not how it was derived) at higher levels (DeAngelis and Rose, 1992; Judson, 1994). It is also at the level of the individual that form components can be utilized to provide an overall estimate of form.

The problem then becomes to take the measured components of form and combine them into an overall, unmeasured estimate of form? One methodology is to use the framework of path analysis to estimate mechanistic effects on form similar to its use for the estimate of mechanistic models for selection (Kingsolver and Schemske, 1991) and fitness (Svensson *et al.*, 2002). Path analysis was first utilized by Sewell Wright for incorporating genetic relatedness into between-generation analyses of quantitative genetic variation (Wright, 1921). However, path analysis is actually part of a larger statistical framework called structural equation or causal modeling that also includes such techniques as principal components analysis and factor analysis (Hatcher, 1994). The usefulness of path models comes from the fact that path coefficients are simply partial regression coefficients on standardized variables (Li, 1975), they can be converted to coefficients of determination (Li, 1975) and path models can contain both manifest (measured) and latent (unmeasured) variables (Hatcher, 1994). In addition, a path model

is a representation of a hypothesis for causal links among the variables in the models so they are well suited for developing mechanistic models. In summary, path analysis is an analytic procedure, which combines both measured and unmeasured variables to produce quantitative assessments (path coefficients) of the proportion of total variation of a trait (or suite of traits) explained by one or more causal factors.

Our objective is to analyze path models for the components of form for the hispid cotton rat (*Sigmodon hispidus*) and interpret them as both evolutionary models and for generating evolutionary effects biomarkers in ecotoxicology. Specifically, we will analyze path models of form components utilizing five individual-level variables (age, sex, heterozygosity, structural size and body mass) and one group-level variable (trapping grid density class). We will then analyze a composite model with all three components of form to assess form change as a single composite character.

MATERIALS AND METHODS

SAMPLING LOCALITIES AND SPECIMENS

A total of 124 cotton rat skulls (Table 10) were obtained from four trapping grids located in Field 3-412, an old-field site currently in a pine savannah successional stage, on the U.S.D.O.E. Savannah River Site, SC, USA (N 33° 14’ W 81° 31’). Each trapping grid consisted of 100 galvanized metal live traps on a 10 x 10 grid with a 15m spacing between traps and rows. Grids were separated by a minimum of 250 m and a maximum of 500 m from the next nearest grid. Grids were trapped during late June through early August of 1993 with each grid being trapped until the assumption of population closure was violated (Otis *et al.*, 1978). Animals were euthanized via cervical dislocation in accordance with our animal use protocol and skulls were prepared using standard

Table 10. Sex and age structure of cotton rats collected from Field 3-412 and estimated density of sampling grids.

Grid	Male			Female			Density (#/ha)
	Adult	Subadult	Juveniles	Adult	Subadult	Juveniles	
1	11	6	8	7	10	9	76
2	7	5	5	8	5	3	53
3	3	0	3	0	3	1	25
4	2	9	5	2	7	5	49
Total	23	20	21	17	25	18	

methods (Martin *et al.*, 2000) at the University of Georgia Museum of Natural History. All skulls have been deposited in the mammal collection of the University of South Dakota, Vermillion, SD, USA.

Each individual was sexed, weighed to the nearest 0.1 g and placed into one of three age classes (juvenile, subadult, or adult) based upon pelage, tooth eruption and skull suture characteristics (Chipman, 1965). Total body length, tail length, left ear length and left hind foot length were also measured for each specimen. Blood and muscle samples were collected and analyzed for variation at 37 isozyme loci of which five were variable in this population (Adenylate Kinase, AK-2, E.C. 2.7.4.3; Glycerol –3-Phosphate Dehydrogenase, GPD, E.C. 1.1.1.8; Phosphoglucomutase, PGM-1, PGM-2, E.C. 5.4.2.2; and Phosphogluconate Dehydrogenase, PGD, E.C. 1.1.1.44). The population density of each trapping grid was estimated utilizing a generalized removal estimator with the assumption of population closure (Otis *et al.*, 1978).

MEASUREMENTS AND ANALYSIS

Individual skulls were placed upon a piece of black felt covering a tray of fine white beach sand and the entire skull was leveled using a small bubble-level balanced upon the molars (Figure 17). A photographic slide of the ventral surface of the skull was taken using a Nikon n90s camera with a flat-field 60mm macro lens (ASA 100; f = 16). The camera was attached to a copy stand and was also leveled using a bubble-level centered upon the back plane of the camera. Slides were taken for a series of skulls, the skulls were repositioned, releveled and a replicate slide was taken for each skull in the series. Thus, each individual was photographed twice with individuals randomized between replicates. Each slide was then scanned to a 7Mb 24bit color bitmap image using a Nikon

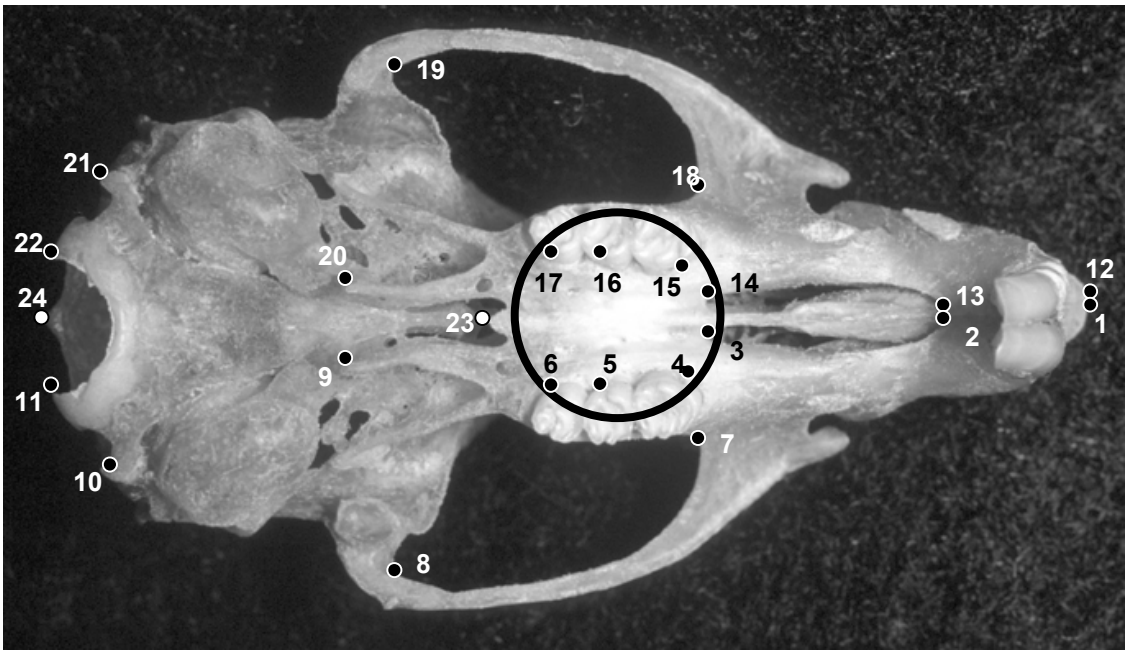

Figure 17. Locations on the ventral view of a cotton rat skull for 24 landmark points utilized in the current study. Midline points are white with a black border (2 landmarks) and paired points are black with a white border (11 pairs of landmarks). The large open circle represents the placement of the bubble-level prior to image acquisition.

LS-2000 slide scanner. Each bitmap was used to digitize a series of 24 landmarks (2 midline and 11 pairs; Figure 17) twice. Again, individuals were randomized prior to digitization of landmarks and between replicates. The final result was each individual having two images, each with two sets of digitized landmarks providing four sets of replicate landmarks per individual.

The basic analysis followed a geometric morphometrics protocol (Adams *et al.*, 2003) and therefore proceeds via the x and y coordinates of each landmark point and not any distances derived from those points. Size was estimated as the centroid size of the configuration of all landmarks, which is simply the square root of the sum of the squared distance between each landmark and the centroid of the configuration (Bookstein, 1991). Centroid size is utilized because it is independent of the shape estimate except for the contribution of allometry (the interaction of size and shape). Antisymmetry was assessed utilizing the test for normality in PROC UNIVARIATE (SAS, 1999) as well as a test of Kurtosis (Zar, 1999). We calculated the best linear unbiased predictor (BLUP) (Robinson, 1991) of the x and y coordinate for each landmark on each individual. The model for BLUP estimation of centroid size utilized individual as a random effect. Fluctuating asymmetry (FA) was estimated using a mixed model analysis of variance (ANOVA) with side (left or right) as a fixed effect, individual as a random effect and the variance component of the interaction of side and individuals providing the measurement error-corrected group estimate of FA (Palmer and Strobeck, 1986; Table 11). The mixed model ANOVA was utilized to generate BLUP values for the x and y coordinates for all landmarks and all individuals as described in Chapter 1. Since we utilized a landmark-based approach, a single measurement error free estimate of symmetric shape variation

Table 11. Mixed-model ANOVA for the estimation of group-level FA.

Effect	Expected Mean Square	Estimated Component
Sides (S)	$\sigma_m^2 + M\left\{\sigma_i^2 + [J/(S-1)]\sum a^2\right\}$	Directional asymmetry
Individuals (J)	$\sigma_m^2 + M\left(\sigma_i^2 + S\,\sigma_j^2\right)$	Size/Shape variation[1]
Interaction(I) (SxJ)	$\sigma_m^2 + M\,\sigma_i^2$	Antisymmetry, FA / # reps, Measurement error
Measurements (M)	σ_m^2	Measurement error

[1] In a Procrustes-based analysis this component represents shape variation and allometric variation (Size x Shape Interaction) since all individuals are scaled to unit centroid size prior to superimpositioning. In addition, for studies performing a Procrustes analysis on a structure with object symmetry, any size asymmetry will be included in this component.

and fluctuating asymmetry was generated utilizing the sum-of-squares summation method of Klingenberg and McIntyre (1998) and Klingenberg *et al.* (2002) to generate estimates of Procrustes sums-of-squares from the path analyses. The Procrustes sums-of-squares were then utilized to calculate the coefficients of the path models by using the statistical definitions of the coefficients (Li, 1975; Hatcher, 1994).

The Procrustes methods of Klingenberg and colleagues are extensions of the work of Goodall (1991), which assumes that variation among landmarks is equal, isotropic (i.e. non-directional) and independent. To assess homogeneity of variance we calculated the centroid of each landmark based upon the digitized points, calculated the squared distance of each point, and summed those distances over all individuals within sex and age classes resulting in 24 estimated variances around each landmark. We then performed an ANOVA on the absolute value of the difference of each squared distance value from the mean value of all squared distances with landmark as a random effect and age and sex as fixed effects including all interactions. The ANOVA is a Levene's test (Palmer and Strobeck, 2003) for testing homogeneity of variances. For visualization of the relative variances around each landmark we used a bubble plot. Independence of landmarks was assessed using a semivariogram based upon a spherical model (Piegorsch and Bailer, 1997). The isotropy of the digitized points around their centroid was assessed using a Rayleigh test for uniformity (Mardia and Jupp, 2000).

A series of path analyses using the components of form as the endogenous variable were performed. Two separate models were run for each component of form. The first model included three ordinal exogenous variables and two mediator variables (Figure 18). Density (Den) was the grid each individual was trapped on ranked by estimated

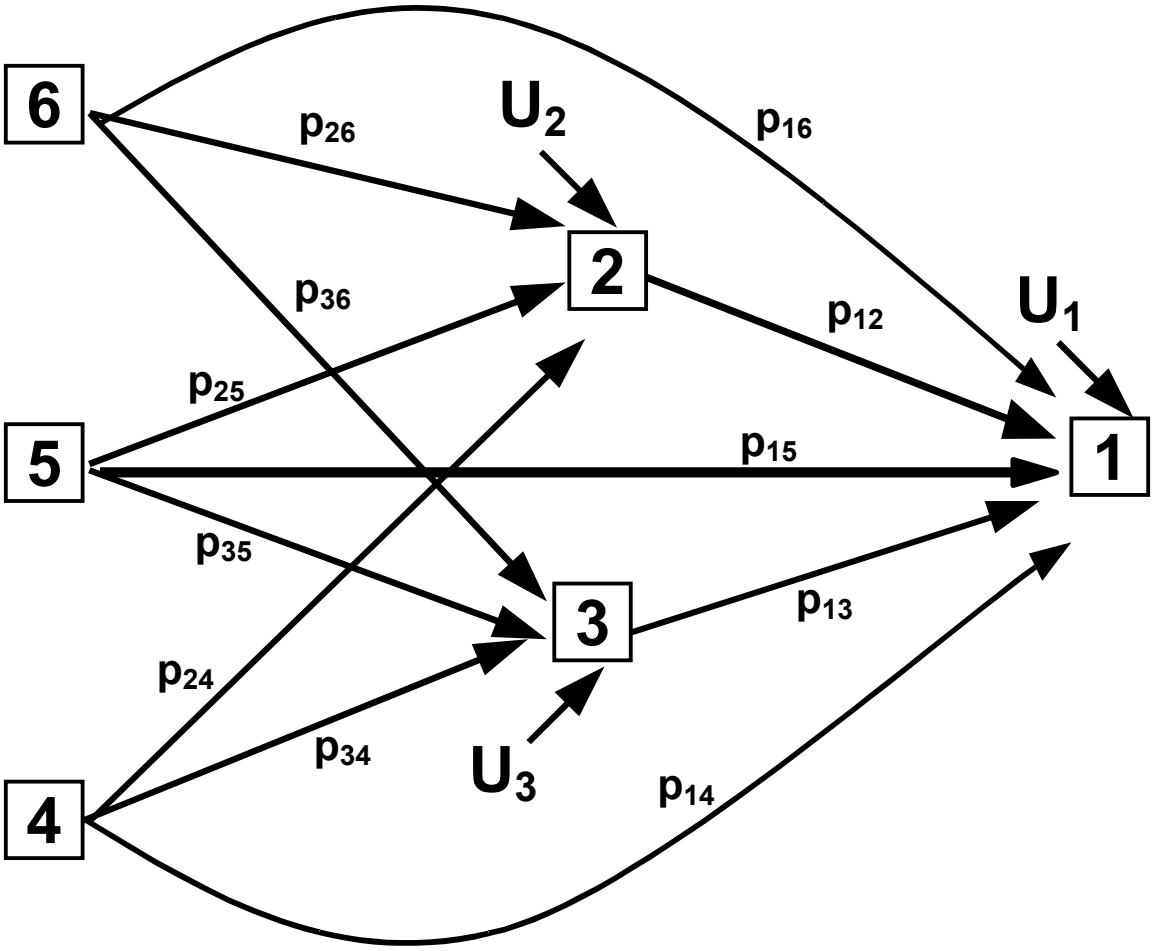

Figure 18. Path diagram for the components of form. Two separate models were run for each endogenous variable; centroid size (1), symmetric shape (1) and fluctuating asymmetry (1). The first model included three exogenous variables, density class (6), age class (5) and multilocus heterozygosity (4) and two mediator variables, body mass (2) and structural size (3). The second model differs in substituting the exogenous variable sex (5) for age. Only the causal paths (p_{ij}) and unexplained variance (U_i) are shown but covariances between exogenous variables and between mediator variables were included in the models. Manifest (measured) variables are indicated by squares.

density, higher ranks being higher densities and represented environmental variation. Age was the age class of the individual coded as 0 for juvenile, 1 for subadult and 2 for adult and represented developmental variation. Heterozygosity (H) was the multilocus direct count heterozygosity of each individual, higher numbers indicated greater heterozygosity and represented genetic variation. Body mass was the log-transformed value of individual body mass and represented condition of an individual. Size was structural body size calculated as the first principal component of body length (total length – tail length), tail length, ear length and hind foot length utilizing the correlation matrix rather than the covariance matrix. All variables loaded in the same direction and the loadings did not vary greatly in magnitude among the variables (Body, 0.53; Tail, 0.41; Ear, 0.51; Foot, 0.54) and accounted for 62.23% of the total variation. Therefore, we assumed this component measured general structural size.

The second model for each of the components of form substituted the exogenous variable, sex, coded as a dummy variable with 0 for female and 1 for male, for age class and this also represents a form of genetic variation since sex is genetically determined in mammals. One composite model including both age and sex would have resulted in empty cells for grid 3 since not all age-sex categories were captured on that low-density grid. Percentage of variance for all models was calculated by converting path coefficients and unexplained variance to coefficients of determination (or nondetermination) as described by (Li, 1975).

All ANOVA calculations to generate BLUP estimates were performed using the SAS® procedure MIXED with restricted maximum likelihood (REML) estimation, the semivariogram was calculated using the SAS® procedures VARIOGRAM and NLIN, the

Levene's test was performed using the SAS® procedure GLM and path analyses were performed using the SAS® procedure CALIS (SAS, 1999). Procrustes superimposition was carried out using the tpsRelw, v. 1.31, program (Rohlf, 2003).

RESULTS

VARIATION OF LANDMARKS

There was heterogeneity of variance among landmarks ($F_{23,16.33} = 3.56$, $P = 0.0058$; Figure 19). The main effects of sex ($F_{1,23} = 1.68$, $P = 0.2073$) and age ($F_{2,46} = 2.75$, $P = 0.0745$) were not significant nor were the two-way interactions (Landmark*Sex, $F_{23,48} = 1.22$, $P = 0.2722$; Landmark*Age, $F_{46,48} = 1.55$, $P = 0.0679$). However the three-way interaction was highly significant ($F_{48,432} = 341.06$, $P < 0.0001$). The midline points and the rostral points appeared to exhibit anisotropy (Figure 20), but the descriptive statistics and a Rayleigh test for circular uniformity showed no deviation from isotropy (Table 12). The variance around landmarks exhibited significant positive spatial autocorrelation for points less than 0.27 units apart (Figure 21).

EXOGENOUS AND MANIFEST VARIABLES

Path coefficients between exogenous and mediator variables and the unexplained variance of the mediator variables remained invariant to changes in endogenous variable. However they did vary when sex is substituted for age in the path model (Table 13). Heterozygosity showed a weak positive association ($p_{24} = 0.0890$) with body mass in model one and an even weaker positive association ($p_{24} = 0.0047$) with body mass in model two. Age exhibited a very strong positive association with body mass ($p_{25} = 0.9409$) in model one but sex exhibited a relatively weak positive association with body mass ($p_{25} = 0.1211$) in model two. The association between density class and body mass

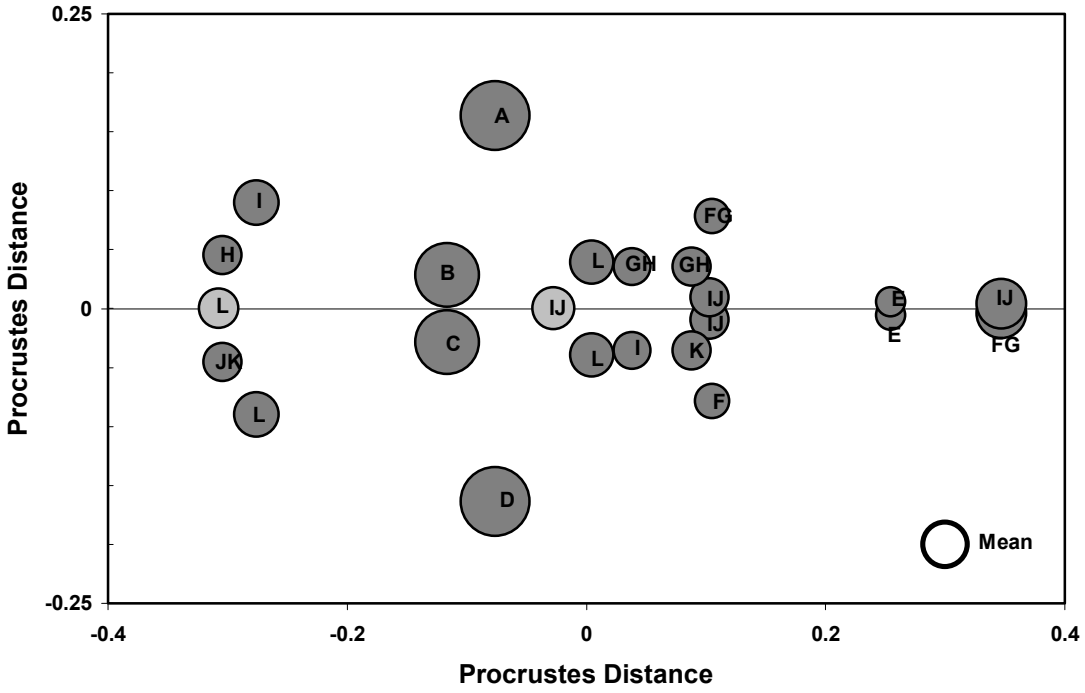

Figure 19. Bubble plot of sum-of-squared distances after Procrustes superimposition for the best linear unbiased prediction estimate for all individuals. The sum of the squared distances was calculated as the sum of the squared distance between each estimated point and the centroid of all estimated points for a landmark. Light gray bubbles represent the midline landmarks and the dark gray bubbles represent the paired landmarks. The diameter of the bubble represents the variation around a landmark relative to all other landmarks. Like letters are not significantly larger or smaller than the mean variance based upon Bonferroni corrected least-squared mean estimates from the Levene's test. The unfilled circle labeled mean represents the overall mean variation for all landmarks and is not an actual landmark point. Procrustes distance is unitless.

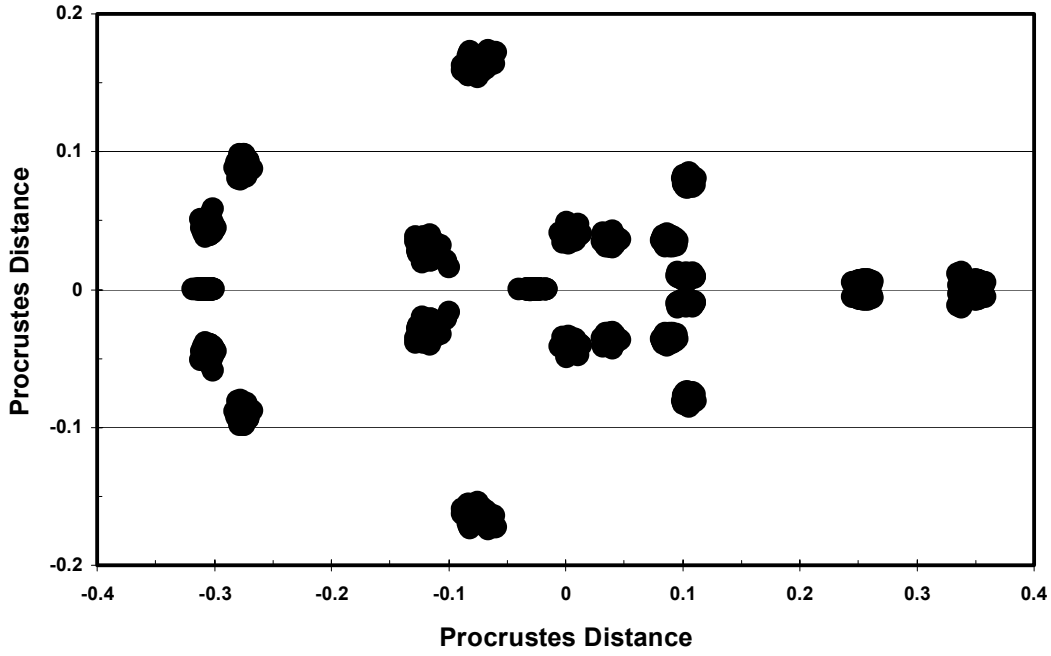

Figure 20. Scatter plot of the best linear unbiased prediction estimate for each of the 24 landmarks after Procrustes superimposition for all individuals. Each cloud consists of 124 points. Procrustes distance is unitless.

Table 12. The mean and median angle, mean length, angular dispersion and Rayleigh test for uniformity of best linear unbiased predictions for each of the 24 landmarks. Landmark numbers are as designated in Figure 17. The sample size for each landmark is 124.

Landmark	Mean Angle	Median Angle	Mean Length	Angular Deviation	Rayleigh Statistic	P
1	40.76	167.04	0.325	66.574	2.4347	0.2960
2	197.93	179.89	0.014	80.471	0.0037	0.9981
3	145.78	178.35	0.141	75.111	0.4048	0.8168
4	352.52	186.51	0.039	79.440	0.0300	0.9851
5	55.44	168.86	0.101	76.816	0.2066	0.9018
6	53.88	187.96	0.033	79.668	0.0220	0.9890
7	49.45	173.36	0.079	77.746	0.1262	0.9389
8	210.73	192.75	0.063	78.444	0.0786	0.9615
9	101.71	169.80	0.043	79.282	0.0362	0.9821
10	80.20	186.21	0.018	80.279	0.0067	0.9966
11	50.95	186.57	0.053	78.861	0.0555	0.9726
12	319.24	192.97	0.325	66.574	2.4346	0.2960
13	162.05	180.11	0.014	80.471	0.0037	0.9981
14	214.23	181.65	0.141	75.111	0.4048	0.8168
15	7.49	173.49	0.039	79.440	0.0300	0.9851
16	304.56	191.14	0.101	76.816	0.2066	0.9019
17	306.13	172.04	0.033	79.667	0.0221	0.9890
18	310.56	186.64	0.079	77.746	0.1262	0.9388
19	149.31	167.25	0.063	78.444	0.0786	0.9614
20	258.24	190.20	0.043	79.283	0.0361	0.9821
21	279.81	173.80	0.018	80.278	0.0067	0.9966
22	309.04	173.43	0.053	78.861	0.0555	0.9726
23	0.01	180.00	0.033	79.689	0.0214	0.9894
24	360.00	180.00	0.230	71.125	1.1295	0.5685

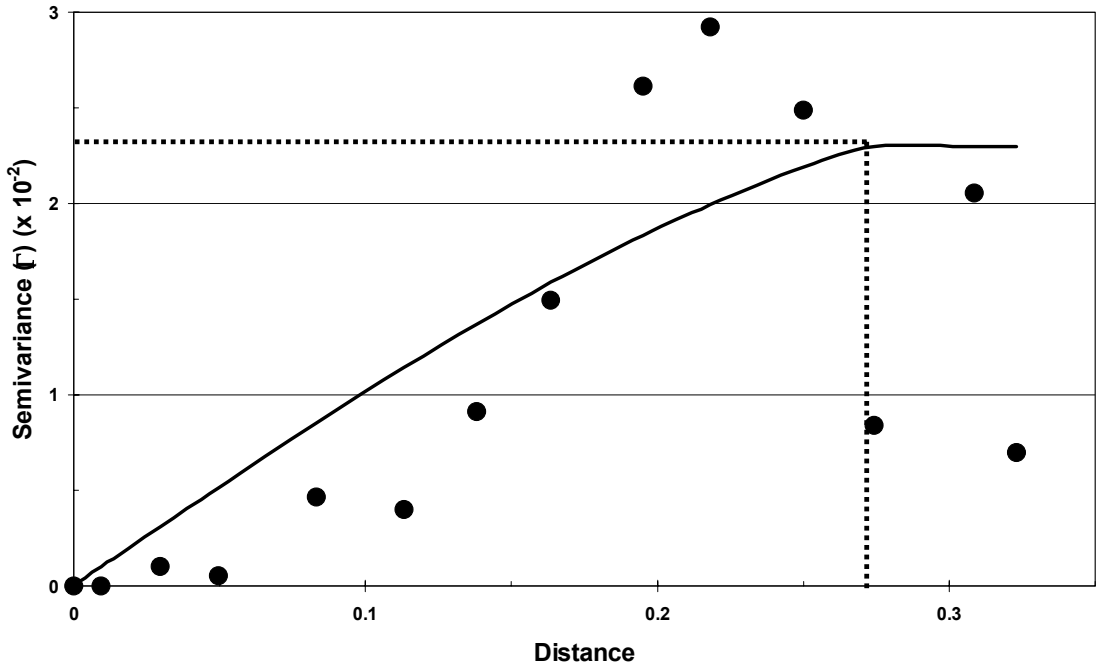

Figure 21. Semivariogram of sum-of-squared distances after Procrustes superimposition for the best linear unbiased prediction estimate for all individuals. The sum of the squared distances was calculated as described in Figure 20. The horizontal dotted line represents the sill and the vertical dotted line the scale or range of the data. The nugget is zero.

Table 13. Path coefficients (p_{ij}) and unexplained variance (U_i) for the two path models for the endogenous variables centroid size (CS), symmetric shape (Shape) and fluctuating asymmetry (FA). The path coefficients between the mediator and exogenous variables and the unexplained variance of the mediator variables remain constant regardless of the endogenous variable analyzed. Coefficients and subscripts are defined in Figure 18.

Coefficient	Age Model			Sex Model		
	CS	Shape	FA	CS	Shape	FA
p_{12}	0.288	-0.319	-0.194	0.246	-0.202	-0.126
p_{13}	0.694	-0.201	0.111	0.739	-0.185	0.124
p_{14}	0.016	-0.084	0.057	0.023	-0.082	0.059
p_{15}	-0.079	0.208	-0.150	0.037	-0.087	-0.100
p_{16}	0.009	0.114	-0.090	0.013	0.104	0.088
p_{24}		0.089			0.005	
p_{25}		0.941			0.121	
p_{26}		-0.053			0.077	
p_{34}		0.059			-0.008	
p_{35}		0.652			0.263	
p_{36}		0.270			0.370	
U_1	0.540	0.939	0.976	0.592	0.939	0.972
U_2		0.365			0.990	
U_3		0.678			0.897	

was negative and weak (p_{26} = -0.0534) in model one and positive and weak (p_{26} = 0.0770) in model two. Structural size and heterozygosity showed a weak positive association (p_{34} = 0.0592) in model one and a weak negative association in (p_{34} = -0.0084) model two. Structural size and age exhibited a relatively strong positive association (p_{35} = 0.6523) in model one while structural size and sex exhibited a moderate positive association (p_{35} = 0.2629) in model two. Structural size and density class exhibited a moderate positive association in both model one (p_{36} = 0.2697) and model two (p_{36} = 0.3697). The unexplained variation in body mass was much smaller in model one (U_2 = 0.3646) compared to model two (U_2 = 0.9902). The unexplained variance in structural size was also smaller in model one (U_3 = 0.6778) compared to model two (U_3 = 0.8972) but the difference was less than for body mass.

CENTROID SIZE

Body mass exhibited a moderate positive association with centroid size in both model one (p_{12} = 0.2883) and model two (p_{12} = 0.2458) while structural size exhibited a strong positive association with centroid size in both models (1: p_{13} = 0.6944; 2: p_{13} = 0.7388). Heterozygosity showed a weak positive association (p_{14} = 0.0156) with centroid size in model one and a slightly stronger positive association (p_{14} = 0.0233) with centroid size in model two. Age exhibited a weak negative association with centroid size (p_{15} = -0.0791) in model one but sex exhibited a weak positive association with centroid size (p_{15} = 0.0367) in model two. The association between density class and centroid size was positive but weak (p_{16} = 0.0085) in both model one and model two (p_{16} = 0.0125). The unexplained variation in centroid size was smaller in model one (U_1 = 0.5404) compared to model two (U_1 = 0.5915). Overall model one explained 50.1% of the total variation

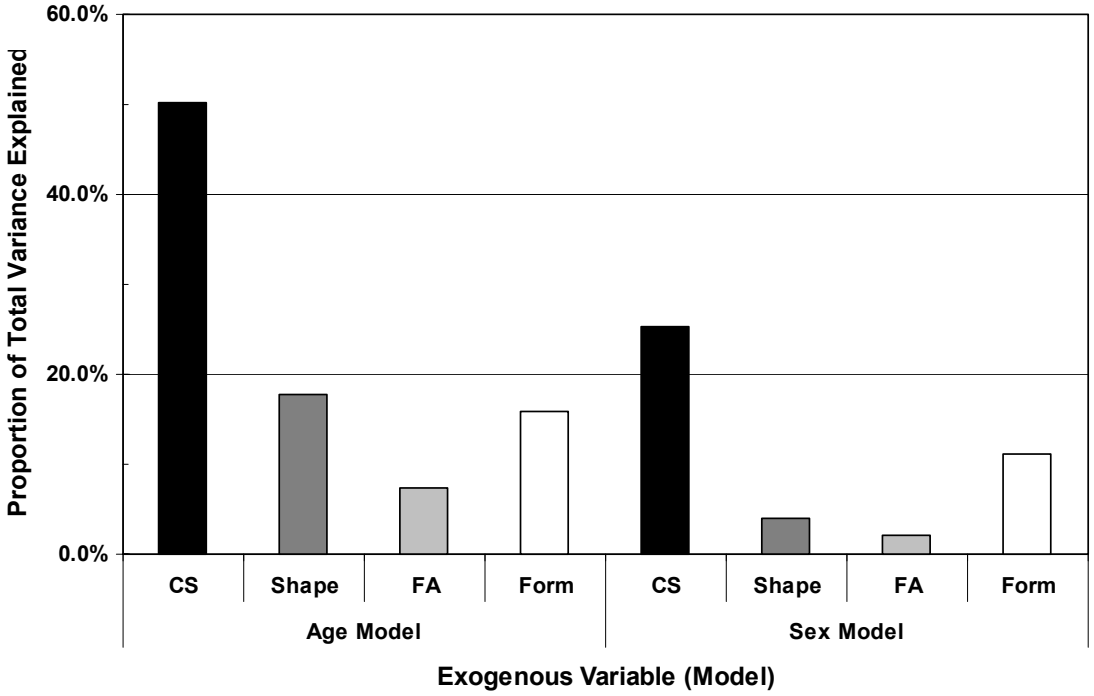

Figure 22. The proportion of total variance explained by the path model for form as well as the three components of form, centroid size, symmetric shape and fluctuating asymmetry for path model one (containing age) and path model two (containing sex).

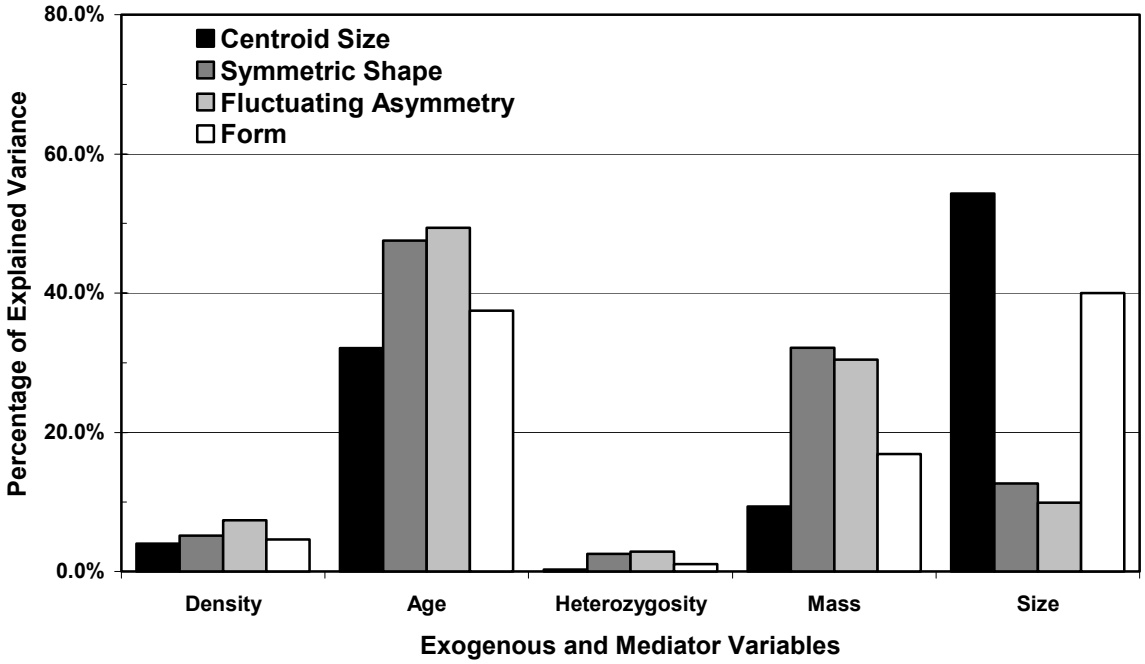

Figure 23. Percentage contribution of each exogenous or mediator variable to the total explained variance for form as well as for each of the three components of form; centroid size, symmetric shape and fluctuating asymmetry for path model one containing the exogenous variable age. Values for the exogenous variables include both direct and indirect paths through the mediator variables.

while model two only accounted for 25.3% of the total variation (Figure 22). In model one structural size and age accounted for most of the explained variance in centroid size (54.3% and 32.1%, respectively) with body mass (9.4%), density class (4.0%), and heterozygosity class (0.3%) accounting for increasingly smaller percentages (Figure 23). In model two the largest percentage of variation in centroid size was accounted for by structural size (75.6%) followed by density class (10.4%), body mass (8.4%), sex (5.5%) and heterozygosity (0.1%) (Figure 24).

SYMMETRIC SHAPE

Body mass exhibited a moderate negative association with symmetric shape in both model one (p_{12} = -0.3192) and model two (p_{12} = -0.2020) as did structural size in both models (1: p_{13} = -0.2005; 2: p_{13} = -0.1846). Heterozygosity showed a weak negative association with symmetric shape in both model one (p_{14} =- 0.0836) and model two (p_{14} = -0.0817). Age exhibited a moderate positive association with symmetric shape (p_{15} = 0.2083) in model one but sex exhibited a weak negative association with symmetric shape (p_{15} = -0.0865) in model two. The association between density class and symmetric shape was positive and relatively weak in both model one (p_{16} = 0.1142) and model two (p_{16} = 0.1041). The unexplained variation in symmetric shape is equal to four decimal places in both models one (U_1 = 0.9387). Overall model one explained 17.7% of the total variation while model two accounted for only 3.9% of the total variation (Figure 22). In model one age and body mass accounted for most of the explained variance (47.5% and 32.1%, respectively) in symmetric shape with structural size (12.7%), density class (5.1%) and heterozygosity (2.5%) accounting for a smaller percentage (Figure 23). In

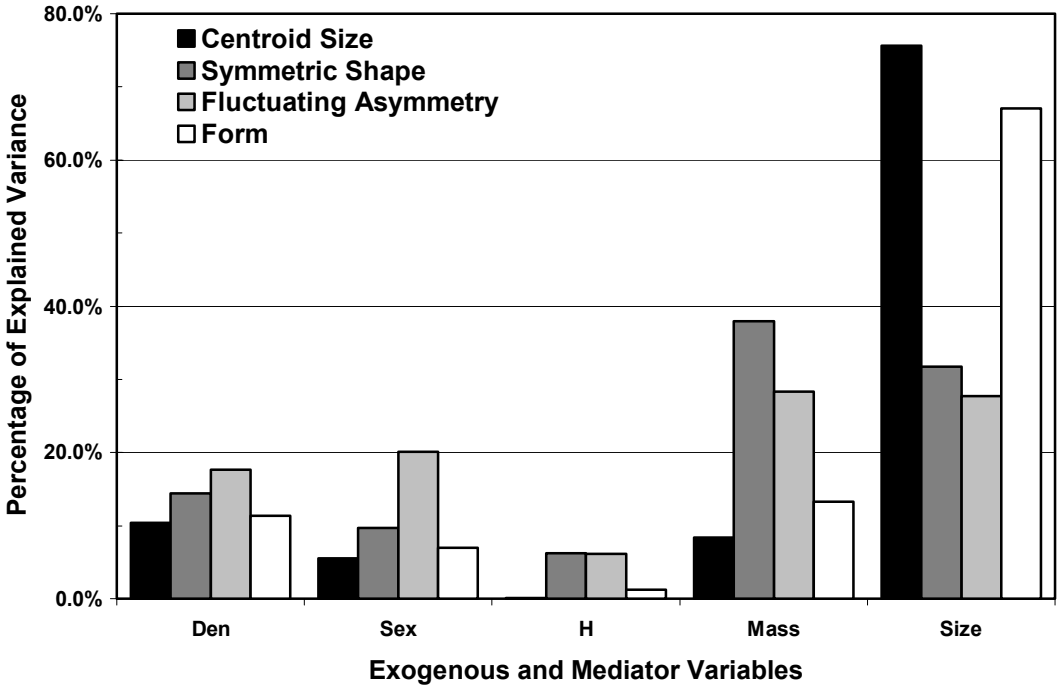

Figure 24. Percentage contribution of each exogenous or mediator variable to the total explained variance for form as well as for each of the three components of form, centroid size, symmetric shape and fluctuating asymmetry for path model two containing the exogenous variable sex. Values for the exogenous variables include both direct and indirect paths through the mediator variables.

model two the greatest percentage of variation in symmetric shape is explained by body mass (38.0%) followed by structural size (31.7%), density class (14.4%), sex (9.7%) and heterozygosity (6.2%) (Figure 24).

FLUCTUATING ASYMMETRY

There was no deviation from normality nor was there a deviation from the normal expectation for kurtosis for the distribution of left-minus-right differences. Body mass exhibited a moderate negative association with fluctuating asymmetry in model one (p_{12} = -0.1942) and a weaker negative association in model two (p_{12} = -0.1258) while structural size exhibited a weaker positive association with fluctuating asymmetry in both models (1: p_{13}= 0.1109; 2: p_{13} = 0.1244). Heterozygosity showed a weak positive association with fluctuating asymmetry in both model one (p_{14} = 0.0565) and model two (p_{14} = 0.0586). Age exhibited a moderate negative association with fluctuating asymmetry (p_{15} = -0.1500) in model one and sex exhibited a slightly weaker negative association with fluctuating asymmetry (p_{15} = -0.0996) in model two. The association between density class and fluctuating asymmetry was negative and relatively weak (p_{16} = -0.0901) in model one and relatively weak and positive in model two (p_{16} = 0.0879). The unexplained variation in fluctuating asymmetry was large and roughly equivalent in model one (U_1 = 0.9757) compared to model two (U_1 = 0.9721). Overall model one explains 7.4% of the total variation while model two only accounted for 2.0% of the total variation (Figure 22). In model one age and body mass accounted for most of the explained variance (49.4% and 30.5%, respectively) in fluctuating asymmetry with structural size (9.9%), density class (7.4%) and heterozygosity (2.9%) accounting for a smaller percentage (Figure 23). In model two the percentage of variation in fluctuating

asymmetry accounted for by body mass (28.4%), structural size (27.7%), age (20.1%), and density class (17.6%) were roughly equal with heterozygosity (6.2%) accounting for a smaller percentage (Figure 24).

OVERALL FORM

An overall model of form, including form as a latent variable and the components of form as mediator variables, is depicted in Figure 25. The path coefficients for all paths other than those going from centroid size (p_{12}), symmetric shape (p_{13}) and fluctuating asymmetry (p_{14}) are the same as in the previous models for each respective component of form (Table 13). The path coefficients for the components of form are roughly equivalent and positive (centroid size, $p_{12} = 0.3763$; symmetric shape, $p_{13} = 0.3811$; fluctuating asymmetry, $p_{14} = 0.3812$). The overall model for form including age accounted for 15.9% of the total variation and the model including sex accounted for 11.1% of the total variation (Figure 22). In the age model, structural size and age accounted for most of the explained variation of form (40.0% and 37.5%, respectively) followed by body mass (16.9%), density class (4.6%) and heterozygosity (1.1%) (Figure 23). In the age model, structural size accounted for most of the explained variance of form (67.1%) followed by body mass (13.3%), density class (11.4%), sex (7.0%) and heterozygosity (1.2%) (Figure 24).

DISCUSSION

The landmark points utilized in this study exhibited significant heterogeneity of variance and appeared more heterogeneous compared to those utilized in the previous study of white-tailed deer (*Odocoileus virginianus*) (Chapter 2). Most of the variation among landmarks evidenced in cotton rat skulls was due to sex and age variance that was

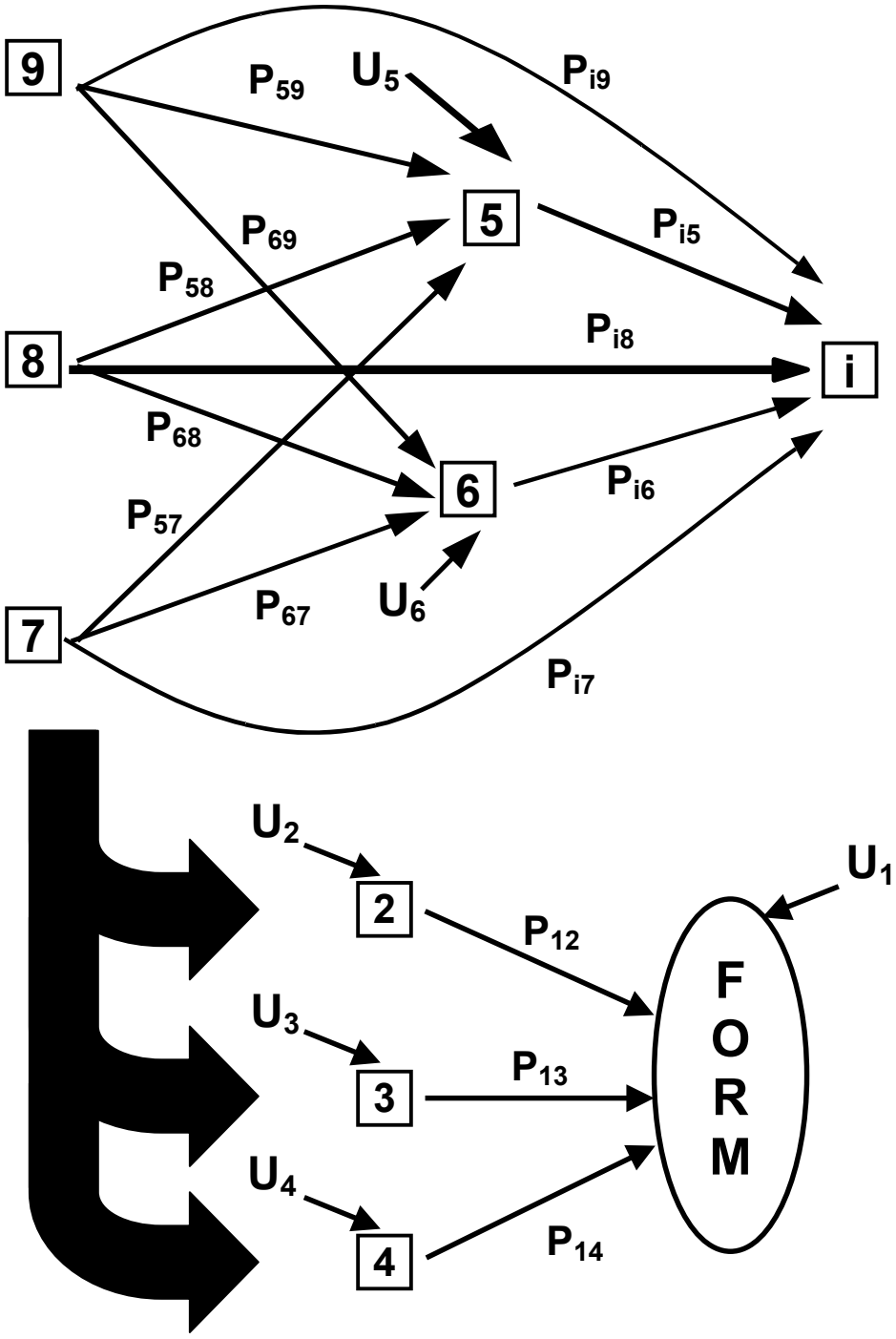

Figure 25. Path model for the composite trait form. The values for all paths other than p_{12}, p_{13}, and p_{14} (which are reported in the text) are given in Table 13. The subscript i refers to the now exogenous variables: centroid size (i = 2), symmetric shape (i = 3)

and fluctuating asymmetry (i = 4). Form (variable 1) is a latent variable in the model and is indicated by an ellipse. All other variables follow the number order in figure 18 and are numbered as: body mass (5), structural size (6), heterozygosity (7), age or sex (8), and density class (9) and are manifest variables. The arrows indicate that the path model in the upper part of the figure determines each of the mediator variables 2 through 4.

not present in the deer sample and created a large landmark-by-sex-by-age interaction. We performed separate analyses for sex and age due to sampling considerations and thus most of the interlandmark variation did not impact our analyses directly. The remaining variance among landmarks was about the same order of magnitude as that in white-tailed deer but was significant in this case because of the larger number of individuals in the study on cotton rats. Nevertheless, the significant interlandmark variance should caution against over-interpreting differences among path models, especially when comparing models with the variable age to those containing the variable sex.

Path coefficients can be interpreted as partial regression coefficients as long as the path model is not over-identified (i.e. there are not fewer causal links than correlations in the model; (Petraitis *et al.*, 1996). In the current study none of the path models were over-identified, therefore we can easily convert our path coefficients to coefficients of determination making it easier to see the relative importance of the exogenous and mediator variables. The mediator variables were all continuous variables and three of the four exogenous variables were ordinal so the directionality of the path coefficient had meaning for all of the continuous and ordinal variables. Sex was a dichotomous categorical variable, which was coded as a dummy variable in the path analyses; therefore the direction of the path coefficient was purely a function of the coding. In this case, positive implied “maleness”.

In an evolutionary sense, path coefficients can be interpreted as coefficients of directional selection (Kingsolver and Schemske, 1991) or with modifications, as coefficients of nonlinear selection (Scheiner *et al.*, 2000). In either case, use of path analyses appears to be a very good way to obtain estimates of selection coefficients from

a phenotypic variance-covariance matrix that are relatively unbiased by environmental variation among individuals (Scheiner *et al.*, 2002; Kruuk *et al.*, 2003). In our models the exogenous variable, density is utilized to estimate the effect of environmental variation. Since density correlates to many other environmental parameters such as habitat quality (Nupp and Swihart, 2000), the competitive environment (Kuang *et al.*, 2003), and numerous others (Andrewartha and Birch, 1954 has an extensive list), it represents a broad-stroke summary variable of the environmental milieu. Since the path coefficients are directional, path models can effectively model evolutionary tradeoffs between direct and indirect effects in the model. The use of coefficients of determination to summarize the direct and indirect paths for exogenous variables takes these tradeoffs, or negative phenotypic correlations, into account. In interpreting our path models of form and form components we preferred to utilize the coefficients of determination to determine the temporal scale of effects rather than as an indication of the relative or absolute importance of effects in the model. The inverse relationship between the magnitude of the path coefficient and the time scale it represents is merely an extension of regarding the path coefficient as a selection coefficient. It is also a better way to interpret the path coefficient as a selection coefficient since it makes explicit the fact that the coefficient represents a rate-of-change over time rather than an indication of magnitude-of-effect.

Skull centroid size was highly positively correlated with structural size in both model one and model two. This positive correlation was an expected result since skull size in mammals is known to positively covary with body size and the relationship has been used extensively to analyze effects on body size due to ecological changes (Yom-Tov *et al.*, 1999), temporal changes (Cooper, 2000) and anthropogenic changes (Wisely *et al.*,

2002). In model one, age also appeared to act on a relatively short time scale but in model two only structural size appeared to affect centroid size on the shortest time scale. Body mass, density class and sex appeared to act over intermediate time scales in both models. Heterozygosity class exhibits a very weak effect on centroid size and thus we interpret its effects as acting over relatively long time periods.

Body mass and age exhibit high correlations with symmetric shape in model one and body mass also appeared to act over a relatively short time scale in model two. However, structural size appeared to be acting over about the same time scale as body mass in model two. Structural size acted over an intermediate time scale in model one. Density class, heterozygosity class and sex also appeared to act over an intermediate time scale. Unlike both centroid size and fluctuating asymmetry, we do not have expectations for either the direction nor magnitude of the exogenous and mediator variables with symmetric shape.

In model one, body mass and age affected fluctuating asymmetry over a relatively short time scale. In model two, structural size also appeared to operate over a relatively short time scale whereas in model one it acted over an intermediate time scale. The effects of density class and heterozygosity class also acted on an intermediate time scale in both models although both appeared to operate over a smaller time scale in model two compared to model one.

From an evolutionary perspective we are really interested in the composite character, form since the components of form may not be truly independent, i.e. they may have non-zero covariances (Klingenberg, 2001a; 2001b). For the cotton rat skull, the covariances among form components did not appear to have been extremely large since all the

components of form have roughly equivalent path coefficients. However, without analyzing form itself we could not have made that determination. The fact that the path coefficients between the components of form and form itself are roughly equivalent does not mean that each component of form has an equal influence on form itself. What it means is that with the given data we can analyze each component of form independently and create a composite form analysis after-the-fact, using the proportion of explained variance for each separate model as a weighting factor. Thus, the final model of form for both model one and model two closely resembled the final models for centroid size, since the path models for centroid size accounted for much more of the explained variance than did the models for symmetric shape and fluctuating asymmetry. Thus our conclusion is that relatively rapid changes in form, within this cotton rat metapopulation, have been primarily a function of structural size and age changes. Changes in body mass, sexual composition, and density affected form over longer time scales and changes in heterozygosity affected form over longer time scales still.

An additional motivation for creating individual-based path models of form was to help in the identification of covariates when using form and form components as ecological and evolutionary biomarkers of toxicological effects (Dieter, 1993; Bickham and Smolen, 1994; Fox, 1995; Fitzgerald *et al.*, 2000). The use of individual-based analysis to compare the effects of toxicants instead of standard analyses comparing impacted to reference sites has great utility. The power of the analysis is increased because sample size for the relevant comparison is now the number of individuals not the number of sites, the effects can be linked to processes at the correct spatio-temporal scale, and the problem of finding replicate impacted sites is alleviated. However, the individual

variation unrelated to the toxicant effects can be large and obfuscate any relevant toxicant effects (Bickham and Smolen, 1994). This individual variation can be reduced with appropriate use of covariates or formal path analyses. For the purpose of identifying covariates, the magnitude of the effect of the variable on form and its components becomes paramount. If only structural size, body mass and age, are included as covariates, 89.8% to 95.7% of the variation explained utilizing all the variables was captured. Collection of individuals would also proceed faster and at less cost if it is determined that density and heterozygosity are unlikely to cause enough change to hinder interpretation of toxicant effects. This assumes that the path relationships are relatively stable over time, which needs to be verified by performing a longitudinal study of form dynamics.

Path analysis provides an excellent framework to analyze the influence of variables of various kinds (environmental, genetic, developmental) and at different scales (individual or group) on evolutionary dynamics of form and its components. It also allows the identification of necessary covariates, and consequently the disuse of others, for analyses of toxicological or other selective effects on form. Although path analysis has many attractive features, a few notes of caution are necessary. First, as cogently pointed out by Petraitis *et al.* (1996) a path model is merely a hypothesis and in fact only one of many possible. Therefore, it is impossible to claim that the path model used here is either the "best" or the "correct" model. In fact, many other models could have been constructed just with the variables utilized in the current analysis and the model used here represented a compromise of theoretical, statistical and logical considerations. It is also impossible to claim that other variables were unimportant. The relatively large amount of unexplained

variance would mitigate against such a claim. Lastly, the results of this analysis cannot be generalized to other species or other populations of hispid cotton rats without additional studies. The additional research necessary to generalize these results over larger spatial areas and to other organisms should provide useful avenues for future research.

LITERATURE CITED

Adams, D. C., F. J. Rohlf, and D. E. Slice. 2003. Geometric morphometrics: Ten years of progress following the 'revolution'. Ital. J. Zool. *In Press*

Akaike, H. 1974. A new look at the statistical model identification. IEEE Trans. Auto. Conf. AC-19:716-723.

Andrewartha, H. G., and L. C. Birch. 1954. The Distribution and Abundance of Animals. University of Chicago Press, Chicago.

Begon, M., C. R. Townsend, and J. L. Harper. 1998. Ecology: Individuals, Populations and Communities, 3rd ed. Blackwell Science Inc, New York.

Bickham, J. W., and M. J. Smolen. 1994. Somatic and heritable effects of environmental genotoxins and the emergence of evolutionary toxicology. Environ. Health Pers. 102:25-28.

Blackard, J. J. 1971. Restoration of the white-tailed deer in the Southeastern United States. M.S. thesis, Louisiana State University, Baton Rouge.

Bookstein, F. L. 1989. A brief history of the morphometric synthesis in L. F. Marcus, E. Bell and A. Garcia-Valdecasas, eds. Contributions to Morphometrics. Museo Nacional De Ciencias Naturales, Madrid, Spain.

Bookstein, F. L. 1991. Morphometric Tools for Landmark Data: Geometry and Biology. Cambridge University Press, Cambridge, UK.

Bookstein, F. L. 1996. Combining the tools of geometric morphometrics. Pp. 131-151 in D. E. Slice, ed. Advances in Morphometrics. Plenum Press, New York.

Bookstein, F. L. 1997. Landmark methods for forms without landmarks: Localizing group differences in outline shape. Med. Image Anal. 1:225-243.

Bullini, L. 1994. Origin and evolution of animal hybrid species. TREE 9:422-426.

Burnham, K. P., and D. R. Anderson. 2002. Model Selection and Multimodel Inference: A Practical Information-Theoretic Approach, 2nd ed. Springer-Verlag, New York.

Caudell, J. N., and R. J. Warren. 1997. Visual estimation of biomass and application of three white-tailed deer HSI models in suburban habitats. Proc. Ann. Conf. SE Assoc. Fish Wildl. Agencies 51:259-268.

Chesser, R. K., and R. J. Baker. 1996. Effective sizes and dynamics of uniparentally and diparentally inherited genes. Genetics 144:1225-1235.

Chipman, R. K. 1965. Age determination of the cotton rat (*Sigmodon hispidus*). Tulane Stud. Zool. 12:19-38.

Cooper, M. L. 2000. Temporal varaiation in skull size and shape in the southern brown bandicoot, *Isodon obesulus* (Peramelidae: Marsupialia) in Western Australia. Austral. J. Zool. 48:47-57.

Dapson, R. W., P. R. Ramsey, M. H. Smith, and D. F. Urbston. 1979. Demographic differences in contiguous populations of white-tailed deer. J. Wildl. Manage. 43:889-898.

DeAngelis, D. L., and K. A. Rose. 1992. Which individual-based approach is most appropriate for a given problem? Pp. 88-111 in D. L. DeAngelis and L. J. Gross, eds. Individual-based Models and Approaches in Ecology: Populations, Communities and Ecosystems. Chapman and Hall, New York.

Deyoung, C. A. 1990. Inefficiency in trophy white-tailed deer harvest. Wildl. Soc. Bull. 18:7-12.

Dieter, M. P. 1993. Identification and quantification of pollutants that have the potential to affect evolutionary processes. Environ. Health Pers. 101:278.

Dryden, I. L., and K. V. Mardia. 1998. Statistical Shape Analysis. John Wiley and Sons, New York.

Edwards, R. J., and C. Hubbs. 1985. Temporal changes in the *Gambusia heterochir* X *G. affinis* hybrid swarm following dam reconstruction. USFWS, Albuquerque, NM End. Spp. Rep. 13:1-31.

Ellsworth, D. L., R. L. Honeycutt, N. J. Silvy, J. W. Bickham, and W. D. Klimstra. 1994a. Historical biogeography and contemporary patterns of mitochondrial DNA variation in white-tailed deer from the Southeastern United States. Evolution 48:122-136.

Ellsworth, D. L., R. L. Honeycutt, N. J. Silvy, M. H. Smith, J. W. Bickham, and W. D. Klimstra. 1994b. White-tailed deer restoration to the Southeastern United States: Evaluating genetic variation. J. Wildl. Manage. 58:686-697.

Fitzgerald, D. G., J. W. Nanson, T. N. Todd, and B. M. Davis. 2000. Truss analysis: Building a bridge between taxonomy and toxicology. SETAC Globe 1:39-40.

Fox, G. A. 1995. Tinkering with the tinkerer: Pollution versus evolution. Environ. Health Pers. 103:93-100.

Futyma, D. J. 1998. Evolutionary Biology, 3rd ed. Sinauer Associates, Sunderland, MA.

Gangestad, S. W., and R. Thornhill. 1999. Individual differences in developmental precision and fluctuating asymmetry: a model and its implication. J. Evol. Biol. 12:402-416.

Goldman, E. A., and R. Kellogg. 1940. Ten new white-tailed deer from North and Middle America. Proc. Biol. Soc. Washington 53:81-90.

Goodall, C. R. 1991. Procrustes methods in the statistical analysis of shape. J. Roy. Stat. Soc., Series B 53:285-339.

Graham, J. H., D. C. Freeman, and J. M. Emlen. 1993. Antisymmetry, directional asymmetry, and dynamic morphogenesis. Genetica 89:121-137.

Greene, D. L. 1984. Fluctuating dental asymmetry and measurement error. Amer. J. Phys. Anthro. 65:283-289.

Hatcher, L. 1994. A Step-by-Step Approach to Using the SAS® System for Factor Analysis and Structural Equation Modeling. SAS Institute, Inc., Cary, NC.

Hillestad, H. O. 1984. Stocking and genetic variability of white-tailed deer in the Southeastern United States. Ph.D dissertation, University of Georgia, Athens.

Hillis, D. M., and J. J. Wiens. 2000. Molecules versus morphology in systematics: Conflicts, artifacts and misconceptions. Pp. 1-19 in J. J. Wiens, ed. Phylogenetic Analysis of Morphological Data. Smithsonian Institution Press, Washington, D.C.

Hoffmann, A. A., and R. E. Woods. 2003. Associating environmental stress with developmental stability: problems and patterns. Pp. 387-401 in M. Polak, ed. Developmental Instability: Causes and Consequences. Oxford University Press, Oxford.

Houle, D. 2000. A simple model of the relationship between asymmetry and developmental stability. J. Evol. Biol. 13:720-730.

Hubbs, C. 1957. *Gambusia heterochir*, a new Poeciliid fish from Texas with an account of its hybridiztion with *G. affinis*. Tulane Stud. Zool. 5:1-16.

Hubbs, C. 1959. Population analysis of a hybrid swarm between *Gambusia affinis* and *G. heterochir*. Evolution 13:236-246.

Hubbs, C. 1971. Competition and isolation mechanisms in the *Gambusia affinis* X *G. heterochir* hybrid swarm. Bull. Texas Mem. Mus. 19:1-46.

Ivey, T. L., and M. K. Causey. 1981. Movements and activity patterns of female white-tailed deer during rut. Proc. Ann. Conf. SE Assoc. Fish Wildl. Agencies 35:149-166.

Jenks, J. A., W. P. Smith, and C. S. DePerno. 2002. Maximum sustained yield harvest versus trophy management. J. Wildl. Manage. 66:528-535.

Jenkins, J. H., and E. E. Provost. 1964. The population status of the larger vertebrates on the Atomic Energy Commission Savannah River Plant site. U.S.A.E.C., Div. Biol. And Med. TID-195652:1-44.

Judson, O. P. 1994. The rise of the individual-based model in ecology. TREE 9:9-14.

Kammermeyer, K. E., and R. L. Marchinton. 1976. Notes on dispersal of male white-tailed deer. J. Mammal. 57:776-778.

Kingsolver, J. G., and D. W. Schemske. 1991. Path analysis of selection. TREE 6:276-280.

Klingenberg, C. P. 2001a. Genetic architecture of mandible shape in mice: Effects of quantitative trait loci analyzed by geometric morphometrics. Genetics 157:785-802.

Klingenberg, C. P. 2001b. Quantitative genetics of geometric shape in the mouse mandible. Evolution 55:2342-2352.

Klingenberg, C. P., M. Barluenga, and A. Meyer. 2002. Shape analysis of symmetric structures: Quantifying variation among individuals and asymmetry. Evolution 56:1909-1920.

Klingenberg, C. P., and G. S. McIntyre. 1998. Geometric morphometrics of developmental instability: Analyzing patterns of fluctuating asymmetry with Procrustes methods. Evolution 52:1363-1375.

Klingenberg, C. P., and H. F. Nijhout. 1999. Genetics of fluctuating asymmetry: A developmental model of developmental instability. Evolution 53:358-375.

Kruuk, L. E. B., J. Merilla, and B. C. Sheldon. 2003. When environmental variation short-circuits natural selection. TREE 18:207-209.

Kuang, Y., W. F. Fagan, and I. Loladze. 2003. Biodiversity, habitat area, resource growth rate and interference competition. Bull. Math. Biol. 65:497-518.

Lamb, T., J. M. Novak, and D. L. Mahoney. 1990. Morphological asymmetry and interspecific hybridization: A case study using hylid frogs. J. Evol. Biol. 3:295-309.

Lehman, N., A. Eisenhawer, K. Hansen, L. D. Mech, R. O. Peterson, P. J. P. Gogan, and R. K. Wayne. 1991. Introgression of coyote mitochondrial DNA into sympatric North American gray wolf populations. Evolution 45:104-119.

Leung, B., and M. R. Forbes. 1997. Fluctuating asymmetry in relation to indices of quality and fitness in the damselfly, *Enallagma ebrium* (Hagen). Oecologia 110:472-477.

Leung, B., L. Knopper, and P. Mineau. 2003. A critical assessment of the utility of fluctuating asymmetry as a biomarker of anthropogenic stress. Pp. 415-426 in M. Polak, ed. Developmental Instability: Causes and Consequences. Oxford University Press, Oxford.

Li, C. C. 1975. Path Analysis - A Primer. Boxwood Press, Pacific Grove, CA.

Littell, R. C., G. A. Milliken, W. W. Stroup, and R. D. Wolfinger. 1996. SAS® System for Mixed Models. SAS Institute Inc., Cary, NC.

Ludwig, W. 1932. Das Rechts-Links Problem im Tierreich und Beim Menschen. Springer Verlag, Berlin.

Lynch, M., and B. Walsh. 1998. Genetics and Analysis of Quantitative Traits. Sinauer Associates, Sunderland, MA.

Mantel, N. 1967. The detection of disease clustering and a generalized regression approach. Cancer Res. 27:209-220.

Marcus, L. F., M. Corti, A. Loy, G. J. P. Naylor, and D. E. Slice. 1996. Advances in Morphometrics. Plenum Press, New York.

Mardia, K. V., and P. E. Jupp. 2000. Directional Statistics. John Wiley, New York.

Markow, T. A. 1994. Developmental Instability: Its Origins and Evolutionary Implications. Kluwer Academic Publishers, Boston.

Martin, R. E., R. H. Pine, and A. F. Deblase. 2000. A Manual of Mammalogy with Keys to Families of the World, 3rd ed. McGraw-Hill, New York.

Mather, K. 1953. Genetical control of stability in development. Heredity 7:297-336.

McCullough, D. R. 1984. Lessons from the George Reserve, Michigan. Pp. 211-242 in L. K. Halls, ed. White-tailed Deer Ecology and Management. Stackpole Books, Harrisburg, PA.

McKechnie, J. L. 1978. Webster's New Twentieth Century Dictionary of the English Language, unabridged, 2nd ed. William Collins and World Publishing Co., Inc, New York.

McKenzie, J. A., and G. M. Clarke. 1988. Diazinon resistance, fluctuating asymmetry and fitness in the australian sheep blowfly, *Lucilia cuprina*. Genetics 120:213-220.

Meacham, C. A., and T. Duncan. 1990. MorphoSys Version 1.26: An automated morphometric system. University Herbarium. University of California, Berkeley, CA.

Mech, L. D., and M. Korb. 1978. An unusually long pursuit of a deer by a wolf. J. Mammal. 59:860-861.

Microsoft. 1995. Microsoft® FORTRAN PowerStation™ V. 4.0 Programmer's Guide. Microsoft Corporation, Seattle, WA.

Møller, A. P. 1994. Directional selection on directional asymmetry: Testes size and secondary sexual characters in birds. Proc. Royal Soc. London, Series B 258:147-151.

Møller, A. P. 1997. Developmental stability and fitness: A review. Amer. Natur. 149:916-932.

Møller, A. P., and J. J. Cuervo. 2003. Asymmetry, size and sexual selection: Factors affecting heterogeneity in relationships between asymmetry and sexual selection. Pp. 262-278 in M. Polak, ed. Developmental Instability: Causes and Consequences. Oxford University Press, Oxford.

Møller, A. P., and A. Pomiankowski. 1993. Fluctuating asymmetry and sexual selection. Genetica Dordrecht 89:267-279.

Møller, A. P., and J. P. Swaddle. 1997. Asymmetry, Developmental Stability, and Evolution. Oxford University Press, Oxford.

Møller, A. P., and R. Thornhill. 1997. A meta-analysis of heritability of developmental stability. J. Evol. Biol. 10:1-16.

Monteiro, L. R., B. Bordin, and S. F. dos Reis. 2000. Shape distances, shape spaces and the comparison of morphometric methods. TREE 15:217-220.

Mood, A. M. 1950. Introduction to the Theory of Statistics. McGraw-Hill, New York.

Nelson, M. E., and L. D. Mech. 1987. Mammalian dispersal patterns: The effects of social structure on population genetics. Pp. 27-40 in B. D. Chepko-Sade and Z. T. Halpin, eds. Mammalian Dispersal Patterns. University of Chicago Press, Chicago.

Nixon, C. M., L. P. Hansen, P. A. Brewer, and J. E. Chelvig. 1991. Ecology of white-tailed deer in an intensively farmed region of Illinois. Wildl. Monogr. 55:1-77.

Novak, J. M., K. T. Scribner, W. D. DuPont, and M. H. Smith. 1991. Catch-effort estimation of white-tailed deer population size. J. Wildl. Manage. 55:31-38.

Nupp, T. E., and R. K. Swihart. 2000. Landscape-level correlates of small-mammal assemblages in forest fragments of farmland. J. Mammal. 81:512-526.

O'Brien, S. J., M. E. Roelke, N. Yuhki, K. W. Richards, W. E. Johnson, W. L. Franklin, A. A. Anderson, J. O. L. Bass, R. C. Belden, and J. S. Martenson. 1990. Genetic introgression within the Florida panther *Felis concolor coryi*. Nat. Geog. Res. 6:485-494.

Otis, D. L., K. P. Burnham, G. C. White, and D. R. Anderson. 1978. Statistical inference from capture data on closed animal populations. Wildl. Monogr. 62:1-135.

Palmer, A. R. 1996. Waltzing with asymmetry. Bioscience 46:518-532.

Palmer, A. R. 1999. Detecting publication bias in meta-analyses: A case study of fluctuating asymmetry and sexual selection. Amer. Natur. 154:220-233.

Palmer, A. R., and C. Strobeck. 1986. Fluctuating asymmetry: Measurement, analysis, patterns. Ann. Rev. Ecol. Syst. 17:391-421.

Palmer, A. R., and C. Strobeck. 1992. Fluctuating asymmetry as a measure of developmental stability: Implications of non-normal distributions and power of statistical tests. Acta Zool. Fennica 191:57-72.

Palmer, A. R., and C. Strobeck. 2003. Fluctuating asymmetry analyses revisited. Pp. 279-319 in M. Polak, ed. Developmental Instability: Causes and Consequences. Oxford University Press, Oxford.

Pascual, M., and S. A. Levin. 1999. From individuals to population densities: Searching for the intermediate scale of nontrivial determinism. Ecology 80:2225-2236.

Petraitis, P. S., A. E. Dunham, and P. H. Niewiarowski. 1996. Inferring multiple causality: The limitations of path analysis. Func. Ecol. 10:421-431.

Piegorsch, W. W., and A. J. Bailer. 1997. Statistics for Environmental Biology and Toxicology. CRC Press, Boca Raton, FL.

Polak, M. 2003. Developmental Instability: Causes and Consequences. Oxford University Press, Oxford.

Purdue, J. R., M. H. Smith, and J. C. Patton. 2000. Female philopatry and extreme spatial genetic heterogeneity in white-tailed deer. J. Mammal. 81:179-185.

Richtsmeier, J. T., V. B. Deleon, and S. R. Lele. 2002. The promise of geometric morphometrics. Yrbk. Phys. Anthro. 45:63-91.

Robinson, G. K. 1991. That BLUP is a good thing: The estimation of random effects. Stat. Sci. 6:15-51.

Roff, D. A. 1992. The Evolution of Life Histories: Theory and Analysis. Chapman and Hall, New York.

Roff, D. A. 1997. Evolutionary Quantitative Genetics. Chapman and Hall, New York.

Rohlf, F. J. 2000a. On the use of shape spaces to compare morphometric methods. Hystrix 11:9-25.

Rohlf, F. J. 2000b. Statistical power comparisons among alternative morphometric methods. Amer. J. Phys. Anthro. 111:463-478.

Rohlf, F. J. 2003. TpsRelW: A Program for Relative Warp Analysis. State University of New York, Stony Brook. Stony Brook, NY.

Rohlf, F. J., and L. F. Marcus. 1993. A Revolution In Morphometrics. TREE 8:129-132.

Ruth, C. 2003. 2001 South Carolina deer harvest report. South Carolina Dept. Nat. Res., Columbia, SC.

SAS Institute. 1999. SAS / STAT® User's Guide, Ver. 8. SAS Institute Inc., Cary, NC.

Scheiner, S. M., K. Donohue, L. A. Dorn, S. J. Mazer, and L. M. Wolfe. 2002. Reducing environmental bias when measuring natural selection. Evolution 56:2156-2167.

Scheiner, S. M., R. J. Mitchell, and H. S. Callahan. 2000. Using path analysis to measure natural selection. J. Evol. Biol. 13:423-433.

Scribner, K. T., M. C. Wooten, M. H. Smith, and P. E. Johns. 1985. Demographic and genetic characteristics of white-tailed deer populations subjected to still or dog

hunting. Pp. 197-212 in S. F. Roberson, ed. Game Harvest Management. Caesar Kleberg Foundation Wildlife Research Institute, Kingsville, TX.

Severinghaus, C. W. 1949. Tooth development and wear as criteria of age in white-tailed deer. J. Wildl. Manage. 13:195-216.

Slice, D. E., F. L. Bookstein, L. F. Marcus, and F. J. Rohlf. 1996. A glossary for geometric morphometrics. Pp. 531-551 in D. E. Slice, ed. Advances in Morphometrics. Plenum Press, New York.

Small, C. G. 1996. The Statistical Theory of Shape. Springer-Verlag, New York.

Smith, M. H., R. Baccus, H. O. Hillstead, and M. N. Manlove. 1984. Population genetics of white-tailed deer. Pp. 119-128 in L. K. Halls, ed. White-tailed Deer Ecology and Management. Stackpole Books, Harrisburg, PA.

Smith, W. P. 1991. *Odocoileus virginianus*. Mammalian Species 388:1-13.

Stearns, S. C. 1992. The Evolution of Life Histories. Oxford University Press, New York.

Svensson, E. I., B. Sinervo, and T. Comendant. 2002. Mechanistic and experimental analysis of condition and reproduction in a polymorphic lizard. J. Evol. Biol. 15

Swaddle, J. P., M. S. Witter, and I. C. Cuthill. 1994. The analysis of fluctuating asymmetry. Anim. Behav. 48:986-989.

Tall Timbers. Research Incorporation. 1992. Population ecology of the Blackbeard Island white-tailed deer. Bull. Tall Timbers Res. Inc. 26:1-108.

Thornhill, R., A. P. Møller, and S. W. Gangestad. 1999. The biological significance of fluctuating asymmetry and sexual selection. Amer. Natur. 154:234-241.

Tomkins, J. L., and L. W. Simmons. 2003. Fluctuating asymmetry and sexual selection: paradigm shifts, publication bias, and observer expectation. Pp. 231-261 in M. Polak,

ed. Developmental Instability: Causes and Consequences. Oxford University Press, Oxford.

Urbston, D. F. 1967. Herd dynamics of a pioneer-like deer population. Proc. Ann. Conf. SE Assoc. Fish Wildl. Agencies 21:42-50.

Van Dongen, S. 2000. Unbiased estimation of individual asymmetry. J. Evol. Biol. 13:107-112.

Van Dongen, S., L. Lens, and G. Molenberghs. 2003. Recent developments and shortcomings in the analysis of individual asymmetry: a review and introduction of a bayesian statistical approach. Pp. 320-342 in M. Polak, ed. Developmental Instability: Causes and Consequences. Oxford University Press, Oxford.

Van Dongen, S., G. Molenberghs, and E. Matthysen. 1999. The statistical analysis of fluctuating asymmetry: REML estimation of a mixed regression model. J. Evol. Biol. 12:94-102.

Van Valen, L. 1962. A study of fluctuating asymmetry. Evolution 16:125-142.

Verbeke, G., and G. Molenberghs. 1997. Linear Mixed Models in Practice: A SAS-Oriented Approach. Springer-Verlag, New York.

Wisely, S. M., J. J. Ososky, and S. W. Buskirk. 2002. Morphological changes to black-footed ferrets (*Mustela nigripes*) resulting from captivity. Can. J. Zool. 80:1562-1568.

Wright, S. 1921. Correlation and causation. J. Agric. Res. 20:557-585.

Yom-Tov, Y., S. Yom-Tov, and H. Moller. 1999. Competition, coexistence, and adaptation amongst rodent invaders to Pacific and New Zealand islands. J. Biogeog. 26:947-958.

Zar, J. H. 1999. Biostatistical Analysis, 4th ed. Prentice Hall, Upper Saddle River, NJ.

APPENDICES

APPENDIX A

DESCRIPTION OF LANDMARKS FOR WHITE-TAILED DEER

Landmark Number[1]	Description
	Paired landmarks
1,2	Point of greatest curvature of the anterior end of the premaxilla
4,5	Point of greatest curvature of the anterior end of the incisive foramen
6,7	Maxilla/premaxilla suture at the exterior margin of the incisive foramen
8,9	Point of greatest curvature of the posterior end of the incisive foramen
12,15	Intersection of the point of greatest curvature of medial invagination of the first molar and the maxilla
13,16	Intersection of the point of greatest curvature of medial invagination of the second molar and the maxilla
14,17	Intersection of the point of greatest curvature of medial invagination of the third molar and the maxilla
19,22	Squamosal/jugal suture at the medial surface of the zygomatic arch
20,21	Intersection of the basisphenoid and the auditory bulla
23,26	Point of greatest curvature of the posterior end of the paraoccipital process
24,25	Intersection of the occipital with the distal anterior margin of the foramen magnum
27,28	Point of greatest curvature of the posterior of the occipital condyle
	Midline Landmarks
3	Anterior medial point of the premaxillary suture
10	Medial intersection of the premaxillary/maxillary suture
11	Medial intersection of the maxillary/palatal suture
18	Posterior medial point of the palatal suture

[1]For paired landmarks, the first number is located on the left side when viewing the skull from the posterior dorsal surface.

APPENDIX B

DESCRIPTION OF LANDMARKS FOR HISPID COTTON RATS

Landmark Number[1]	Description
	Paired landmarks
1,12	Point of least curvature of the nasal
2,13	Point of greatest curvature of the anterior end of the incisive foramen
3,14	Point of greatest curvature of the posterior end of the incisive foramen
4,15	Intersection of the point of greatest curvature of medial invagination of the first molar and the maxilla
5,16	Intersection of the point of greatest curvature of medial invagination of the second molar and the maxilla
6,17	Intersection of the point of greatest curvature of medial invagination of the third molar and the maxilla
7,18	Point of greatest curvature of the medial anterior end of the orbit
8,19	Point of greatest curvature of the medial posterior end of the orbit
9,20	Intersection of the basisphenoid and the auditory bulla
10,21	Point of greatest curvature of the posterior end of the paraoccipital process
11,22	Point of greatest curvature of the posterior of the occipital condyle
	Midline Landmarks
23	Posterior-most point of the palatal suture
24	Point of greatest curvature of the posterior end of the occipital condyle

[1]For paired landmarks, the first number is located on the left side when viewing the skull from the posterior dorsal surface.